UMEÅ UNIVERSITY

Using patient-derived cell models to investigate the role of misfolded SOD1 in ALS

Elin Forsgren

Pharmacology and Clinical Neuroscience
Umeå 2017

Cover : Immunostaining of induced pluripotent stem cell-derived motor neurons differentiated from an ALS patient heterozygous for the L144F *SOD1* mutation and stained with antibody against phosphorylated neurofilament heavy chain (SMI31).

Responsible publisher under swedish law: the Dean of the Medical Faculty

ISBN: 978-91-7601-759-3
ISSN: 0346-6612
New series no: 1913
Cover illustration: Image by Jonathan Gilthorpe
Figure design: Elin Forsgren
E-version available at: http://umu.diva-portal.org/
Printed by: Print & Media, Umeå University, Umeå, Sweden 2017

To my family

Table of Contents

TABLE OF CONTENTS I

ABSTRACT III

ORIGINAL PAPERS V

ABBREVIATIONS VI

ENKEL SAMMANFATTNING PÅ SVENSKA VIII

INTRODUCTION 1

Amyotrophic Lateral Sclerosis 1
- Motor system overview 1
- Epidemiology 2
- Risk factors 3
- Diagnosis 3
- Treatment 4
- General neuropathology 4
- Genetics of ALS 5

Superoxide dismutase 7
- SOD1 8
- SOD2 8
- SOD3 8

SOD1 9
- Structure 9
- Stability 10
- *SOD1* mutations 11

Models of SOD1 ALS 12
- Transgenic mouse models 12
- *In vitro* model systems 13

SOD1 and ALS 16
- Mutant SOD1 toxicity 16
- Wt SOD1 in ALS 16

Mechanisms of SOD1 toxicity 17
- Disturbances in protein degradation 17
- Endoplasmatic reticulum stress 20
- Glutamate excitotoxicity 21
- Hyperexcitability 22
- Mitochondrial damage 22
- Misfolded SOD1 interaction partners 23

RNA-interaction and processing 23
Prion-like transmission of misfolded SOD1 23
Non cell-autonomous toxicity 24

Induced pluripotent stem (iPS) cells **27**
History and discovery 27
Reprogramming methods 28
Motor neuron organization 29
MN classification 30
MN differentiation 31

IPSC-based models of ALS **32**

AIMS OF THESIS **35**

MATERIAL AND METHODS **36**
Human materials 36
Cell culture 36
Fibroblasts 36
Induced pluripotent stem cells 39
IPSC-derived motor neuron cultures 39
IPSC-derived astrocytes 40
IPSC-derived sensory neuron cultures 40
Cell treatments 41
Quantification of SOD1 by ELISA 42
Size exclusion chromatography 42
CytoTox-Glo Cytotoxicity Assay 43
Proteasome analysis 43
Immunocapture of misfolded SOD1 44
Immunocytochemistry 44
Western Blotting 44
Statistical analysis 45

RESULTS **47**
Paper I 47
Paper II 49
Paper III 53
Paper IV 56

DISCUSSION **59**

CONCLUSIONS **65**

ACKNOWLEDGEMENTS **66**

REFERENCES **68**

Abstract

Protein misfolding and aggregation underlie several neurodegenerative proteinopathies including amyotrophic lateral sclerosis (ALS). *Superoxide dismutase 1 (SOD1)* was the first gene found to be associated with familial ALS. Overexpression of human mutant or wild type SOD1 in transgenic mouse models induces motor neuron (MN) degeneration and an ALS-like phenotype. *SOD1* mutations, leading to the destabilization of the SOD1 protein is associated with ALS pathogenesis. However, how misfolded SOD1 toxicity specifically affects human MNs is not clear. The aim of this thesis was to develop patient-derived, cellular models of ALS to help understand the pathogenic mechanisms underlying *SOD1* ALS.

To understand which cellular pathways impact on the level of misfolded SOD1 in human cells, we established a model using patient-derived fibroblasts and quantified misfolded SOD1 in relation to disturbances in several ALS-related cellular pathways. Misfolded SOD1 levels did not change following reduction in autophagy, inhibition of the mitochondrial respiratory chain, or induction of endoplasmic reticulum (ER)-stress. However, inhibition of the ubiquitin-proteasome system (UPS) lead to a dramatic increase in misfolded SOD1 levels. Hence, an age-related decline in proteasome activity might underlie the late-life onset that is typically seen in *SOD1* ALS.

To address whether or not SOD1 misfolding is enhanced in human MNs, we used mixed MN/astrocyte cultures (MNCs) generated *in vitro* from patient-specific induced pluripotent stem cells (iPSCs). Levels of soluble misfolded SOD1 were increased in MNCs as well as in pure iPSC-derived astrocytes compared to other cell types, including sensory neuron cultures. Interestingly, this was the case for both mutant and wild type human SOD1, although the increase was enhanced in *SOD1* FALS MNCs. Misfolded SOD1 was also found to exist in the same form as in mouse SOD1 overexpression models and was identified as a substrate for 20S proteasome degradation. Hence, the vulnerability of motor areas to ALS could be explained by increased SOD1 misfolding, specifically in MNs and astrocytes.

To investigate factors that might promote SOD1 misfolding, we focussed on the stability of SOD1 mediated by a crucial, stabilizing C57-C146 disulphide bond and its redox status. Formation of disulphide bond is dependent on oxidation by O_2 and catalysed by CCS. To investigate whether low O_2 tension affects the stability of SOD1 *in vitro* we cultured fibroblasts and iPSC-derived MNCs under different oxygen tensions. Low oxygen tension promoted disulphide-reduction, SOD1 misfolding and aggregation. This response was much greater in MNCs compared to fibroblasts, suggesting that MNs may be especially sensitive to low oxygen tension and areas with low oxygen supply could serve as foci for ALS initiation.

SOD1 truncation mutations often lack C146, and cannot adopt a native fold and are rapidly degraded. We characterized soluble misfolded and aggregated SOD1 in patient-derived cells carrying a novel *SOD1* D96Mfs*8 mutation as well as in cells fom an unaffected mutation carrier. The

truncated protein has a C-terminal fusion of seven non-native amino acids and was found to be extremely prone to aggregation *in vitro*. Since not all mutation carriers develop ALS, our results suggested this novel mutation is associated with reduced penetrance.

In summary, patient derived cells are useful models to study factors affecting SOD1 misfolded and aggregation. We show for the first time that misfolding of a disordered and disease associated protein is enhanced in disease-related cell types. Showing that misfolded SOD1 exists in human cells in the same form as in transgenic mouse models strengthens the translatability of results obtained in the two species. Our results demonstrate disulphide-reduction and misfolding/aggregation of SOD1 and suggest that 20S proteasome could be an important therapeutic target for early stages of disease. This model provides a great opportunity to study pathogenic mechanisms of both familial and sporadic ALS in patient-derived models of ALS.

Keywords: ALS, SOD1, patient-derived models, induced pluripotent stem cells, motor neurons, astrocytes, 20S proteasome low oxygen tension, misfolded SOD1.

Original papers

The thesis is based on the following papers, referred to in the text by their Roman numeral:

I. Isil Keskin, **Elin Forsgren,** Dale J. Lange, Markus Weber, Anna Birve, Matthis Synofzik, Jonathan D. Gilthorpe, Peter M. Andersen and Stefan L. Marklund. Effects of Cellular Pathway Disturbances on Misfolded *Superoxide Dismutase-1* in Fibroblasts Derived from ALS Patients. PloS one. (2016) 11 (2): e0150133.

II. **Elin Forsgren,** Manuela Lehmann, Mackenzie Weygandt Mathis, Isil Keskin, Per Zetterström, Jik Nijssen, Emily R Lowry, Alejandro Garcia, Jackson Sandoe, Eva Hedlund, Hynek Wichterle, Christopher Henderson, Kevin Eggan, Evangelos Kiskinis, Peter M. Andersen, Stefan L. Marklund and Jonathan D. Gilthorpe. Enhanced protein misfolding in patient-derived models of amyotrophic lateral sclerosis. *2017 manuscript under review*.

III. Isil Keskin, **Elin Forsgren,** Peter M. Andersen, Dale J. Lange, Matthis Synofzik, Ulrika Nordström, Per Zetterström, Stefan L. Marklund and Jonathan D. Gilthorpe. Low oxygen tension induces misfolding and aggregation of superoxide dismutase in ALS patient-derived motor neurons. *2017 Manuscript*.

IV. **Elin Forsgren,** Frida Nordin, Ulrika Nordström, Reza Rofougaran, Jens Danielsson, Stefan L. Marklund, Jonathan D. Gilthorpe and Peter M. Andersen. A Novel mutation D96Mfs*8 in *SOD1* identified in a Swedish ALS patient results in a truncated and heavily aggregation-prone protein. *2017 Manuscript*

Abbreviations

AD	Alzheimer's disease
ALS	amyotrophic lateral sclerosis
ANG	angiogenin
ANOVA	analysis of variance
ATF6	activating transcriptions factor 6
ATP	adenosine triphosphate
BCA	bicinchoninic acid assay
BDNF	brain derived neurotrophic factor
BMP	bone morphogenic factor
C9ORF72	chromosome 9 open reading frame 72
CCS	copper chaperone for SOD
CHAT	choline acetyltransferase
CNS	central nervous system
CNTF	ciliary neurotrophic factor
CSF	cerebrospinal fluid
CST	corticospinal tract
CuZn SOD	copper zinc superoxide dismutase (=SOD1)
DNA	deoxyribonucleic acid
DMEM	Dulbecco's Modified Eagle Medium
EC-SOD	extracellular superoxide dismutase (=SOD3)
ER	endoplasmatic reticulum
ERAD	ER-associated protein degradation
FACS	fluorescence-activated cell sorting
FALS	familial amyotrophic lateral sclerosis
FBS	fetal bovine serum
FF-MNs	fast twitch fatigable motor neurons
FGF	fibroblast growth factor
FR-MNs	fast twitch fatigue resistant motor neurons
FTD	frontotemporal dementia
FUS	FUS RNA binding protein
GDNF	glial cell line-derived neurotrophic factor
GFAP	glilal fibrillary acidic protein
GFP	green fluorescent protein
Grp78	ER chaperone glucose-regulated protein 78
GSH	glutathione
HB9	motor neuron and pancreas homeobox 1, MNX1
hESC	human embryonic stem cell
Hox	homeobox
HSC70	heat shock cognate 70
HSP	heat shock protein
IAM	iodoacetamide
IGF1	insulin-like growth factor 1
iPSC	induced pluripotent stem cell
iPSC-Astros	iPSC-derived astrocytes
IRE1	inositol-requiring enzyme 1

ISL1/2	ISL LIM homeobox 1/2
LC3	microtubule-associated protein 1 light chain 3
LMC	lateral motor column
LMN	lower motor neuron
MAP2	microtubule associated protein 2
MAPT	microtubule associated protein tau
mESC	mouse embryonic stem cell
misELISA	misfolded SOD1 specific ELISA
MN	motor neuron
MNC	iPSC mixed motor neuron/astrocyte cultures
Mn SOD	manganese superoxide dismutase (=SOD2)
mRNA	messenger ribonucleic acid
miRNA	micro ribonucleic acid
NEAA	non-essential amino acids
NEFL	neurofilament light
NEFH	neurofilament heavy
NGF	nerve growth factor
PAGE	polyacrylamide gel electrophoresis
PBS	phosphate buffered saline
PD	Parkinson's disease
PERK	protein kinase RNA-like endoplasmic reticulum kinase
RA	retinoic acid
RNA	ribonucleic acid
ROS	reactive oxygen species
SALS	sporadic amyotrophic lateral sclerosis
SHH	sonic hedgehog
SMI32	neurofilament heavy chain, non-phosphorylated
S-MNs	slow twitch fatigue resistant MNs
SNC	mixed sensory neuron cultures
SOD	superoxide dismutase
TBK1	TANK-binding kinase-1
TARDBP	TAR DNA binding protein (TDP-43)
UMN	upper motor neuron
UPR	unfolded protein response
UPS	ubiquitin-proteasome system
VDAC	voltage dependent anion channels
Wt	wild type
XBP	x-box binding protein 1
3-MA	3-methyladenine

Enkel sammanfattning på svenska

Varje år insjuknar omkring 5300 personer i världen i motorneuronsjukdomen Amyotrofisk lateralskleros (ALS). Sjukdomen kännetecknas av degeneration av motorneuron i hjärnan och ryggmärgen, de nervceller som styr kroppens muskler, vilket leder till musklerförtvining och gradvis förlamning. ALS-patienter avlider oftast till följd av andningssvikt när sjukdomen når andningsmuskulaturen. I de allra flesta fall uppkommer ALS sporadiskt (SALS), det vill säga utan känd genetisk orsak, medan ärftliga fall (FALS) drabbar omkring 10 % och beror på mutationer i ett antal kända gener. Upp till 6 % av alla ALS fall kan härledas till mutationer i genen *superoxid dismutas 1* (*SOD1*).

SOD1 är ett enzym som ansvarar för att omvandla och oskadliggöra fria syreradikaler som bildas vid normal ämnesomsättning. 206 olika *SOD1* mutationer har identifierats, alla orsakar inte ALS men många leder till att den tredimensionella proteinstrukturen förändras, vilket ökar proteinets benägenhet att felveckas. Initialt trodde man att *SOD1* mutationer förhindrade proteinets normalfunktion och följaktligen orsakade ALS. Studier har emellertid visat att den enzymatiska funktionen ofta bevaras, även hos muterade proteiner. Däremot kan små mängder felveckat SOD1 störa andra viktiga cellulära funktioner. Felveckat SOD1 har en benägenhet att klumpa ihop sig och bilda aggregat i det centrala nervsystemet (CNS). Dessa aggregat återfinns hos patienter med såväl FALS som SALS vilket tyder på att även vildtyps-SOD1 kan felveckas och vara involverat i sjukdomsutvecklingen. De flesta studier är baserade på transgena musmodeller som uttrycker extremt stora mängder av muterat humant *SOD1*. Det är dock oklart hur väl studier i möss överensstämmer med sjukdomsutvecklingen hos ALS-patienter, där mängden SOD1 är betydligt lägre. En central fråga som fortfarande står obesvarad är varför just motorneuron degenererar i ALS, trots att SOD1 uttrycks i alla kroppens celler.

Det övergripande syftet med den här avhandlingen har varit att karakterisera felveckat SOD1 i patientceller för att studera dess roll i ALS-relaterade sjukdomsmekanismer med fysiologiskt relevanta nivåer av *SOD1*. Samtliga studier är gjorda *in vitro* med celler från friska donatorer med vildtyps-SOD1, celler från patienter med *SOD1*-FALS, FALS som bär andra ALS-associerade gener, samt SALS. I de allra flesta fallen har vi analyserat både lösligt felveckat SOD1 samt aggregerade former av SOD1 proteinet.

Studie I: Syftet med denna studie var att inducera förändringar i ALS-relaterade cellulära funktioner i fibroblaster (hudceller) och därefter studera dess inverkan på felveckat SOD1. Våra resultat visar att mängderna felveckat och aggregerat SOD1 inte nämnvärt påverkas av vare sig nedreglerad autofagi (nedbrytning av felaktiga proteiner), induktion av stress i endoplasmatiska nätverket (ansvarar för proteinveckning) eller inhibering av mitokondriefunktionen (energiproduktion). Däremot visar vi att ubiquitin-proteasomsystemet (UPS) bär huvudansvaret för nedbrytning av felveckat

SOD1. Våra resultat visar att en åldersrelaterad eller annan typ av försämring av UPS funktion skulle kunna föranleda utveckling av ALS.

Studie II: För att studera felveckat SOD1 i de celler som degenererar i ALS använde vi oss av fibroblaster som reprogrammerats till stamceller. Vi utvecklade protokoll för att differentiera stamcellerna till motorneuron och astrocyter. Genom att undersöka olika typer av neurala och icke-neurala patientceller har vi visat att nivåerna av lösligt felveckat SOD1 är högre i motorneuroner, de celler som är mest utsatta vid ALS. Detta gäller såväl friska kontrollceller, med vildtyps-SOD1, som patientceller, med muterat SOD1. Däremot är mängden högre vid närvaro av *SOD1* mutationer. Uttryck av felveckat SOD1 i astrocyter leder till snabbare sjukdomsutveckling hos möss. Vi identifierade höga nivåer i astrocyter från ALS patienter. De felveckade SOD1 proteiner vi analyserat i patientceller är mestadels SOD1 monomerer som saknar en intramolekylär disulfidbrygga, vilken är viktig för proteinets stabilitet. Därmed är felveckat SOD1 i patientceller av samma slag som tidigare påvisats i ryggmärgen hos transgena musmodeller. Detta resultat främjar jämförelser av SOD1-relaterade sjukdomsmekanismer modellsystemen emellan.

I likhet med fibroblaster leder inhibering av UPS-degradering i motorneuron till ansamling av såväl viltyps-, som muterat, felveckat SOD1 i löslig form. Däremot bildas inte olösliga SOD1-aggregat i samma utsträckning. Vi har vidare visat att felveckat SOD1, i likhet med felveckade proteiner i Alzheimers och Parkinsons sjukdom, i huvudsak bryts ner av 20S proteasomen oberoende av ubiquitin. Därmed kan 20S proteasomen utgöra ett gemensamt läkemedelsmål för flertalet neurodegernerativasjukdomar, inklusive ALS.

Sammanfattningsvis visar våra resultat att felveckat SOD1 i patientceller är av samma slag som återfinns hos transgena musmodeller, samt att 20S proteasomens funktion är viktig för nedbrytning av felveckat SOD1. Vi visar att nivåerna är specifikt förhöjda i motorneuron och astrocyter, vilket överensstämmer med deras utsatthet i ALS. Vidare studier av de mekanismer som styr felveckning av SOD1, och 20S proteasomens funktion, med hjälp av patientderiverade celler kan bidra till identifiering av nya behandlingsstrategier för ALS.

Studie III: Åldrande, manligt kön, rökning, stroke eller mekanisk skada på CNS, är faktorer som associerats med högre risk att drabbas av ALS. Gemensamt för många av dessa faktorer är att de leder degeneration av små kapillärer och sämre syresättning till vävnaden. Syftet med denna studie var att undersöka om försämrad syresättning påverkar mängden felveckat SOD1 i patientcellinjer. Våra resultat visar att låga syrekoncentrationer leder till ökade mängder lösligt felveckat och aggregerat SOD1 i både fibroblaster och motorneuronkulturer *in vitro*. Mängden felveckat SOD1 till följd av låga syrenivåer var både dos- och tidsberoende och resulterade i protein som saknade den stabiliserande disulfidbryggan. Effekten var störst hos fullängd- och muterade SOD1 proteiner. Detta indikerar att effekten av låga syrenivåer är beroende av att proteinet kan stabiliseras av en disulfidbrygga, vilken sedan reduceras under odling vid låg syrehalt. Ökad mängd felveckat SOD1

förekom hos celler med vildtyps-*SOD1*, samt celler med muterat *SOD1* och var mest påtaglig i motorneuronkulturer. Våra resultat tyder därför på att motorneuron är extra känsliga och att områden i CNS med låg syretillförsel skulle kunna vara en riskzon där SOD1 initialt börjar felveckas och aggregera.

Studie IV: Syftet med denna studie var att karakterisera SOD1 i celler från en ALS-patient med en ej tidigare beskriven *SOD1* mutation, D96Mfs*8. Mutationen resulterar i ett förkortat SOD1 protein med en främmande, 7 aminosyror lång, neo-peptid. D96Mfs*8 proteinet saknar C146 av disulfidbryggan, och enzymatisk funktion. Det kodade proteinet är instabilt och effektivt nedbrutet av UPS. Vi identifierade ändå förhöjda nivåer av lösligt felveckat SOD1 i fibroblaster samt motorneuronkulturer och proteinet med just denna mutation visade sig vara väldigt aggregationsbenäget. Mutationen återfanns hos en ALS patient samt hos en frisk anlagsbärare, vilka hade nära på identiska mängder lösligt felveckat SOD1, däremot fann vi större mängder aggregat i motorneuron deriverade från ALS patienten. Våra resultat visar på skillnader i hanteringen av felveckat SOD1 mellan fibroblaster och motorneuron samt mellan bärare av mutationen. Våra resultat påvisar även vikten av välfungerande UPS-degradering för att minska mängden felaktiga proteiner, vilka har potential att bilda toxiska aggregat och bidra till utveckling av ALS.

Våra studier har varit inriktade på att undersöka potentialen av patientceller, i form av fibroblaster, motorneuron och astrocyter, som modell för att för att undersöka vilka faktorer och möjliga terapier som påverkar ansamling av felveckat och aggregerat SOD1 protein. Vi har visat att dessa patientceller är en relevant modell för att mäta hur felvekning och aggregering påverkas av ALS associerade faktorer. Våra studier främjar också jämförelser mellan SOD1-relaterade sjukdomsmekanismer identifierade i möss och humana celler samt likheter mellan degradering av felveckade proteiner i såväl ALS som Parkinsons och Alzheimers sjukdom. Våra resultat visar även att motoriska nervceller och astrocyter, som är särskilt utsatta vid ALS, även *in vitro*, har en särkild benägenhet att bygga upp ansamlingar av felveckat SOD1. Sammanfattningsvis stärker våra resultat patientderiverade celler som modell för fortsatta studier av sjukdomsmekanismer och utveckling av nya behandlingsmetoder för ALS.

Introduction

Amyotrophic Lateral Sclerosis

In 1869, the French neurologist Jean-Pierre Charcot first described a connection between symptoms and pathology of a neurodegenerative disease he later called amyotrophic lateral sclerosis (ALS) [1, 2]. It is still referred to as Charcot's disease in France or motor neuron disease in the UK. In the US it is known as Lou Gehrig's disease, after the well-known American baseball player who died from ALS in 1941. ALS is defined by symptoms of muscle weakness, atrophy and hyporeflexia with an asymmetric and focal onset that spread progressively to anatomically related areas [5, 6]. The majority of ALS patients die from causes related to respiratory complications and denervation of the muscles innervating the diaphragm and intercostal muscles [7, 8].

In 1873, Charcot held a lecture describing the symptoms of ALS with exceptional accuracy. This lecture has been translated and published [1, 2] and more recently reviewed by Goetz [9]. Charcot's descriptive name provides an accurate depiction of the degeneration of upper motor neurons (UMNs) in the motor cortex and lower motor neurons (LMNs) in the brain stem and spinal cord representing the major neuropathological hallmark of the disease that has endured for 150 years. The term "amyotrophic" refers to the loss of muscle tissue that occurs when the connection to motor neurons (MNs), and thereby the trophic signals that support them, are lost. "Lateral sclerosis" refers to lesions seen as a hardening of the lateral spinal cord where connective tissue replaces the areas of degenerated corticospinal tracts (CST) [10].

Motor system overview

An overview of the motor neuron system is illustrated in Figure 1.
Cell bodies of UMNs are positioned in the motor cortex with their axons located in the CST. The CST descends via the brain stem and medulla oblongata where the majority of axons cross over to the opposite, contralateral side of the central nervous system (CNS). Hence, axons emanating from UMNs located in the right cortical hemisphere will form the lateral CST on left side of the spinal cord. CST axons are myelinated and lie within the white matter of the spinal cord until they reach their appropriate level of muscle innervation in cervical, thoracic or lumbar levels. They project down the spinal cord to synapse, either directly on LMNs, or indirectly via interneurons that coordinate the activity of LMNs.

A large proportion of UMN axons terminate on a pool of interneurons in the lateral motor column (LMN) along the ventral spinal cord and represent their major synaptic inputs. A smaller proportion of UMNs terminates directly on LMNs that in turn innervate target muscles and regulated fine motor control. UMNs also form the corticobulbar tract that innervates nuclei of the cranial nerves controlling muscles in the face, tongue and jaw.

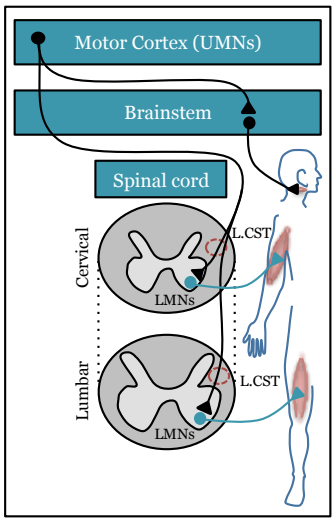

Figure 1: Overview of the motor system. Illustration of motor system with axons of upper motor neuron (UMNs) in the motor cortex descending via the brainstem to the spinal cord within the corticospinal tract (CST) to reach lower motor neurons (LMNs) that project to innervate muscles.

Clinical symptoms

A majority of ALS cases present with a spinal onset of classical ALS, with features described by Charcot 1869 involving both LMNs and UMNs. Symptoms start in a localized area but spread contiguously and lead to a more generalized involvement of all extremities [5, 11]. Signs of LMN symptoms involve localized muscle weakness followed by muscle wasting that initiates in upper or lower limbs. Patients may also experience exaggerated reflexes, fasciculation's (involuntary muscle twitching) and cramps. Signs of UMN involvement include Babinski's sign, a pathological extension reflex of the big toe, hyperreflexia, spasticity and weakness [12, 13].

Bulbar onset ALS involves the degeneration of LMNs that initiates in the bulbar nuclei of the brainstem and initially affects speech and swallowing. It occurs in approximately 20% of all cases and generally presents at an older age with a median age onset of 68 years, compared to classical ALS where the median age of onset is 60 years [14, 15]. Bulbar ALS is also associated with a more rapid progression compared to classical ALS [14-16].

About 50% of ALS patients die within 30 months of diagnosis, 15-20% survive for more than 5 years, and 5% survive for more than 10 years [17, 18]. Although different clinical patterns are discernable, the progressive nature of the disease causes almost all regions of the motor system to become affected. However, some MNs and related functions are relatively spared in ALS. These include MNs in Onuf's nuclei, controlling bladder muscles and oculomotor nuclei controlling eye movements. The reasons behind the heterogeneity of clinical symptoms found in ALS are not well understood. However, defining the factors that lead to late versus early onset, or fast versus slow progression, is likely to lead to a greater understanding of the mechanisms underlying ALS.

Epidemiology

The lifetime risk of developing ALS is slightly higher for men (1:350) than women (1:400) [19]. ALS typically shows a midlife onset that presents between the ages of 45-60 [20]. The incidence of ALS worldwide is 1.75/100 000 person-years [21] with a prevalence of 5/100 000 persons [20]. A number of studies have reported an increased incidence of ALS with age, reaching a plateau around the 7th decade of life [22-26]. The number of cases of ALS cases is predicted to increase, mainly due to increased life expectancy [27].

Risk factors

Although the most commonly identified risk factors of ALS are genetic, the majority of cases have no known genetic involvement. Non-genetic risk factors such as lifestyle, environmental and occupational factors [28, 29] and stroke [30] have been investigated in relation to the disease. However, it has been difficult to link any of these conclusively to ALS [31, 32]. Intense physical activity has been proposed to increase the risk of ALS in soccer [33, 34], as well as players in the National Football League [35]. However, other studies have found no correlation with strenuous physical activity [36-38]. Reasons for these disparities may include heterogeneous study methods or patient classifications, confounding biases, or a lack of well-defined exposure [29].

As in many other diseases, smoking may be associated with higher risk of developing ALS [39, 40]. Although limited evidence is available [41], there appears to be an association between smoking and ALS [37], which increase with the duration of smoking [40]. Nevertheless, family history, male sex and age are the only confirmed factors that increase the risk of ALS [31, 32].

Diagnosis

Early stages of ALS often show a broad clinical presentation shared by several other diseases, which need to be excluded to confirm a diagnosis of ALS. Standard procedures include an investigation of a family history of disease, physical and neurological examinations, as well as electrophysiological examinations and neuroimaging [17, 42, 43]. ALS is a progressive disease and examination should be followed up after six months to establish an advancement of disease manifestations, in order to distinguish ALS from other neurological disorders involving the motor system, such as Kennedy's disease, Myasthenia gravis, or other myopathies [10, 44]. Because there are no biomarkers available to help confirm or exclude a diagnosis of ALS, misdiagnosis is not uncommon [44].

Early stages of ALS often present with intermittent symptoms and the average time between symptom onset and diagnosis is 13-18 months [45]. Delayed diagnosis will postpone opportunities for early treatment and could also hinder enrollment into suitable clinical trials. To aid in this matter the World Federation of Neurology has established El Escorial criteria for ALS diagnosis [46]. This aims to standardize the steps leading to diagnosis and to enhance the sensitivity and specificity of an ALS diagnosis. The criteria have been revised [42] and currently, at least one of the following criteria must be met for a definitive ALS diagnosis [42, 43]:

1) Progressive deficits in at least one limb, or other body region as a result of UMN and LMN degeneration.
2) LMN signs in one region established by clinical examination.
3) Electromyography deficits in two regions.

ALS diagnoses are categorized as 'suspected', 'possible', 'probable' or 'definite' and depend on how the clinical signs fulfill these criteria [42].

Treatment

Riluzole (Rilutek) was developed in the 1950s and was approved for treatment of ALS 1995 in the US and 1996 in Sweden. Until recently it was the only US Food and Drug Administration approved treatment for ALS. Riluzole is well-tolerated [47-49] but results in only a modest increase in survival time [50-53], typically between two to three months [48, 54]. The drug has several potential mechanisms of action including blocking glutamate release [55 56] and glutamate receptors [57] and thereby protecting against excitotoxicity [58]. It is also reported to modulate voltage-dependent Na^+ currents [59] but which mechanism(s) convey the protective effect in ALS is not clear. Early administration is associated with longer survival time [60] compared to more advanced stages [47], further emphasizing a need for early and accurate diagnosis.

The US Food and Drug Administration approved edaravone (Radicava, Mitsubishi Tanabe Pharma America) for the treatment of ALS in 2017. It acts as a free radical scavenger [61] that was initially developed to treat stroke. Phase II clinical trials found no adverse drug reaction but failed to show a significant delay in disease progression [62]. However, *post hoc* analysis revealed a subgroup of patients with a possible delay in disease progression in response to edaravone treatment. Another phase III study was performed with inclusion criteria based on this subpopulation. The trial resulted in a significant delay in disease progression with edaravone compared to placebo but no indications that the treatment would be beneficial for a wider population of patients [63].

General neuropathology

Upon histological examination, spinal cord tissue from ALS patients *post mortem* shows morphological alterations with signs of atrophy and a reduction in the number of MNs. The MNs that remain show swollen and/or disrupted axons and a disorganized cytoskeleton [64 65]. MN loss and subsequent sclerosis of the spinal cord is a hallmark of ALS, and although MNs are affected selectively, other cell types are also involved in disease. Reactive gliosis is commonly reported in the white and grey matters of the spinal cord [66, 67 68, 69] along with activated microglia and an inflammatory response [70-72].

As seen in other neurodegenerative proteinopathies, such as Alzheimer's disease (AD) and Parkinson's disease (PD), protein aggregation has long been associated with ALS [73]. A number of cytoplasmic protein inclusions in motor area cells are linked to ALS. However, these can also be found as a result of normal ageing [74, 75]. The most common ones are presented below.

Ubiquitinylated inclusions

Ubiquitin-positive inclusions represent the majority of inclusions present in MNs of ALS patients [74]. They are identified by immunohistochemistry using anti-ubiquitin antibodies. Inclusions are composed of aggregated proteins, the majority of which has been identified as TAR DNA binding protein (TARDBP) [76, 77]. Ubiquitin-positive inclusions are common in other neurodegenerative diseases as well as ALS [78] and can be divided into

subgroups based on their morphology. Immunohistochemical classification of inclusions is helpful in *post mortem* diagnosis of ALS [79].

Skein-like inclusions
Skein-like inclusions, or skeins, are one of the most common types of ubiquitin-positive inclusion found in ALS. Skeins are composed of thread-like structures that form loose aggregates in MNs [80]. They are present in both Familial ALS (FALS) and sporadic ALS (SALS) but are not specific to ALS [81]. In addition to being ubiquitin-positive, these inclusions also stain positively for p62 [82], TARDBP [76, 77] and SOD1 [83] but not microtubule associated protein tau (MAPT).

Lewy body-like hyaline inclusions
Lewy body-like hyaline inclusions are tightly packed filamentous aggregates located in the cytoplasm of MNs in *TARDBP* FALS patients [84]. The inclusions are also present in *SOD1* FALS patients [85] and SALS [86] where they stain positively for ubiquitin and SOD1 [85-87]. However, Lewy body-like hyaline inclusions do not contain α-synuclein, which separates them from Lewy bodies found in PD [88].

Bränström bodies
These inclusions are small, cytoplasmic and SOD1-positive aggregates found in the brainstem and spinal cord *SOD1* FALS and non-*SOD1* FALS patients [83, 85, 89]. Aggregates are also present in the nuclei of glial cells and stain positively for ubiquitin, but not p62 and TARDBP [90]. These results suggest a general role for SOD1 in ALS pathogenesis, not restricted to *SOD1* FALS.

Hyaline conglomerate inclusions
Hyaline conglomerate inclusions are large inclusions with a glassy appearance following hematoxylin and eosin staining [91]. The inclusions contain both non-phosphorylated and phosphorylated neurofilament heavy proteins (NEFH), which are not present in ubiquitin-positive inclusions [91, 92]. These inclusions are not specific for ALS and are also present in other neurodegenerative diseases and controls [78, 93]

Bunina bodies
Bunina bodies are small inclusions found in the ventral horn of the spinal cord that are generally considered to be specific to ALS. Bunina bodies are best visualized by hematoxylin and eosin staining and contain cystatin C [94] and transferrin [95] but are ubiquitin-negative [96]. Bunina bodies are found in both FALS and SALS [97] and while some studies report no TARDBP-positive inclusions in SALS and non-*SOD1* FALS [98] others suggest a co-localization with early stage inclusions in LMNs [97].

Genetics of ALS
ALS is categorized as either FALS or SALS, where the hereditary cases account for 1-13% but the majorities are sporadic without a known genetic cause [99]. Family history with minimum one affected first-and/or second-degree relative is required for a FALS diagnosis. Due to frequent

misclassification of SALS patients as a result of incomplete disease penetrance or inadequate family history [100], the number of FALS cases is likely to be underestimated.

FALS is most commonly inherited in an autosomal dominant fashion but could also be passed on in an autosomal recessive, or and X-linked manner [101]. Mutations in 36 different genes are known to cause ALS [20] and several other candidates are associated with the disease [101-103]. No common biological function can be described to these genes and none of them are associated exclusively with ALS. However, they can be grouped into functional categories, such as ribonucleic acid (RNA) processing, regulation of angiogenesis, ubiquitination and oxidative stress [101, 104].

TAR DNA binding protein

The TAR DNA binding protein (TARDBP, TDP-43) encodes a nuclear protein that binds to RNA/deoxyribonucleic acid (DNA) and regulates transcription and alternative splicing. ALS associated *TARDBP* mutations [77, 105-108] have been identified in 1-5% of FALS [100, 109] and < 2% of SALS patients [109, 110]. Mutant TARDBP is known to translocate to the cytoplasm where it forms the major component of ubiquitin-positive inclusions [76, 108]. TARDBP is also localized to cytoplasmic stress granule complexes in patients with both ALS and frontotemporal dementia (FTD) [111]. Stress granules form in response to rapid environmental changes, such as oxidative stress, leading to polysome (mRNA and ribosome) disassembly and translational arrest [112]. The formation of aggregates in stress granules is reversible and contains, and thus protects, proteins and RNA that are not required to cope with the stress response [113].

FUS RNA binding protein

FUS RNA binding protein (FUS) is ubiquitously expressed and encodes a nuclear RNA/DNA protein that is structurally and functionally related to TARDBP [114]. FUS regulates transcription and is involved in DNA repair, as well as RNA splicing [115, 116]. The mutant protein is associated with 4% of FALS cases [117, 118] and < 1% of SALS cases [118, 119]. Mutant FUS displays many similarities with mutant TARDBP including cytoplasmic mislocalization and colocalization with stress granules [120-122]. Cytoplasmic inclusions of mutant FUS have also been reported in sporadic FTD patients providing a genetic association between FTD and ALS [123].

Angiogenin

Angiogenin (ANG) encodes an inducer of angiogenesis as a response to hypoxia and is suggested to have neuroprotective functions [124]. Mutations in *ANG* are found to segregate with a small number FALS cases and few SALS cases [125, 126] but also in patients with FTD and Parkinsonism [127]. ANG has functional similarities with vascular endothelial growth factor (VEGF), another angiogenic factor to be linked to ALS pathogenesis [128].

Chromosome 9 open reading frame 72

Non-coding hexanucleotide repeat expansion in *Chromosome 9 open reading frame 72* (*C9ORF72*) [129, 130] has been identified as the most common

genetic cause of ALS and ALS/FTD. A pathological expansion (>25-30 repeats) [131] is found in 40% of FALS and 7% of SALS cases [132]. C9ORF72 has an important function in both intracellular and extracellular vesicle trafficking [133] [134]. There are three hypothesis regarding pathogenicity of C9ORF72 as reviewed by Gitler and colleagues [135].

1. Toxicity is caused by loss of protein function and haploinsufficiency if the expression of the wild type (wt) allele is not enough to maintain normal function [129] [136].
2. RNA toxicity induced by foci containing both sense and antisense transcripts that are thought to sequester important RNA binding proteins found in brain and spinal cord [129], patient fibroblasts [137] and patient derived MNs [138].
3. Proteotoxicity caused by unconventional, non-ATG initiated translation of the repeat expansion that results in dipeptide repeat proteins, which accumulate into insoluble inclusions [139, 140] [141].

TANK-binding kinase-1

Mutations leading to loss of function of TANK-binding kinase-1 (TBK1) was found to cause ALS and ALS/FTD in 0.4-4% of all patients [142, 143]. A French cohort study disclosed even higher frequencies in ALS/FTD (10.8%) compared to isolated ALS [144]. TBK1 is involved in multiple cellular processes [145], including the immune response, where it induces the production of type 1 interferon in response to viral infections or DNA damage [146]. Its' role in degradation of aggregated proteins [145] is perhaps the most significant from an ALS perspective. TBK1 is involved in formation of autophagosomes [147]. Autophagosomes are a double membrane vesicle that engulfs aggregated proteins, which are degraded by lysosomal hydrolases when the autophagosome fuse with lysosomes. The C-terminal part of TBK1 mediates interaction with adaptor proteins such as Optineurin and p62, leading to the degradation of pathogens and aggregated proteins via autophagy [142]. Both Optineurin [148] and p62 [149] are candidate genes associated with ALS and the identification of TBK-1 further links them to disease as well as it highlights the importance of autophagy in ALS pathogenesis.

Superoxide dismutase

Reactive oxygen species

Reactive oxygen species (ROS) are highly reactive metabolites of oxygen (O_2) including, e.g. the superoxide free radial ($O_2^{\cdot-}$), hydrogen peroxide (H_2O_2) and the nitric oxide radical ($NO\cdot$), which are formed as a byproduct of aerobic energy production [150]. Although not very reactive themselves, these metabolites can undergo further reactions such as between $O_2^{\cdot-}$ and nitric oxide, resulting in peroxynitrite (ONOO-), or H_2O_2 decomposure to the hydroxyl radical ($OH^{\cdot-}$). These products are highly reactive oxidative agents that are capable of damaging proteins, membranes and nucleic acids etc. [151]. This process is termed oxidative stress and is a result of an imbalance

between the production of ROS and removal/repair of toxic species [152-154]. Glutathione is one of the main redox buffers in cells, which exists in either a reduced (GSH) or an oxidized form (GSSG) [155]. Removal of H_2O_2 is catalyzed by glutathione peroxidase, which couples the reduction of H_2O_2 to the oxidation of GSH to GSSG. GSSG is then reduced to by glutathione reductase to maintain the high levels of GSH/GSSH within cells. The ratio of GSH/GSSG can be used as an indicator of oxidative stress [155].

Superoxide dismutase (SOD) enzymes are a class of ancient antioxidants present in bacteria, fungi, plants and animal cells that act as the main defense system against $O_2^{\cdot -}$ [152]. Humans have three different SOD isoenzymes; the intracellular copper zinc SOD (CuZn SOD or SOD1) and manganese SOD (Mn SOD or SOD2) and the extracellular SOD (EC SOD or SOD3). The dismutase activity of SODs refers to reactions where metal ions in the different isoforms undergo alternate reduction and oxidation in separate reactions resulting in dismutation (or partitioning) of $O_2^{\cdot -}$ to H_2O_2 and O_2 as the net result. SOD1 and SOD3 catalyze the reaction via $Cu^{+/2+}$ whereas SOD2 uses $Mn^{2+/3+}$ [156].

SOD1

SOD1 was first described in 1938 when Mann and colleagues isolated a copper-binding protein from bovine erythrocytes and named it haemocuprein [157]. A related protein was later identified in human erythrocytes and called erythrocuprein [158]. However, no apparent enzymatic activity was detected [159]. A decade later, McCord and Fridovich isolated a bovine erythrocyte protein that acted as a catalyst for the dismutation of $O_2^{\cdot -}$ to H_2O_2 and O_2. The protein was identified as bovine haemocuprein and the enzymatic activity was found to be copper-dependent [160]. The protein was renamed to SOD and is now known as SOD1. Partitioning of $O_2^{\cdot -}$ to H_2O_2 with SOD1 as a catalyst is shown below:

1) SOD1-Cu^{2+} + $O_2^{\cdot -}$ → SOD1-Cu^{+} + O_2 (reduction of Cu^{2+} and oxidation of $O_2^{\cdot -}$)
2) SOD1-Cu^{+} + $O_2^{\cdot -}$ + $2H^{+}$ → SOD1-Cu^{2+} + H_2O_2 (oxidation of Cu^{2+} and reduction of $O_2^{\cdot -}$)

With the net reaction:
$O_2^{\cdot -} + O_2^{\cdot -} + 2H^{+} \rightarrow O_2 + H_2O_2$

SOD2

The SOD2 protein is localized to the mitochondrial matrix where it exerts its' dismutase activity [161-163]. Hence, SOD2 is the first line of defense against $O_2^{\cdot -}$ produced during oxidative phosphorylation. SOD2 is a tetramer [164] and can be distinguished from SOD1 by its insensitivity to cyanide. Knockout of SOD2 in mice is embryonic lethal [165], emphasizing the importance of superoxide metabolism in mitochondria.

SOD3

SOD3 has been identified in a wide range of tissues [166 {Marklund, 1984 #734]. It is structurally similar to SOD1 and uses the same metal cofactor (copper), but in contrast to SOD1, it is located extracellularly [167, 168]. Thus, SOD3 contains a

signal peptide that targets it for secretion via the endoplasmatic reticulum (ER)-trans Golgi pathway, where it acquires copper [169, 170].

SOD1

Structure

An overview of the amino acid sequence of SOD1 and important structural features are presented in Figure 2.

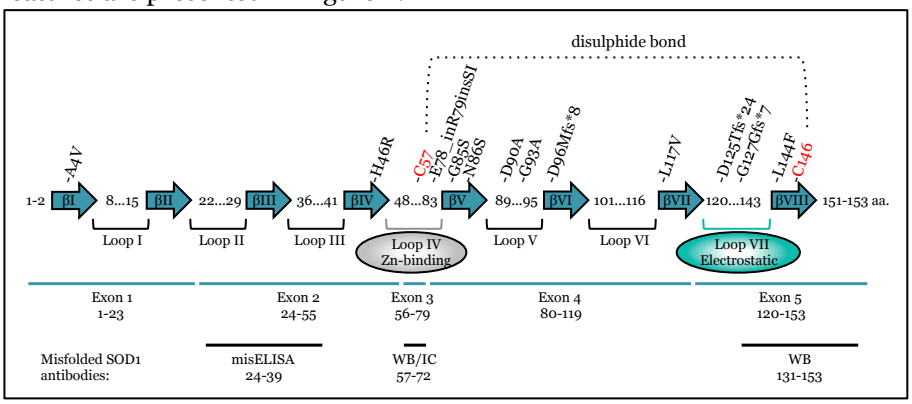

Figure 2: Overview of the SOD1 sequence. Diagram showing the position of structural motifs as well as mutations analysed in this study and sequences used to raise antibodies. Positions of exons 1-5 and as well as missense and SOD1 truncation mutations are indicated. β-strands shown as arrows connected by loops of which Zn-binding loop is coloured in grey and electrostatic loop is coloured in turquoise. The disulfide bond connecting C57 and C146 is depicted by a dotted line. Primary antibodies against misfolded SOD1 sequence 24-39, 57-72 and 131-153 (black lines) used for misfolded SOD1 ELISA (misELISA) and immunocapture (IC) as well as western blotting (WB).

The amino acid sequence of SOD1 was determined in 1980 [171] and the 3D structure (Figure 3) was solved in 1992 [172]. SOD1 is a 32-kDa homodimer where each monomer consists of 153 amino acids [171, 173]. Each monomer carries a copper ion and a zinc ion, which are important for enzymatic function and stability, respectively [174].

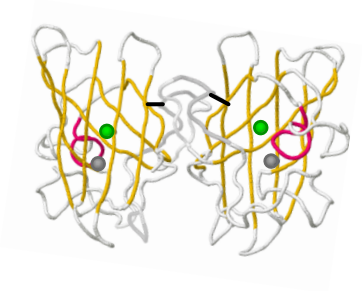

Figure 3: 3D-trace presentation of dimeric human SOD1 structure with metals and oxidized disulfide bonds. Human SOD1 protein modelled in RCSB protein data bank (PDB code 1HL5 [3]) with key structures coloured as; β-strands in yellow, α-helix in pink and C57-C146 disulphide bond in black. Cu-ion is shown in green and Zn-ion in grey.

Another feature of the protein that is important for structural stability is an intrasubunit disulphide bond positioned between C57-C146 [175, 176]. The individual monomers are formed by a β-barrel made up by eight antiparallel β-strands connected by seven loops (I-VII). The metal binding loop IV between βI and βV (residues 49-84) has major contribution to the protein stability as it harbors both the zinc active site, C57-site of the disulphide bond and the dimer interface [172, 177]. The electrostatic loop VII positioned between βVII and βVIII (residues 121-141) functions as a protective lid that covers the metal binding sites [177]. Together with the metal binding loop, the electrostatic loop forms a channel [3] through which the negatively charged superoxide is guided to the active site [178].

Stability

The fully mature, homodimeric SOD1 protein (holo-SOD1) is extremely stable with a melting point of 92°C [179]. The protein also retains its enzymatic activity in the presence of strong denaturants, such as 10 M urea or 4% (w/v) sodium dodecyl sulfate [174]. The thermochemical stability of native SOD1 is a result of several posttranslational modifications, all of which are essential for SOD1 maturation [180, 181]. The process of maturation can be divided into four steps, metal loading of zinc and copper, formation of disulphide bond and dimerization [180, 182], where metallation is most important for SOD1 stability [182]. The process of maturation is described below and summarized in Figure 4.

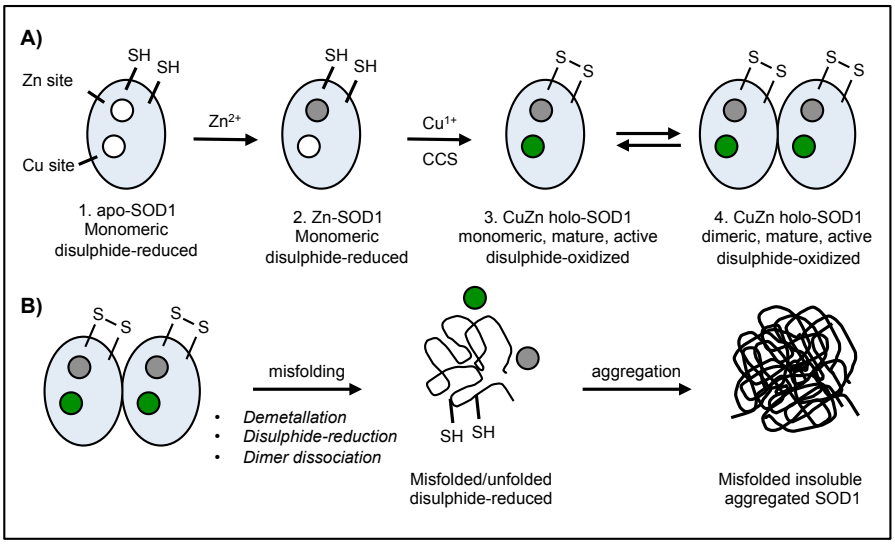

Figure 4: SOD1 maturation. A) Maturation of apo-SOD1 (1) by the acquisition of a Zn ion (2), Cu ion delivery and disulphide bond formation by CCS (3) followed by dimerization of metallated and oxidized holo-SOD1 (4). **B)** Misfolding and aggregation of disulphide-reduced SOD1.

1: *Acquisition of Zn^{2+}*
Zinc binding is necessary for stabilizing the native SOD1 structure but the mechanism of Zn^{2+} insertion is not understood [181, 183]. However, Zn^{2+}-loading is required for the subsequent insertion of copper [184].

2: *Acquisition of Cu^{1+}*
Once Zn^{2+} is bound, the SOD1 monomer forms a dimer with copper-chaperone for SOD (CCS), which transfers Cu^{+} to SOD1 [184-188]. CCS is structurally related to SOD1 and is also ubiquitously expressed [185] but with a 12-30-fold lower level of expression [189].

3: *Formation of stabilizing intrasubunit disulphide bond*
Following Cu-insertion, the intermolecular disulphide bond between CCS and SOD1 is transferred to an intrasubunit disulphide bond in the SOD1 monomer before the CCS-SOD1 complex is dissolved [175, 176]. The disulphide bond is formed through oxidation of thiol groups in C57 and C146 [175].

4: *Dimerization:*
In the final step of maturation, inactive, fully metallated and mature SOD1 monomers dimerize and form the active SOD1 protein. It is not known whether dimerization occurs spontaneously or by the means of other factors [180, 182]. Holo-SOD1 is extremely stable, however, reduced apo-SOD1 (lacking the disulphide bond and metals) is on the other hand very unstable [190].

The CCS-dependent activation described above requires O_2 [175, 191]. Before the discovery that *CCS* knockout mice retain some SOD1 activity [192], CCS was thought to be essential for SOD1 activation. However, SOD1 can be activated independently of CCS and O_2, although not to the same extent as CCS dependent activation [193].

Mutation in the *SOD1* gene can affect the folding properties of the protein [194, 195] and FALS-associated SOD1 mutant proteins are more susceptible to disulphide reduction, which can lead to misfolding [194, 196, 197]. Reduction of the stabilizing intrasubunit bond promotes misfolded SOD1 aggregation *in vitro* [198-200] and *in vivo* [201] where also soluble misfolded SOD1 is disulphide-reduced SOD1 in transgenic models [202, 203]. This suggests that the C57-146 disulphide bond represents an 'Achilles heel' of the otherwise stable SOD1 protein [204].

SOD1 mutations
Mutations in the *SOD1* gene were the first genetic link to FALS [205]. Approximately 206 ALS-associated *SOD1* mutations have been reported (http://alsod.iop.kcl.ac.uk/ and Peter Andersen, personal communication; August, 2017), which are spread over the entire primary protein sequence [206]. Not all *SOD1* mutations are pathogenic [207] but mutations have been found in 2-6% of all ALS patients and about 20-25 % of all FALS cases [208, 209]. The majority of mutations are missense, resulting in an exchange of amino acids, whereas others are nonsense and alter the length of the protein by introducing a premature stop codon. Frameshift mutations caused by deletions or insertions have also been identified, which change the protein sequence or lead to the formation of truncated proteins [101].

ALS-associated mutations in *SOD1* often reduce the stability of the protein [197] and make it more prone to misfold [210]. Mutations that severely destabilize the protein are associated with a shorter survival [210]. Mutations that result in a truncation lacking the C-terminal part of the protein, e.g. G127X [211] and D125Tfs*24, lack C146 and are unable to form the C57-146 disulphide bond. Such truncated proteins cannot adapt to a native conformation and are thus completely unfolded. These highly unstable proteins are quickly degraded *in vitro* [212].

Soluble disulphide-reduced SOD1 monomers are found in several transgenic mouse models expressing mutant human *SOD1* [202]. This type of unfolded monomeric SOD1 is prone to aggregation [199, 200, 213]. Therefore, disulphide-reduced and demetallated SOD1 has been proposed to be central to *SOD1* FALS pathogenesis [176, 196, 199, 214, 215].

The majority of *SOD1* mutations result in reduced protein activity in erythrocytes [211]. However, there are mutations that have little or no effect on the stability or activity *in vitro* [216, 217] in patient erythrocytes [218-220] or in CNS tissue [221]. Stable, wt-like mutant proteins include, e.g. D90A [218] and L117V [220] and often present with limb-onset, slower disease progression and reduced disease penetrance. Consequently, the stability of mutant SOD1 can be in the range of wt SOD1 and levels of soluble misfolded SOD1 are undistinguishable between wt and stable SOD1 mutants [220]. Hence, only minor changes in SOD1 are necessary to induce protein misfolding and very small amounts of misfolded protein are sufficient to cause ALS in mice [222]. Together these results suggest a role of wt SOD1 in ALS, which will be discussed in section 'SOD1 and ALS –wt SOD1 in ALS'.

Models of SOD1 ALS

Transgenic mouse models

Genetically modified mice enable the contribution of human genes and mutations to disease processes to be studied in a rodent model. ALS pathology in mice bears a strong resemblance to ALS in humans, making it a useful model system [223]. Transgenic mice overexpressing human mutant *SOD1* develop SOD1 aggregates within the spinal cord [224] similar to those present in the spinal cord of ALS patients [83] and have been a valuable tool to study SOD1 toxicity [225].

A transgenic model expressing human *SOD1* G93A was generated soon after the discovery of *SOD1* mutations as a cause of ALS [217]. Mice expressing the highest levels of SOD1, with around 18 copies of the transgene, showed signs of hind limb weakness around 3-4 months of age and were paralyzed in one or more limbs before 6 months of age. Analysis of the spinal cord from these mice revealed a loss of MNs and remaining ones staining positively for SOD1 and neurofibrillary material [217]. Subsequently, a G93A mouse model expressing 10 copies of the transgene was established [226]. These mice developed an ALS-like disease with MN loss, astrocytosis and Lewy body-like inclusions and were considered to more accurately reflect the pathological findings in humans [226]. Although the G93A mouse model is one of the most commonly used, mice expressing other *SOD1* mutations have

been developed [225] including G37R [216], G85R [224], G127X [222], D90A [227] as well as models expressing human wt SOD1 [228].

A high level of SOD1 overexpression is typically required to cause disease, for example in the G37R model where mutant SOD1 expression is increased between 5-12–fold (range of four different lines) compared to the endogenous murine SOD1 [216]. On the other hand, the G85R model expresses mutant human SOD1 at level of 0.2-1-fold compared to the endogenous murine SOD1 in eight different lines and develop a rapidly progressive disease at 8 months of age [224]. In young mice, the levels of endogenous murine and human G85R SOD1 are similar. However, at end stage of disease, human G85R levels increase 2-fold suggesting a reduced degradation of mutant protein with age [224].

The D90A mutation is inherited in a recessive fashion [218] and mice expressing human *SOD1* D90A develop symptoms that bear a close resemblance to the human disease [227]. Heterozygous mice remain unaffected even in old age (800 days). However, homozygous D90A mice develop symptoms around 350 days of age [227]. Furthermore, D90A homozygous mice also develop bladder involvement, a function that is usually spared in ALS, but is common in *SOD1* D90A patients [229].

Early attempts to develop a mouse model overexpressing human wt SOD1 did not result in a motor neuron phenotype by 18 months of age [216]. However, mice showed mild pathological changes in muscle innervation that was indicative of premature ageing [217]. Further investigation of the same model identified pathogenic alterations in MNs including mitochondrial swelling, axon degeneration and mild motor symptoms [230]. By overexpressing human wt SOD1 to the same level as the first G93A model with high overexpression (18 copies of the transgene), an ALS-like disease resulted in mice becoming terminally ill at approximately 370 days of age [231]. Both spinal cord and brain from human wt SOD1 mice stain positively for aggregated SOD1 and the degree of MN loss is similar to that found in mice expressing mutant human SOD1 [231], demonstrating that wt SOD1 has the capacity to cause ALS in mice.

In summary, a number of transgenic models of ALS have been established that recreate important aspects of the disease including axonal degeneration and vacuolization, SOD1 positive inclusions and loss of neurons in the spinal cord [216, 217, 224]. Of these, the G93A model is used most widely. However, when used to test potential treatments for ALS, the vast majority of compounds have failed to show efficacy in this model [232]. The drugs tested include anti-glutamatergic compound such as ceftriaxone [233], anti oxidative compounds like creatine [234, 235] and neurotrophic factors [236], among others. A possible explanation could lie in the reliance of G93A model for preclinical testing since overexpression of mutant SOD1 is not seen in ALS patients. Furthermore, the majority of ALS patients have SALS, with no known genetic cause [232, 237].

In vitro model systems

In vitro cell culture models offer several advantages compared to *in vivo* models. Cultures are relatively easy and rapid to work with compared with animals. They enable the analysis of ALS-related events with cellular and

subcellular resolution, in live cells. *In vitro* models also facilitate the analysis of specific interventions, such as controlled exposure to pharmacological treatments over time when screening for therapeutic agents. A further advantage is that cell types can be isolated and co-cultured, which enables interaction between mutant and wt cells to be investigated as well as cell autonomous and non cell-autonomous aspects of disease. Using cell models it is also possible to study cells derived from patients, including the individuals' genetic background, or introducing mutations in the same genetic background to study the effect of two or more genes on the disease process.

Embryonic day 12-14 mouse spinal cord cultures

MNs are normally isolated from the ventral horn of the murine spinal cord with high purity at embryonic day (E) 12.5-13.5, when the expression of the MN marker ISL LIM homeobox 1/2 (ISL1/2) is at its highest [238, 239]. However, an even greater yield is achieved with isolation at E14.5, possible due to larger cells allowing for better separation from other cell types [240]. From the same material, it is also possible to culture isolated astrocytes and microglia [240, 241]. Cell types can be cultured separately, but the greatest survival of MNs (up to 7 weeks) is seen when neuronal and glial cells are cultured together [242]. MN cultures are typically grown on culture vessels coated with laminin and a synthetic polypeptide such as poly-L-ornithine, which gives the substrate a positive net charge and facilitates cell adhesion [243-245].

Once isolated *in vitro*, MNs can be purified by fluorescence-activated cell sorting (FACS). FACS is a useful method to enrich for a specific cell type if a suitable antibody to a cell surface marker is available [246, 247], or if the desired cell population is fluorescently labeled, e.g. with green fluorescent protein (GFP) [248] [246, 247]. To increase survival, purified cultures require supplementation with trophic factors that are normally provided by glia cells *in vitro* and *in vivo* [243, 246, 249]. Purified MNs can also be cultured on a feeder-layer of primary astrocytes that, in addition to supplying trophic factors, also provide suitable growth substrate for MNs. This increase the time MNs can be maintained in culture and enable MNs to be studied at more mature stages [246, 249, 250]. Moreover, supplements of different neurotrophic factors to embryonic cultures further supports the survival of specific subtypes of MNs. One example is an addition of hepatocyte growth factor promoting the survival of limb innervating MNs [251]. A disadvantage of *in vitro* culture methods is the need for timed matings in mice and a relatively low yield of post-mitotic MNs.

NSC-34 cells

Mature neurons are post-mitotic and cannot be expanded in culture. To create an immortalized cell line with characteristics of MNs, mouse embryonic spinal MNs were fused with a mouse neuroblastoma cell line to create the hybrid cell line NSC-34 [252]. This line has been widely used as a cell model to study ALS as the cells possess neuron-like properties with a multipolar phenotype, generate action potentials and are positive for MN-specific markers including choline acetyltransferase (CHAT) and

neurofilament proteins [252]. Differentiation of NCS-34 by serum deprivation and an addition of retinoic acid (RA) induce higher expression of CHAT, as well as expression of motor neuron and pancreas homeobox 1, MNX1 (HB9) and Isl1/2 [253].

Upon exposure to SALS-derived cerebrospinal fluid (CSF), NSC-34 cells showed reduced survival and developed ubiquitin-positive inclusions of neurofilament proteins [254] and ER-stress [255]. NCS-34 neurons have also been shown to respond to neurotoxic chemicals in a similar way to mouse primary MN cultures [256]. However, they are less suited to study the effects of excitotoxicity due to the lack of a response of calcium influx following glutamate exposure [257].

Embryonic stem cells

Embryonic stem cells (ESCs) can be established from the inner cell mass of the blastocyst of fertilized eggs in mice (mESC) [258] or humans (hESC) [259]. Most hESCs used for research comes from frozen fertilized eggs that are produced *in vitro* in fertility clinics and subsequently donated and used for research purposes [260].

As pluripotent cells, ESCs can be differentiated to any cell type present in the body, including neurons and glial cells [258, 261]. Typically, ESCs are differentiated as three-dimensional aggregates known as embryoid bodies (EBs). Through spontaneous differentiation, EBs can differentiate and express markers of all three germ layers (endoderm, mesoderm and ectoderm) [262] and by directed differentiation through addition of specific factors they can be guided to develop into a desired cells type, such as MNs [248]. EBs are formed when culturing partly dissociated ESCs on a non-adherent substrate [261]. Neural induction, and a forebrain identity, of ectodermal cells is achieved by blocking bone morphogenic protein (BMP) signaling, which otherwise would lead to an epidermal fate [263, 264]. Neurons can be instructed to adopt a spinal cord identity by providing a caudalizing signal from RA [265]. Specification towards MN progenitors is achieved by activating the ventralizing signals of the sonic hedgehog (SHH) signaling pathway. SHH signaling is also required for the final specification of MNs [266, 267]. Using established protocols for MN differentiation [248], both mouse [268] and human ESC-derived MNs have been established. The possibility to expand and differentiate ESC cultures *in vitro* has been of great value for studying neurodegenerative. For example in ALS where hESC-derived MNs have been shown to display pathological changes with reduced survival and presence of SOD1 inclusions upon co-culture with murine *SOD1* mutant glial cells [269].

Human post mortem-derived neural precursor cells

Routine isolation of neural tissue from patients with ALS is not possible. However, patient-derived neural precursor cells can be isolated and propagated from tissues *post mortem*. Brain and spinal cord biopsies have been isolated from donors of various ages up to 20 h *post mortem* [270]. Neural precursor cells can be amplified and differentiated into neurons, astrocytes and oligodendrocytes [271]. This type of model enables studies of both SALS and FALS and together with mouse ESC-derived MNs, neural precursor-

derived cells have aided in the characterization of mechanisms of non-cell autonomous toxicity of patient-derived astrocytes towards MNs [271]. Nevertheless, the availability of *post mortem* tissue is limited, and the material is only usually available at the end stage of disease.

Induced pluripotent stem cell-derived cultures
The work in this thesis is based on the use of induced pluripotent stem cells (iPSCs) and cells derived from them as a model system to study misfolded SOD1 in ALS. The iPSC model will be discussed in further detail in Section 'Induced pluripotent stem cells'.

SOD1 and ALS

Mutant SOD1 toxicity

When mutations in *SOD1* were identified as a cause of ALS, a loss of enzymatic function was thought to be the underlying cause of disease. However, a number of lines of evidence have shown that this is not the case. Most *SOD1* mutations result in a protein with reduced enzymatic activity [211, 272, 273]. However, several ALS-associated *SOD1* mutations, e.g. D90A [218], G73R, [274] or L117V [220], result in SOD1 proteins with normal, or close to normal, enzymatic activities. *SOD1* FALS is usually inherited in a dominant fashion [101, 275], meaning that carriers of mutations retain around 50% SOD1 activity from the wt allele, which should be sufficient to exert its' function. Moreover, deletion of *SOD1* in mice results in MN vulnerability upon axonal injury but does not lead to an ALS-like disease *per se* [276]. Overexpression of several forms of human mutant [217, 224] or wt *SOD1* cause ALS in mice [231]. Hence, ALS is believed to be a result of a toxic gain of function and not a result of a lost enzymatic activity.

Wt SOD1 in ALS

SOD1 mutations have been identified in about 2-6% of all ALS patients [277] but the majority of ALS cases are sporadic. Wt forms of disease-associated proteins have been shown to be involved in in PD as well as AD [278] and several findings suggestes that this is also the case for ALS.

Disease-associated mutations are spread over the whole SOD1 sequence [206] and not only found in functionally or structurally important residues (see Figure 2). This suggests that even small structural changes can cause disease. Certain *SOD1* mutations, known to cause ALS, generate proteins with the same characteristics at wt SOD1, including stability, activity and folding pattern [220, 227]. Exposure of wt SOD1 to oxidizing reagents can induce protein misfolding and aggregation *in vitro* [215] and these aggregates are as toxic to MNs in culture as those formed from mutant SOD1 [279]. Overexpression of wt *SOD1* also results in ALS-like disease in mice [231]. Further involvement of wt *SOD1* in ALS is evident by the presence of misfolded wt SOD1 in *post mortem* samples from SALS patients [280-282]. Together, these data support a role for wt SOD1 in ALS pathogenesis and points towards a possible common pathogenic mechanism of SOD1 toxicity in FALS and SALS.

Mechanisms of SOD1 toxicity

Several mechanisms of SOD1-mediated toxicity have been proposed, many related to the misfolding propensity of SOD1. Among these are disturbances in protein degradation, ER-stress, excitotoxicity, excitability and mitochondrial dysfunction, which are discussed below.

Disturbances in protein degradation

Chaperones have an important function in protein quality control and are required to maintain proper protein folding [283]. Before degradation is initiated, attempts to disaggregate and refold proteins may be initiated, mainly by a bi-chaperone system consisting of heat shock protein (HSP) 70 and HSP100 [284, 285]. HSP70 binds to aggregated proteins and recruits HSP100 and through an ATP-dependent activity, aggregates are dissolved and unfolded proteins can then refold, either by themselves or with the help of additional chaperones [283, 284].

In cases where refolding fails, or protein damage is too severe, misfolded and/or aggregated proteins are cleared through two main processes; the ubiquitin-proteasome system (UPS) or autophagy; the latter mediated through chaperones, or by macroautophagy [286, 287]. In chaperone-mediated autophagy, the protein intended for degradation is recognized and bound by heat shock cognate 70 (HSC70), and transported to the lysosome where it is degraded [283, 287]. In macroautophagy, on the other hand, proteins are enclosed by a double-membrane vesicle term the autophagosome. This then fuses with the lysosome to form the autolysosome, where proteins are degraded. In addition to soluble protein, studies have also shown that the UPS, together with ubiquilin 2 (UBQLN2) and the chaperones HSP70 and HSP110 can clear aggregated proteins [288].

Failure to clear misfolded and aggregated protein is associated with several neurodegenerative diseases, including AD and PD and Huntington's disease, as well as ALS [74, 75, 278, 289]. If not degraded, misfolded proteins can aggregate and form larger macromolecular assemblies of various sizes. Aggregates can be amorphous or have an ordered, amyloid-like structure referred to as oligomers, protofilaments and filaments/fibers [75]. Aggregates are partly resistant to degradation, and their accumulation is especially harmful to neurons [286] as they are post mitotic cells and unable to 'dilute' misfolded or aggregated proteins by cell division. Moreover, the large size and complex morphology of neurons make them highly dependent on functional intracellular transport processes for the efficient degradation of misfolded and/or aggregated proteins [290].

Ubiquitin-proteasome system

The UPS is the main pathway for clearance of soluble misfolded proteins, including misfolded SOD1 (Figure 5A-B) [291]. The UPS involves the combined actions of two consecutive steps; ubiquitinylation and proteasomal degradation [292]. In the first step, proteins are tagged with a poly-ubiquitin chain through the sequential activity of three classes of enzymes (E1-3),

which activate, conjugate and ligate ubiquitin to the protein substrate [293]. These actions mark proteins for degradation by the proteasome [292]. Ubiquitinylated proteins are degraded by the barrel-shaped 26S proteasome in an ATP dependent manner. The 26S proteasome is composed of two 19S caps arranged on either end of the 20S catalytic subunit. The 19S caps, also referred to as the regulatory subunit, recognize the polyubiquitin tag, unfolds the protein and also removes the ubiquitin chain [294-296]. 19S is also responsible for opening up the gated channel of the 20S subunit so that the polypeptide can enter the barrel containing the catalytic sites and thus regulates the degradative activity [297].

The 20S core proteasome contains the constitutively expressed β1 (caspase-like protease), β2 (trypsin-like protease) and β5 (chymotrypsin-like protease) subunits, which are responsible for peptide cleavage (Figure 5C) [286]. The 20S subunit can degrade proteins in an ubiquitin- and ATP-dependent manner as part of the 26S proteasome. However, the 20S subunit alone is also capable of degrading unfolded or disordered proteins in an ubiquitin-and ATP-independent manner [298-301]. This is the case for alpha synuclein [302] and tau [303, 304]. Levels of free 20S proteasomes can be increased by dissociation of 26S proteasomes when there is a need for enhanced protein degradation, e.g. during oxidative stress [305, 306] and also during mitochondrial dysfunction in neurons [307]. In the absence of 19S, other activators can stimulate the 20S proteasome including e.g. PA28, also referred to as the 11S complex, and PA200 [308], which together with 20S are upregulated during oxidative stress [298]. The activity/specificity of the 20S proteasome can also be elevated by variation of the subunit composition in response to oxidative stress [309, 310]. The most common substitution is the replacement of the β1, β2 and β5 subunits with their interferon gamma-inducible variants; β1i, β2i and β5i, forming the 20S immunoproteasome, also known as i20S [298 311].

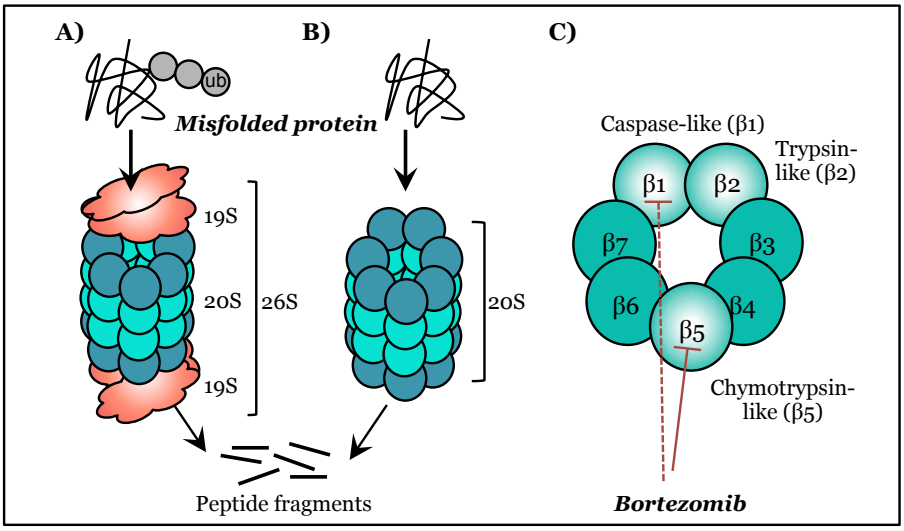

Figure 5: Proteasomal degradation of misfolded protein substrates. (A) Ubiquitin-dependent 26S degradation (A; 19S regulatory cap + 20S core) and ubiquitin-independent 20S degradation **(B)**. The β1, β2 and β5 subunits are located in catalytic core of 20S and. Bortezomib mainly inhibit the chymotrypsin-like β5-site but also caspase-like β1-site.

Misfolded SOD1 is mainly degraded by the chymotrypsin-like and caspase-like protease activities [212, 291, 312]. Inhibition of proteasome activity leads to an increase in misfolded SOD1 and formation of SOD1 aggregates *in vitro* [212, 313, 314]. A misfolded SOD1-related reduction of the constitutively active subunits has been identified in the Neuro2a cell model expressing mutant *SOD1* [314]. Reduction was also evident in G93A mouse spinal cord at early [315, 316], as well as symptomatic [317, 318] stages. Along with decreased activity of the constitutive subunits, G93A mice also displayed a pre-symptomatic increase of the i20S. This increase was induced by elevated cytokines from reactive astrocytes and microglia [317, 318]. Reduced proteasome activity is also seen in SALS patient spinal cord homogenates [319].

Expression β1, β2 and β5 in spinal cord are known to decrease with age [320]. As previously mentioned, age is a major risk factor for ALS, perhaps be due to the accumulation of misfolded and aggregated proteins [320-322]. Continuous degradation of misfolded proteins has been suggested to overwhelm the UPS, resulting not only in an accumulation of aberrant proteins but also in a failure to maintain normal protein homeostasis [313]. However, the identified reduction of proteasome activity is a relatively late event in ALS, and accompanied by induction of i20 activity and possibly also other mechanisms of degradation [317] such as autophagy [323] making the role of UPS dysfunction in ALS unclear. Although the UPS is involved in the pathogenesis of several protein diseases, its' function is preserved in polyglutamine diseases such as Huntington's disease. Hence, there is no support for an overall proteasome impairment underlying proteinopathies, but evidence does exist for an ability to, at least initially, compensate for reduced or inadequate function [324].

Autophagy

Protein aggregates and other macromolecular structures that are too large to be handled by the UPS are degraded by autophagy. Autophagy has an important role in maintaining normal proteostasis [325] and can be induced by starvation when amino acids are needed for new protein synthesis [287, 326].

The first step of the process involves the formation of a double-membrane vesicle, termed the autophagosome, involving microtubule-associated protein 1 light chain 3 (LC3) and p62 [327]. LC3-I is a soluble cytosolic form of the protein involved in elongation and maturation of the autophagosome. Upon binding to the membrane of the vesicle, LC3-I is processed to LC3-II by a set of enzymes, similar to the E1-3 activation and elongation of ubiquitin in UPS [328]. The p62 protein recognizes and binds to aggregated, ubiquitinylated proteins and helps to mediate their degradation [287, 329, 330]. P62 and its bound protein substrate are incorporated with the autophagosome by binding to LC3 [331, 332]. The autophagosome and its enclosed proteins then fuse with the lysosome, where its' contents are degraded by lysosomal hydrolases [287, 328, 333]. Degradation of p62 and conversion of LC3-I to LC3-II can thus be used as markers of autophagy and autophagic flux.

Studies *in vitro* have shown that both wt and mutant SOD1 aggregates are degraded by autophagy [334]. An elevation of markers of autophagosome formation, including LC3-II and p62, is seen in *SOD1* G93A mice [335, 336]. This has also been found in MNs from SALS patient [337] but it has not been determined if the increase is due to an induction of autophagy or an inhibition of autophagic flux. An increase in p62, but not LC3-II, levels in *SOD1* FALS patients indicates that reduced autophagic flux, or a possible dysfunction in autophagy, occurs in *SOD1* ALS [338].

As with the proteasome [320], autophagic activity also declines with age [335, 339]. The importance of removal of aggregated proteins by autophagy was shown by heterozygous deletion of the autophagy regulator protein beclin1 in G127X mice, resulting in an accumulation of SOD1 aggregates, loss of MNs and reduced survival [338]. An inverse relationship was observed between soluble and aggregated SOD1, where the soluble protein decreased upon the initiation of aggregation [338].

Endoplasmatic reticulum stress

Within the ER, newly synthesized proteins are folded with the help of chaperones. Accumulation of misfolded proteins in the ER induces a stress response termed the unfolded protein response (UPR) [340]. ER-stress and UPR-activation are features of ALS, as well as several other neurodegenerative diseases [341]. ER-stress and UPR induce three main sensors, which produce transcription factors that activate pathways resulting in increased protein folding capacity [342]. Two of these are activating transcriptions factor 6 (ATF6) [343] and inositol-requiring enzyme 1 (IRE1), the latter mediating splicing and activation of the transcription factor x-box binding protein 1 (XBP1) mRNA [344](Cox 1993). This first branch leads to upregulation of proteins that assist in protein folding, including a production of ER-directed chaperones, such as ER chaperone glucose-regulated protein 78 (Grp78) and protein disulphide isomerase [345]. Activation of the third

sensor, protein kinase RNA-like endoplasmic reticulum kinase (PERK) [342], results in phosphorylation and thereby inactivation of translation initiation factor 2 alpha (eIF2α), causing a reduction in protein translation and, ultimately, cell cycle arrest [346].

The ER also has a protein quality control system termed endoplasmic-reticulum-associated protein degradation (ERAD). This consists of chaperones and ubiquitin-associated enzymes that detect and modify proteins for retro-translocation to the cytoplasm, where misfolded proteins can be degraded by the proteasome [347, 348]. One of the proteins that 'dislocate' misfolded proteins to the cytoplasm in ERAD is derlin 1 (DERL1) [349].

Overexpression of mutant SOD1 *in vitro* leads to ER-stress and activation of the UPR [350]. UPR activation is also seen in the spinal cord of symptomatic and end stage mice expressing *SOD1* G93A, H46R or L84V [350-354]. The UPR is especially prominent in vulnerable fast fatigable (FF)-MNs compared to MNs that are more resistant to the disease, including fast fatigue resistant (FR) and slow (S) fatigue resistant MNs [355]. Analysis of pre-symptomatic G93A mice suggests that ER-stress is an early event in ALS pathogenesis [353, 355]. Expression of mutant G93A in NSC-34 and human embryonic kidney cells lead to PERK and IRE-1 activation. Moreover, by binding to DERL1, misfolded SOD1 also inhibits ERAD, which leads to reduced survival of MNs *in vitro* [356].

ER-stress and increased an UPR is also present in patient-derived *SOD1* A4V MNs *in vitro* and increases with maturation [357]. In SALS patient material, UPR activation is evident by increased expression of ATF6, IRE1 and PERK at the end stage of the disease [353]. Hence, ER-stress is an early pathological event in ALS and increase throughout disease, but whether it is a cause or consequence of the disease is not understood.

Glutamate excitotoxicity

Glutamate is the main excitatory neurotransmitter and is released from vesicles in presynaptic neurons in a Ca^{2+}-dependent manner [358]. Extracellular glutamate binds to neuronal N-methyl-D-aspartate (NMDA) receptors or α-amino-3-hydroxy-5-methyl-4-isoxazolepropionic acid (AMPA) receptors and induces Ca^{2+} influx, for example in MNs [359, 360]. A failure to clear glutamate rapidly from the extracellular space may lead to excitotoxicity due to overstimulation of neurons and Ca^{2+} -dependent damage and degeneration [360-364].

Elevated extracellular glutamate can result from increased glutamate release from presynaptic neurons, or reduced uptake from the synaptic cleft [365]. Excitatory amino acid transporter (EAAT) 1 and 2 bind glutamate in and transport it from the extracellular space. Hence, they can terminate synaptic transmission and restore the extracellular glutamate concentration to basal levels. Expression EAAT2 is decreased in the lumbar spinal cord of ALS patients [366], as is the rate of glutamate transport in the spinal cord and motor cortex of SALS patients [367]. However, it is not known whether the decreased expression is a cause or consequence of neuron death [366]. There are also conflicting reports as to whether glutamate levels are increased [368] or decreased [369] in cerebrospinal fluid (CSF) from patients. A role of excitotoxicity has been proposed in several neurodegenerative diseases

including AD, PD, Huntington's disease and ALS [370]. In ALS it is supported by the clinical effects of riluzole [51], which increases survival time moderately [50-53]. However, the consequence of changes in the excitability of neurons resulting from excessive glutamate is under debate.

Hyperexcitability

Muscle cramps and fasciculation are characteristic symptoms of ALS, resulting from hyperexcitable MNs [12, 13, 17]. Changes in excitability could be due to either increased Na^+, or decreased K^+, currents, which would lead to increased depolarization or decreased hyperpolarization of MNs, respectively [65, 371-373]. Hyperexcitability is thought to occur in ALS patients but is not the only cause of fasciculations, which is a normal event also without underlying pathology.

The role of excitability in ALS and whether it is protective, or damaging, remains inconclusive. Hyperexcitability was not found to trigger MN death in young *SOD1* G93A mice [374]. In the same model, excitability was found early in the disease course and proposed to act as a protective mechanism by reducing ER-stress and protein aggregation [375]. Other studies propose that reduced K^+ currents are responsible for hyperexcitability and reduced survival of patient-derived MNs [376]. In this study, excessive neuronal firing led to an enhanced cellular uptake of Ca^{2+}, which is known to cause mitochondrial damage and ROS production [359, 360]. ROS further inhibit EAAT2, which results in decreased uptake of glutamate and even more calcium uptake [7]. Hyperexcitability can perhaps be considered as a secondary effect of excitotoxicity, caused by overstimulation of glutamate. However, hyperexcitable neurons also contribute to release of glutamate that can lead to MN damage through excitotoxicity. Hence, excitotoxicity and hyperexcitability are interconnected and contribute to MN vulnerability in ALS.

Mitochondrial damage

Mitochondria dysfunction is thought to induce MN death by Ca^{2+}-mediated excitotoxicity, increased production of ROS and activation of apoptosis [377, 378]. Several mutant SOD1 variants are associated with mitochondria in the spinal cord of *SOD1* transgenic mice [379 380, 381] where mutant SOD1 binds to the apoptosis-related protein BCL2 [382]. This interaction was also found in a homogenate of a *SOD1* FALS patient-derived spinal cord [382]. Aggregates bound to mitochondria obstruct import channels, which ledas to mitochondrial dysfunction [379]. Misfolded mutant SOD1 was further found to bind to voltage dependent anion channels (VDAC) isolated from *SOD1* transgenic rats [383] that, together with a conformational change in BCL2 [384], induce apoptosis through release of cytochrome c [385].

SOD1 is mainly a cytoplasmic protein but it is also present in the intermembrane space of mitochondria [386]. High-level overexpression of mutant SOD1 in transgenic models has been suggested to result in an artificial overloading of mutant protein within mitochondria, especially with stable mutant proteins, such as D90A [387], which could affect interactions with mitochondrial proteins. However, a pathogenic involvement of mitochondrial dysfunction in ALS is also supported by studies in patient-

derived MNs, which show a SOD1-dependent change in mitochondrial motility and morphology without overexpression of mutant protein [357].

Misfolded SOD1 interaction partners

A toxic gain of function of soluble, or aggregated, misfolded and disulphide-reduced SOD1 is involved in ALS pathology. Toxicity is likely exerted by misfolded SOD1 binding to and disrupting the function of other cellular proteins. Immunocapture of misfolded SOD1 from G93A and G127X mouse spinal cord followed by proteomic analysis found chaperones to be the major interaction partners of misfolded SOD1 [388]. The most abundant protein was HSC70, a constitutively expressed chaperone that is involved in protein quality control [287] and enriched in MNs [389]. However, because misfolded SOD1 only bound 1% of the total HSC70 present in the spinal cord, toxicity cannot be explained by chaperone depletion [388]. Misfolded SOD1 is also associated with VDAC1 in mitochondrial membranes and DERL1 in the ER, leading to accelerated disease progression in G37R [383] and G93A mice [356], respectively.

Activation of NADPH oxidase (NOX) leads production of superoxide and is associated with reduced survival in G93A mice [390, 391]. The activity of NOX is regulated by the ubiquitous protein Rac family small GTPase 1 (RAC1) in microglia [392]. In G93A mice, misfolded SOD1 binds to RAC1 and causes sustained NOX activation that results in excessive and harmful production of superoxides [393]. Increased NOX2 activation and ROS production is also involved in MN degeneration in SALS patients [390]. Hence, misfolded SOD1 is known to interact with several disease-associated proteins supporting its general role in ALS pathology.

RNA-interaction and processing

Several ALS associated genes encode RNA binding proteins [394] including TARDBP [105, 106, 108], FUS [115, 116] and C9ORF72 [129, 130], which are thought to sequester RNA binding proteins into foci [129, 137, 138].

Although generally not associated with RNA toxicity [394], SOD1 D90A binds to and dysregulates neurofilament light (NEFL) mRNA in patient-derived MNs Chen, 2014 #281} and G93A binds to VEGF mRNA resulting in down regulation *in vitro* and nuclear translocation *in vitro* and *in vivo* [395]. Together, these studies imply that deregulated RNA processing, or depletion of RNA, could be a common mechanism in the pathogenesis of ALS and FTD [396, 397], with the potential involvement of misfolded SOD1.

Prion-like transmission of misfolded SOD1

The prion-like-propagation of aggregation occurs via nucleation [398]. In this process, a misfolded protein acts as a template or seed that induces misfolding of native proteins, which are incorporated into a growing protein fibril [398]. Fragmentation of fibrils both amplifies the number of fibrils and enables their propagation to neighbouring cells [399, 400]. *In vitro* studies of mutant and wt recombinant SOD1 have shown that induction of misfolding cause fibrillation in a nucleation-dependent manner, similar to that observed in prion transmission [401-404]. Recombinant disulphide-reduced mutant SOD1 [200], or homogenates from *SOD1* G93A spinal cords [404], can induce fibrillation

of wt and mutant SOD1 and thereby enabling the spread of misfolding from cell to cell *in vitro* [405, 406].

Injection of end-stage spinal cord homogenates from a G93A or G37R mice into recipient mice also induces the propagation of ALS-like disease *in vivo* [407, 408]. Two different strains of SOD1 aggregates have been described in the spinal cord of end-stage mice expressing human mutant *SOD1*. Two kinds of aggregate structures, strain-A (including G93A, G85R and wt SOD1) and -B (D90A), were associated with different disease progression and were dissimilar to aggregates produced *in vitro* [409]. Injection of isolated strain-A and -B aggregates into the spinal cord of recipient G85R mice resulted in a premature, and strain specific transmission of ALS-like disease [410]. These results suggest that templated SOD1 aggregation, which is dependent on the presence of misfolded SOD1 monomers, could spread in a prion-like manner and act as a central mechanism behind SOD1 ALS pathology.

Non cell-autonomous toxicity

Because *SOD1* is ubiquitously expressed, mutant SOD1 is not just present in MNs. Cell autonomous toxicity, e.g. to MNs is derived from mechanisms acting in MNs themselves. However, other cell types can also be involved in toxicity to MNs via non-cell autonomous mechanisms. Attempts to induce ALS-like disease in transgenic mice by selectively overexpressing mutant SOD1 in different cell types has led to the understanding that mutant SOD1 toxicity has both cell autonomous and non-cell autonomous components [411-416].

Cell autonomous/non-cell autonomous components of ALS was first defined in mouse models [417-424] and then *in vitro* in co-culture systems [268, 269, 425, 426]. Constitutive expression of G73R, G85R and G93A mutant SOD1 only in neurons driven by the Thy-1.2 expression cassette [427], or the NEFL promotor, either failed to cause disease [417, 418] or led to a slowly progressing disease with late onset [419]. Expression of mutant SOD1 in MNs is required for disease onset as established by selective expression in MNs using the Thy1.2 expression cassett [419] or selective Cre-mediated inactivation of G37R in MNs [420, 422]. However, it does not affect the rate of progression [422, 428] suggesting that other cells types are involved in pathogenesis [411, 413, 429]. The normal function and role in disease for some of these motor area cells will be discussed below.

Microglia

Microglia serves as the main phagocytic, macrophage-like cell in the CNS [430]. Degeneration of neurons is followed by neuroinflammation [413]. Microglia have an important function in the inhibition, as well as in the activation, of neuroinflammation, depending on the environmental cues. There are two main types of microglia, the quiescent or resting type termed M2, which are non-reactive and neuroprotective, and the reactive and neurotoxic M1 type [431].

Microglia can be activated by three main pathways; classical, alternative and acquired activation, which induce either the M1 or M2 microglial phenotype [431]. Alternative activation by interleukin 4 and 13, as well as acquired activation by interleukin 10 or transforming growth factor

beta (TGFβ), promote the anti-inflammatory M2 type. M2 microglia are involved in phagocytosis of misfolded proteins and promote neuronal survival by secreting neurotrophic factors, such as insulin-like growth factor 1 (IGF1) [431]. Hence, activated microglia can have a cytoprotective role in ALS through the release of trophic or anti-inflammatory factors [415, 423].

Classical activation is enhanced by interferon gamma and lipopolysaccharides and promotes the proinflammatory M1 type. M1 activation induces production of proinflammatory cytokines such as interleukin 1β and 6 as well as leading to enhanced production of ROS [431]. Initiation of an inflammatory response and activation of M2 microglia occurs early in the disease course of G93A mice [432, 433]. Activated M2 microglia are also found in the spinal cord of both FALS and SALS patients [434]. Expression of mutant *SOD1* in microglia is not sufficient to initiate disease onset but contributes to disease progression [420, 422, 423]. Disease progression is also associated with the phenotypic conversion of activated M2 microglia to the cytotoxic M1 type [415, 432], which further associates activated M1 microglia to ALS progression and MN degeneration by increased production of ROS and inflammatory factors [415]. Consequently, a reduction of mutant protein in microglia slows disease onset and extends survival in mice [422].

Oligodendrocytes

The axons of UMNs and initial segments of LMNs in the CNS are insulated and supported by a myelin sheath provided by oligodendrocytes. Myelination is the main function of oligodendrocytes, but they also provide metabolic support to axons by delivering energy metabolites, such as lactate, at the nodes of Ranvier [435].

Degeneration of oligodendrocytes starts before disease onset in G93A mice [436] and induce a sustained proliferation of neural/glial antigen 2 (NG2) positive oligodendrocyte precursor cells, which is evident until end stage [437]. As a result, oligodendrocytes are continuously produced but fail to mature, leading to ongoing demyelination and axon degeneration [436]. Selective depletion of mutant SOD1 from oligodendrocyte precursor cells in G37R mice delays disease onset and prolongs survival [436], defining their role in non-cell autonomous mechanisms of SOD1-mediated toxicity.

In vitro studies using *SOD1* FALS or SALS patient-derived oligodendrocytes have confirmed their toxic effect on MNs [414]. Toxicity was found to be mediated both directly by cell-cell contact in co-culture [438] as well as indirectly, via decreased levels of lactate in oligodendrocyte conditioned medium. Silencing of G93A mutant *SOD1* by short hairpin RNA in mature oligodendrocytes did not affect the survival of MNs *in vitro* [438]. However, as previously seen in mice, deletion in oligodendrocyte precursor cells could rescue the cytotoxic phenotype leading to MN loss [436, 438].

Astrocytes

Astrocytes are the most abundant glial cell type in the CNS and are also involved in non-cell autonomous toxicity to MNs. The normal function of astrocytes includes, e.g. providing metabolic, trophic and structural support to neurons, maintaining ion homeostasis, and also regulating the synaptic activity via uptake and recycling of neurotransmitters [439, 440].

Under pathological conditions, astrocytes become reactive and proliferate in a process known as astrogliosis. This is a common feature in areas around MN degeneration in both mouse models of ALS [432, 433] as well as in ALS patients [441, 442]. A number of molecular signals that trigger astrocyte activation have been defined, such as interleukin 6 that acts through the Jak family tyrosine kinases/signal transducer and activator of transcription 3 (JAK/STAT3) pathway, or interleukin 1β and tumor necrosis factor α that act through the nuclear factor kappa B (NFκβ) pathway [439]. The activating signals are produced, e.g. by reactive microglia or degenerating neurons, but could also be a result of deposits of misfolded proteins such as mutant SOD1 [421 439, 440, 443].

Studies in animal models have identified inclusions of mutant SOD1 within astrocytes of G85R mice before the onset of symptoms, which increase with disease progression [224]. However, selective expression of *SOD1* G86R in astrocytes is not sufficient to cause ALS, although it does induce astrogliosis [421]. SOD1 inclusions are also found in nuclei of astrocytes in FALS patients with D90A or G127X mutations [90] and in a patient with a two base pair deletion in codon 126 [83].

Chimeric mice expressing wt, G37R or G85R mutant *SOD1* established that degeneration of MNs is dependent on neighboring, non-neuronal cells, expressing mutant *SOD1*. The survival of mutant *SOD1* expressing MNs could be further preserved in the presence of non-neuronal cells expressing wt *SOD1* [444]. Although this study confirmed a non-cell autonomous effect, the cell types involved could not be defined in chimeric mice. Expression of mutant *SOD1* in MNs is required for onset of disease but does not affect progression [420, 422, 424]. However, a reduction of G37R in astrocytes [424], or G37S or G85R in microglia and macrophages [420, 422] slows disease progression. Delayed onset is also seen in mice by cre-mediated removal of G85R expression in astrocytes using the glial fibrillary acidic protein (GFAP) promoter [445]. Hence, a reduction of mutant SOD1 in astrocytes delays both disease onset [445] and progression [422, 424, 445].

In vitro co-culture experiments have confirmed the non-cell autonomous toxic effect of glial cells on MNs. Primary MNs expressing mutant SOD1 do not degenerate *in vitro* [425]. However, reduced survival of both mouse and human ESC-derived MNs was evident when co-cultured with mutant *SOD1*-expressing astrocytes [268, 269, 425, 426]. This effect has been attributed to soluble toxic factors released by astrocytes in to the culture media [269, 425]. Secreted factors upregulated in G93A glia included three different cytokines (chemokine ligand 5 and 7 and 8), glial maturation factor beta, an agonist of the SHH pathway, and prostaglandin D2 [269] of which prostaglandin D2 had a negative effect on the survival of hESC-MNs [269].

The majority of studies on non-cell autonomous toxicity mediated by astrocytes have been performed in models overexpressing mutant SOD1. However, the majority of ALS cases are sporadic and thus express wt SOD1 at normal levels [99]. Patient-derived astrocytes cultured from spinal cord tissue *post mortem*, from both SALS and FALS patients, led to the same degree of degeneration of mouse ESC-derived MNs [271]. Since both FALS and SALS astrocytes express *SOD1* at physiological levels, astrocytes toxicity does not require high levels of *SOD1* expression. Astrocyte-derived toxicity was

further attenuated by *SOD1* knockdown in SALS cells using short interfering RNAs, demonstrating the involvement of non-neuronal cell types, as well as a role for wt SOD1, in MN toxicity [271]. Hence, the toxicity of astrocytes is not dependent on overexpression of mutant SOD1 protein and also involves wt SOD1 [271]. This highlights the role of astrocytes in ALS pathology and suggests that therapeutics targeting astrocytes could be beneficial in *SOD1* FALS, non-*SOD1* FALS and also SALS.

MN degeneration is associated with an increased influx of Ca^{2+}, which can overwhelm the capacity for intracellular storage and initiate degenerative cascades [360-362]. Normally, astrocytes reduce susceptibility to excitotoxicity by upregulating the glutamate receptor 2 subunit of the Ca^{2+} permeable AMPA receptors and thereby decreasing Ca^{2+} uptake and reducing Ca^{2+}-dependent toxicity [446, 447]. This protective function of astrocytes is lost in astrocytes expressing mutant SOD1 [448]. Mutant SOD1-expressing astrocytes also cause activation of microglia, highlighting the crosstalk that exists between different glial cell types in disease progression [443]. Loss of glutamate transporters in mutant *SOD1* rodent models [224, 449] and decreased transport in ALS patients [450] further contribute to astrocyte-mediated non-cell autonomous toxicity.

Induced pluripotent stem (iPS) cells

History and discovery

In nuclear transplantation, a nucleus is isolated from a somatic donor cell and fused with an enucleated host oocyte. This can result in 'reprogramming' of the somatic nucleus by factors in the host oocyte [451]. With this technique, adult somatic tadpole cells were shown to have the capacity to be reprogrammed and develop into juvenile tadpoles [451]. The technique was developed further in mammals with the cloning of the sheep Dolly [452]. These findings inspired further investigation of the factors that could induce reprogramming but circumventing the time consuming and technically difficult methods associated with nuclear transfer [451, 452]. In 2006, Takahashi and coworkers reported a successful reprogramming of mouse embryonic fibroblasts and adult fibroblasts to pluripotent stem cells using four transcription factors (referred to as Yamanaka factors [453].

The Yamanaka factors include octamer-binding transcription factor 4 (OCT3/4), SRY (sex determining region Y)-box 2 (SOX2), Kruppel-like factor 4 (KLF4) and c-MYC and cells reprogrammed using this method are referred to as iPSCs [453]. Human somatic cells were also reprogrammed using the same Yamanaka factors [454], or by replacement of KLF4 and c-MYC with NANOG and LIN28 [455]. Reprogramming was also accomplished with three of the Yamanaka factors (OCT3/4, SOX2, KLF4), albeit with lower efficiency [456]. IPSCs resemble human ESCs in several aspects including, e.g. their morphology, proliferation and telomerase activity, gene expression, cell surface markers, and most importantly, their capacity to differentiate into cells present in all three germ layers [454, 455].

Reprogramming methods

A range of techniques has been developed for the reprogramming of somatic cells to iPSCs. Only the methods relevant to this thesis will be introduced here.

Initial reprogramming methods were based on retroviral [453, 454], or lentiviral, transduction [455], both resulting in genomic integration of vectors expressing the Yamanaka factors. Viral integration into host chromosomes can result in insertional mutagenesis with the addition of new bases to the DNA, or otherwise interfere with transcription [457]. However, non-integrating methods have also been developed that generate iPSCs with similar characteristics as those produced by retroviral and lentiviral transduction [458].

Non-integrative reprogramming of fibroblasts [459, 460] and keratinocytes [460] has been achieved by transfection of mRNA encoding the four Yamanaka factors, as well as LIN28, reaching a reprogramming efficiency of up to 4%. Another method was developed using human foreskin fibroblasts with a single transfection of Epstein-Barr nuclear antigen 1 (EBNA1)-based episomal plasmids, which enabled high-level and long-term expression of OCT4, SOX2, LIN28 and NANOG, However, the efficiency of reprogramming was was relatively low [461]. A combination of non-integrating plasmids expressing OCT3/4, SOX2, KLF4, L-MYC and LIN28 as well as a short hairpin RNA against p53, increased the efficacy [462]. Hence, non-integrating factors offer a useful alternative to retrviral or lentiviral transduction, although repeated transfections are sometimes required to obtain successful reprogramming.

When comparing non-integrating methods, mRNA reprogramming has the highest efficiency, but it is also the most time-consuming method and requires daily, time-sensitive transfections [460]. Episomal reprogramming, on the other hand, has a higher success rate, likely due to the requirement for a single transfection, but the total time before colonies can be picked and expanded is slightly longer compared to mRNA reprogrammed cells [463]. IPSCs also need to be repeatedly passaged to ensure that episomal vectors are removed.

The iPSCs used in this thesis all originate from fibroblasts. Cells were reprogrammed using retroviral transduction of the Yamanaka factors (Paper II) and non-integrating methods including mRNA (Paper III) and transfection of Yamanaka factors and LIN28 in episomal plasmids in papers III and IV. IPSCs were further differentiated to MN cultures (Figure 6).

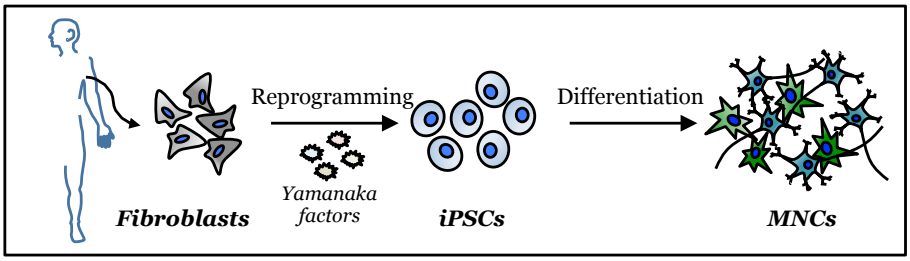

Figure 6: Isolation, reprogramming and differentiation of patient derived cells. Fibroblasts were isolated from skin biopsies, reprogrammed to iPSCs and differentiated to iPSC-derived motor neuron cultures (MNCs) containing MNs of a limb innervating subtype and their associated astrocytes.

Motor neuron organization

MNs are organized into groups along the rostral-caudal axis of the spinal cord by the combined action of transcription factor expression, diffusible factors and adhesion molecules, which facilitate the matching of MNs with their target muscles. These groups are termed motor columns, of which there are four different types in the spinal cord. Once the organization of motor columns is complete, MNs become further subdivided into motor pools, which are defined as the collection of MNs within a motor column that innervate a single muscle (reviewed in [246, 464-467]). A summary of MN development is illustrated in Figure 7.

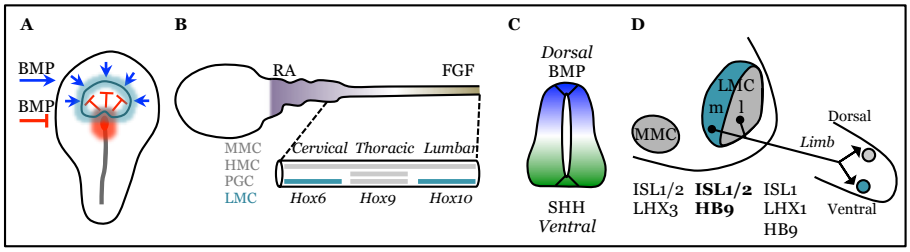

Figure 7: Schematic overview of MN development. (A) Neural induction is established by secretion of bone morphogenic protein (BMP) inhibitors (red) from the node forming neuroectoderm in the developing embryo. These counteract the activity of BMPs from the surrounding non-neural ectoderm (blue). **(B)** Motor neurons specification is achieved by a gradient of retinoic acid (RA; purple) that positions motor neurons and column formation in the spinal cord. **(C)** In combination with a ventro-dorsal gradient of sonic hedgehog (SHH; green), which leads to the development of MN precursors in the ventral spinal cord. **(D)** We have used differentiation protocols that result in the development of medial lateral motor column MNs (LMCm; turquoise) expressing ISL1/2, LHX1 and HB9 [4].

Neural induction results from inhibition of BMP signals in the developing embryo (Figure 7A). The rostral-caudal patterning of the motor columns inducing a spinal cord identity is established by opposing gradients of RA and fibroblast growth factor (FGF), which induces expression of

members of the *Hox* gene family at different axial levels of the spinal cord [265, 468, 469] (Figure 7B). Hox proteins are transcription factors that regulate expression of target genes involved in the establishment of both motor column- and motor pool-identity, as well as of the target muscles [469, 470]. One example is forkhead box protein 1, which is involved in column specification and the formation of limb innervating MNs [471, 472]. The four motor columns include the preganglionic- and hypaxial motor columns at the thoracic level of the spinal cord and comprise visceral MNs innervating sympathetic ganglia and MNs innervating abdominal wall, respectively. MNs in the medial motor column innervate proximal muscles along the spinal cord, whereas MNs in the LMC are located at cervical and lumbar levels and innervate limb muscles [246, 465-467].

In the ventral neural tube of a developing embryo, SHH is secreted from the notochord and floor plate (Figure 7C). It forms a gradient where different pools of neural progenitor are induced, depending on the SHH concentration [266, 473, 474]. SHH is crucial for the dorsoventral organization of the spinal cord.

The LMC is further divided into a lateral (LMCl) and medial (LMCm) segment with expression of LIM class homeobox proteins, including ISL1/2 and LIM homeobox 1 (LHX1)[475-477]. MNs in the LMCl project to dorsal muscles and express LHX1 and ISL2, whereas MNs in LMCm project to ventral muscles and express ISL1 and ISL2 [465, 475, 478]. Both subgroups also express HB9 [465, 479] (Figure 7D).

MN classification

MNs can be classified as alpha (α), beta- (β) and gamma (γ) subtypes based on the muscle fibers that they innervate. α-MNs innervate extrafusal muscle fibers in skeletal muscle and generate muscle contraction and force, whereas γ-MNs innervate intrafusal muscle fibers of the muscle spindle. γ-MNs also have a slower conduction speed and sense muscle stretch [246, 464, 466]. β-MNs are less well defined, but include a mixture of α- and γ-MNs and thus innervate both intra- and extrafusal fibers [466]. Features that distinguish α- from γ-MNs are their larger soma size, fast conduction velocity and more extensive and complicated branching [480]. α-MNs are most abundant and can be classified according to their contractile properties, slow twitch and fatigue resistant-MNs (S-MNs), fast-twitch and fatigue resistant-MNs (FR-MNs) and fast-twitch fatigable MNs (FF-MNs). FF-MNs generally have a large soma size and axon diameter, produce a large amount of force and can only remain active for a short period of time. S-MNs, on the other hand, are smaller and generate less force but can remain activated for a longer duration. Hence, S-type α-MNs are generally involved in maintaining posture whereas FF-type α-MNs are used for intense movements requiring much force, such as jumping.

A motor unit is defined as a MN and the muscle fibers that it innervates. Activation of muscles requires recruitment of motor units in response to stimulation. The order in which units are used is decided by the 'size principle' presented in the 1960s by Henneman and colleagues [481]. Smaller S-MNs require less synaptic activation and are recruited first in response to weak stimuli, followed by FR-MNs and FF-MNs when the

strength of stimulation increase and requires more force [466]. By recruiting FR-MNs first, 'exhaustion' is minimized and fatigable fibers are only used when high forces are needed.

ALS primarily affects the limb innervating MNs of the LMC in both G93A mice [466, 482] and ALS patients [483]. In G93A mice, muscle weakness is apparent around 90 days of age. However, denervation of muscles is initiated already at 50 days of age, demonstrating that MNs start to degenerate long before symptom onset [482]. However, all MN subtypes are not equally affected. FF α-MNs are the first ones affected in G93A mice [484]. Initial degeneration of the neuromuscular junction can be rescued by re-innervation of the muscle by FR-MNs and S-MNs [485]. Hence, re-innervation can compensate for MN degeneration and postpone symptom onset [466, 485]. However, with disease progression, more muscular connections will be lost, and degeneration extends to include FR- and S-MNs and muscle atrophy.

MN differentiation

Protocols have been developed for directed differentiation MNs from both mouse and human ESCs [244, 248, 268, 269, 486, 487] and more recently iPSCs [4, 244, 488-494]. These protocols make use of the signaling factors and pathways that specify MNs *in vivo* and have been identified by studying the development of MNs in amphibian, chick, fish and mouse embryos [464-466, 495].

Differentiation protocols can be generally divided in to three parts; neuronal induction, MN specification and MN maturation [248, 496 497]. IPSCs (and ESCs) can be differentiated through EBs gown in suspension cultures [4, 244, 357, 488, 489, 491, 498]. Alternatively, they can be differentiated as adherent cells, referred to in this thesis as '2D cultures' [490, 493, 499, 500]. A summary of the *in vitro* differentation of MNs and the factors used is shown in Figure 8.

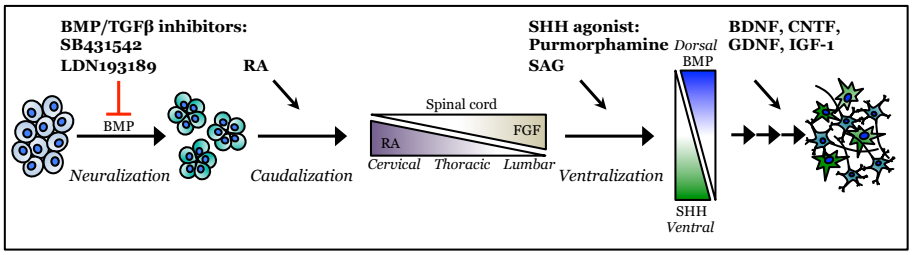

Figure 8: Directed differentiation of iPSCs to MNs *in vitro*. Neural induction is established by Dual SMAD inhibition of bone morphogenic protein (BMP) and transforming growth factor β (TGFβ) signalling using SB431542 and LDN193189, respectively. Retinoic acid (RA) is supplemented to induce caudalization and the appropriate sonic hedgehog (SHH) concentration is established by addition of smoothened agonist (SAG) and purmorphamine. Differentiated MNCs are matured for ten days in the presence of brain derived neurotrophic factor (BdNF); ciliary neurotrophic factor (CNFT), glial derived neurotrophic factor (GDNF) and insulin-like growth factor (IGF1).

Protocols largely rely upon neural induction by inhibition of BMP and TGFβ using SB431542 and LDN193189, respectively, a method referred to as dual SMAD inhibition. These small molecules block endodermal and

mesodermal cell fates and promote neural conversion [496]. This method has enabled a significant reduction in the length of time needed for neural conversion, resulting in shorter protocols as well as an enhanced neuronal yield. MN specification includes caudalization, which is initiated by RA, and ventralization by SHH, e.g. through smoothened agonists or purmorphamine. RA signalling specifies the rostrocaudal ('head-tail') axis of organization of the spinal cord, whereas SHH signalling mimicks the high concentration of SHH that establish ventral identity *in vivo,* from which MN progenitors arise. In the last main step, MN cultures are matured by addition of neurotrophic factors including glial-derived neurotrophic factor (GDNF), ciliary neurotrophic factor (CNTF), brain derived neurotrophic factor (BDNF), nerve growth factor (NGF), and IGF1 [501]. These factors are normally supplied by surrounding cells, including targets of innervation *in vivo,* but can be added to differentiating cells to improve survival and maturation.

RA, FGF, BMP and SHH are all extrinsic factors present in the developing spinal cord that act by inducing transcriptional programs, thereby guiding the formation and specification of MNs [465, 495]. When differentiating MNs *in vitro*, an addition of these extrinsic factors, or their agonists or antagonists, drives their differentiation and the expression of specific transcription factors that are characteristic markers of MN subtypes. MNs differentiated from iPSCs express several markers that can be used to classify them. For LMC MNs these include ISL1/2, LHX1, HB9, forkhead box protein 1, non-phosphorylated neurofilament heavy chain (SMI32), CHAT and microtubule associated protein 2 (MAP2) [4, 244, 490, 491].

A range of both '2D' and '3D' differentiation protocols have been established based on the developmental principles summarized above. In these protocols, a large variation exists in the duration of neural induction, as well as in MN specification and maturation. Hence, the total length of different protocols may differ. A slightly altered timing of patterning, plating densities and small molecules used to induce differentiation could have a great effect on the yield and purity of MNs, and also on their subtype identity and maturity [497]. The majority of protocols have a duration of around 30-50 days from onset of differentiation to the time of analysis [4, 244, 488, 491]. However, the generation of ISL1/2 and HB9 expressing cells can vary from 10 days of differentiation [493], up to 130 days [498]. Longer differentiation protocols might be of benefit over shorter ones when it comes to maturity and assays involving measurements of electrical activity [4, 376, 488, 498], whereas 'fast track' protocols could be beneficial for screening studies, e.g. including toxicity or factors that improve disease phenotypes and/or survival.

IPSC-based models of ALS

ALS is a disease in the nervous system, which can be followed, e.g. by sampling of CSF as a measure of progressive alterations in the CNS [368, 369]. However, the affected MNs and the surrounding glia cells can only be studied *post mortem,* by which time a severe loss of MNs has already

occurred, thus making studies of early pathogenesis difficult. Transgenic mouse models overexpressing human *SOD1* have been used widely to circumvent these issues [217, 224]. Apart from being a rodent and not human models, high levels of expression could induce an artificial overload of mutant SOD1 that is not typical for disease in ALS patients. Hence, the mechanism of misfolded SOD1 toxicity in patients with a physiological level of expression remains unclear.

The development of iPSCs offered a new approach for stem cell-based research, bypassing the reliance on overexpression models and also ethical concerns of using human ESCs. Somatic cells for iPSC reprogramming are relatively accessible and preserve at least some aspects of the genetic and environmental backgrounds of the individual donors [454, 455].

In 2008, the first MNs were successfully differentiated from iPSCs [489]. These iPSCs were reprogrammed from fibroblasts from an 82-year-old patient donor carrying a *SOD1* L144F mutation and showed that neither advanced age, nor disease stage, affected the reprogramming ability [489]. The differentiation of these iPSCs was further validated in two independent laboratories where iPSC clones from several donors were differentiated with similar results [488]. These studies demonstrated a robustness of the method, which was followed by several other differentiations protocols for human MNs as reviewed [497, 502, 503].

An advantage when working with iPSCs is the possibility to correct, or induce, mutations by gene editing and thereby investigating the contribution of specific genes to the disease phenotype [357, 376, 504]. Modeling *SOD1* FALS with iPSC-derived MNs has recapitulated several known pathological findings in patient-derived cells, reinforcing the utility of the approach. *SOD1* D90A patient–derived MNs demonstrated NEFL aggregation and axonal degeneration [504]. Aggregation was attributed to mutant SOD1 binding to and deregulating NEFL mRNA and both aggregation and degeneration were reversed upon correction of the D90A mutation [504]. By electron microscopy, SOD1 aggregates were also detected in the nuclei, cytoplasm and neurites of D90A MNs, as well as in mitochondria of both MNs and non-MNs [504]. Degenerating axons and a reduction in soma size were further features of A4V MNs, which also was associated with decreased survival [357]. Correction of this mutation reversed the observed phenotypes connected the degeneration of MNs to the presence of a *SOD1* mutation in patient-derived MNs [357].

UPR and ER-stress were found to be increased in A4V MNs compared with their wt counterparts, as measured by increased splicing of XBP1 and phosphorylation of elF2α. The UPR was also linked to degeneration since knockdown of XBP1 by small interfering RNA led to a significant improvement in MN survival. IPSC-derived MNs also demonstrated alterations in excitability. *SOD1* A4V, D90A and G85S MNs were found to be hyperexcitable compared to wt MNs, and by reducing activity with the potassium channel opener retigabine, survival of A4V MNs was improved [376]. Blocking action potentials using the sodium channel blocker tetrodotoxin also reduced levels of spliced XBP1, thus connecting the UPR to hyperexcitability and survival [357]. A slight increase of the UPR was also evident in wt MNs, which increased with maturation. This suggests that

there is a basal level of ER-stress in MNs, which could be related to their vulnerability to ALS [357].

Several ALS-associated genes have been investigated using iPSC models and aspects of the disease phenotype have been recapitulated. Importantly, iPSC-based models also enable studies of SALS [505], which is not possible in overexpression models. By analyzing gene expression in MNs from SALS patients compared to MNs from healthy controls, a deregulation of genes associated with oxidative phosphorylation, including VDAC1, cytochrome C and several ATP synthases was demonstrated, leading to a role of mitochondrial dysfunction in SALS pathogenesis to be proposed [506]. MNs with mutant [507, 508] and wt [505] *TARDBP* expression demonstrate increased levels of both the soluble [508] and aggregated protein [505, 507, 508], which is associated with reduced survival [508]. The TDP43 M337V mutant protein also shows characteristic cytoplasmic mislocalization, which is reduced upon mutant allele-specific knock down using small interfering RNA [509]. Cytoplasmic mislocalization is also a feature of iPSC-derived MNs derived from patients with *FUS* mutations [510, 511]. The MNs contain aggregates of mutant FUS protein [511] that were associated with stress granules after induction of oxidative stress using sodium arsenite [510].

TARDBP models, expressing both mutant and wt protein, have been used to screen for candidate drugs that improved disease phenotype as well as protein aggregation, without reducing protein expression [505, 507]. IPSC-derived MN with hexanuleotide repeat expansion in *C9ORF72* demonstrate RNA foci [396, 492] and sequestration of the RNA binding protein adenosine deaminase, RNA specific B2 (ADARB2) [396]. iPSC-derived MNs also demonstrate hyperexcitability in *SOD1*, *TARDBP* and *C9ORF72* models [376, 498]. In *TARDBP* and *C9ORF72* models, initial hyperexcitability was followed by a reduction of action potentials [492, 498] as well as increased sensitivity to excitotoxicity [396]. Treatments with antisense oligonucleotides that target the repeat RNA sequence led to a reduction in RNA foci [396].

The studies above show the utility of iPSC-derived MNs to study pathogenic mechanisms in ALS and for testing potential interventions aimed at reducing the disease phenotype. However, misfolded SOD1 has not been characterized in different patient-derived cell types *in vitro* in relation to known cellular disturbances in ALS in *SOD1* FALS, non-SOD1 *FALS* and SALS lines.

Aims of thesis

The pathogenic mechanisms of SOD1-related ALS have mainly been investigated in models overexpressing mutant SOD1 *in vitro* and *in vivo*. How well the identified pathogenic mechanisms translate to ALS in patients is unclear. The overall aim of this thesis was to characterize misfolded SOD1 in patient-derived models with physiological levels of *SOD1* expression and investigate its relation to disease-associated processes. The thesis includes four studies with the following specific aims:

Paper I

- Investigate the effects of pathways known to be disturbed in ALS on the levels of soluble and aggregated misfolded SOD1 in FALS patient-derived fibroblasts.

Paper II

- Characterize misfolded SOD1 in patient-derived motor neurons and astrocytes to analyse misfolding in disease-relevant cell models from *SOD1* FALS, non-*SOD1* FALS or SALS.

Paper III

- Investigate the role of low oxygen tension on disulphide bond stability and levels of soluble and aggregated misfolded SOD1 in patient-derived cells *in vitro*.

Paper IV

- Characterize soluble misfolded and aggregated SOD1 in patient-derived cells carrying a novel SOD1 truncation mutation resulting in a loss of the electrostatic loop and the stabilizing disulphide bond.

Material and Methods

Human materials

Studies were performed in accordance with the ethical principles for medical research involving human subjects outlined in the Declaration of Helsinki (WMA, 1964) and approved by Etikprövningsnämnden (EPN) at Umeå University, DNR 2014-137-31M.

Human patient and control samples used in papers I, III and IV were provided by Prof. Peter M. Andersen following written informed consent from the donors. Cell lines used in Paper II were obtained through collaboration with Project ALS and Prof. Christopher E Henderson's lab at Colombia University and Prof. Kevin Eggan's lab at Harvard University. These were covered by material transfer agreements between Umeå University, Columbia University, Harvard University and Howard Hughes Medical Institute.

Cell culture

All cells were maintained routinley at 37°C and 5% (v/v) CO_2 in a humidified incubator. Cell lines were cultured using standard protocols and media components supplied by Thermo Fisher Scientific, unless stated.

Fibroblasts

Fibroblast lines included in paper I, III, and IV were expanded from 3 mm dermal biopsies from the upper arm of healthy controls and ALS patients with mutations in *SOD1* (A4V, H46R, E78_R79insSI, N86S, D90A, G93A, D96Mfs*8 (two lines), L117V, D125Tfs*24, G127X (two lines, one diagnosed with ALS three years after biopsy and one asymptomatic carrier), *FUS* (Q23L), *TBK1* (A417X (two lines, one diagnosed with ALS and one asymptomatic carrier), I450Kfs*14, p.690-713del, M598V) and *C9ORF72* (two lines, one with a diagnosis of ALS and one with FTD). The control lines were obtained from unaffected family members of ALS patients and did not carry any identified mutation in ALS associated genes [142, 512]. ALS patients were heterozygous for their respective mutation except for the *SOD1* D90A patient that was homozygous.

Paper II includes lines with mutations in *SOD1* (A4V, L144F and G85S), *FUS* (H517Q), *TARDBP* (Q343R and G298S), *ANG* (not determined) and one SALS line [357, 489, 513]. Two healthy control individuals are included as well as a genetically modified isogenic control line where the *SOD1* A4V mutation was corrected to wt [357, 376]. Fibroblast in papers I, II and IV were maintained in Roswell Park Memorial Institute medium 1640 medium, supplemented with fetal bovine serum (FBS), L-glutamine and penicillin (Meda). Fibroblasts in Paper II were maintained in Dulbecco's Modified Eagle Medium (DMEM) supplemented with FBS, L-glutamine and Penicillin-Streptomycin. A summary of all lines used is presented in Table 1 and 2.

Table 1: Details of patient and control lines (Papers I, III and IV).

Genotype	Cell type	Diagnosis	Repr.	Sex	Age onset	Paper
Non-disease wt controls						
wt	Fb/MNC	NA	mRNA	F	NA	I and III
wt	Fb/MNC	NA	mRNA	F	NA	I and III
wt	Fb	NA	-	F	NA	I and III
wt	Fb	NA	-	M	NA	I and III
wt	Fb/MNC	NA	Epi	F	NA	IV
SOD1						
A4V	Fb/MNC	ALS	mRNA	M	62	I, III and IV
H46R	Fb/MNC	ALS	mRNA	M	54	I and III
E78_R79insSI	Fb/MNC	ALS	mRNA	F	42	I and III
N86S	Fb/MNC	ALS	Epi	M	77	I and III
D90A/D90A	Fb/MNC	ALS	mRNA	F	52	I and III
G93A	Fb/MNC	ALS	Epi	M	42	I, III and IV
D96Mfs*8	Fb/MNC	ALS	Epi	M	57	IV
D96Mfs*8	Fb/MNC	NA	Epl	M	NA	IV
L117V	Fb/MNC	ALS	mRNA	F	36	I and III
D125Tfs*24	Fb/MNC	ALS	mRNA	M	55	I and III
G127X (I)	Fb/MNC	NA	mRNA	M	NA	I and III
G127X (II)	Fb	Later ALS	mRNA	M	71	I, III and IV
Non-*SOD1* FALS						
FUS^{Q23L}	Fb	PBP	-	M	35	III
TBK^{A417X}	Fb	ALS	-	F	65	III
TBK^{A417X}	Fb	NA	-	F	NA	III
TBK^{I450Kfs*14}	Fb	ALS	-	M	55	III
TBK^{M598V}	Fb	ALS	-	F	63	III
TBK$^{690\text{-}713del/wt}$	Fb	NA	-	F	NA	III
C9orf72^{exp}	Fb	ALS	mRNA	F	53	I and III
C9orf72^{exp}	Fb	FTD	mRNA	M	65	I and III

Table 1: Cell types include fibroblasts (Fb) and induced pluripotent stem cell (iPSC)-derived mixed motor neuron cultures (MNCs). Lines from patients with a diagnosis of amyotrophic lateral sclerosis (ALS) or frontotemporal dementia (FTD) and asymptomatic mutation carriers (defined as NA; not applicable under diagnosis section). iPSCs were reprogrammed by transfection of *OCT3/4*, *SOX2*, *KLF4, cMYC* and *LIN28* mRNAs or by nucleofection of Episomal (Epi) plasmids encoding *OCT3/4, SOX2, KLF4, L-MYC, LIN28* and a *short hairpin RNA against P53*. Patient-lines included both female (F) and male (M) donors. All mutations are heterozygous unless otherwise stated. NA; not applicable/not determined.

Table 2: Details of patient and control lines (Paper II).

Name and Genotype	Cell type	Clone	Diagnosis	Sex	Age	Ref.
Non-disease controls and *SOD1*						
Control A wt	Fb/iPS/ MNC	11a/b	NA	M	36	[488]
Control B wt	Fb/iPS/MNC	18a/b/c	NA	F	48	[488]
Isogenic control	MNC/SNC	39b$^{+/+}$	NA	F	44	[357]
AV4	MNC/SNC/Ast	39b	ALS	F	44	[357]
G85S	MNC/Ast	27B/e	ALS	F	29	[488]
L144F	MNC	29A/B/e	ALS	F	82	[489]
Non-*SOD1*						
ANGND	MNC	027	ALS	M	55	[513]
FUS^{H517Q}	MNC	025	ALS	F	50	[513]
TDP-43^{Q343R} A	MNC	36a	ALS	M	53	This study
TDP-43^{G298S} B	MNC	47a	ALS	M	43	This study
SALS	MNC	16b	ALS	M	49	This study
mESCs						
SOD1^{wt}	MNC	NA	NA	M	NA	
SOD1^{G93A}	MNC	NA	NA	M	NA	

Table 2: Cell types include fibroblasts (Fb), induced pluripotent stem cell (iPSC)-derived mixed motor neuron cultures (MNCs), iPSC-mixed sensory neuron cultures (SNC), iPS-derived astrocytes (Ast) and mouse embryonic stem cell-derived MNCs. IPSCs were preprogrammed by lentiviral transduction *OCT3/4*, *SOX2* and *KLF4* (clone reference in lowercase suffix) or *OCT3/4*, *SOX2*, *KLF* and *cMYC* (clone reference in uppercase suffix). Patient-lines included both female (F) and male (M) donors. All mutations are heterozygous. NA; not applicable/not determined.

Induced pluripotent stem cells

Retroviral reprogramming (Paper II)
IPSCs in Paper II were reprogrammed by retroviral transduction of three (OCT4, KLF4, SOX2) or four (OCT4, KLF4, SOX2 and cMYC) of the Yamanaka factors [357, 488, 489, 513].

mRNA reprogramming (Paper III)
The majority of iPSC lines in paper III were reprogrammed by Cellartis (Takara Bio Europe AB, Gothenburg, Sweden) using the mRNA Reprogramming Kit (Stemgent).

Episomal reprogramming (Papers III and IV)
Two lines used in paper III (*SOD1* G93A and N86S) and all iPSCs in paper IV were reprogrammed by nucleofection of episomal plasmids [462]. Approximately 0.5x10^6 dermal fibroblasts were transfected with the Amaxa Human Dermal Fibroblast Nucleofector Kit (Lonza) using plasmids of OCT3/4, SOX2, KLF4, L-MYC, LIN28, short hairpin RNA-p53 and Epstein–Barr nuclear antigen 1 plasmids [462]. Cells were re-plated in 6-well tissue culture vessels (9.6 cm^2) one week after transfection and maintained in DEF-CS Culture System (Takara Bio). Colonies were picked and expanded after another 1-2 weeks in culture.

Feeder-dependent culture of iPSCs (Paper II)
IPSCs in paper II were initially maintained on gamma irradiated mouse embryonic feeder cells in DMEM/F12 supplemented with Knock-Out Serum Replacer (KOSR), 1x Non-Essential Amino Acids (NEAA) (Millipore), 2-mercaptoethanol (Sigma Aldrich) and basic FGF and passaged weekly using Dispase II [488, 489]. IPSCs were adapted to the feeder free culture system later on (DEF-CS, Takara Bio).

Feeder-free culture (Papers II-IV)
IPSCs in papers III–IV and some parts of Paper II, were cultured without feeder cells in the DEF-CS Culture System (Takara Bio). Cells were maintained as a monolayer and passaged using TrypLE Express Enzyme twice per week after reaching a density of approximately 150-200,000 cells per cm^2 and re-seeded at approximately 0.4-0.5 x10^5 cells per cm^2. This method of culture was more convenient compared to feeder-dependent culture with reduced expansion time and better accuracy of iPSC numbers used to initiate differentiation. Hence, feeder-dependent cultures were adapted to this culture system by changing the culture media and coating substrate to that of the feeder-free system and passaging cells > 5 rounds with no apparent changes in pluripotency or differentiation capacity.

IPSC-derived motor neuron cultures
2D and 3D protocols were used to differentiate iPSCs to MNs according to protocols optimized for the generation of MNs of a limb-innervating identity [4]. The differentiated MNs within this thesis contained a mixture of MNs and

astrocytes and are referred to as iPSC-derived mixed motor neuron/astrocyte cultures (MNCs).

3D differentiation (Papers II-IV)
Undifferentiated iPSCs were seeded in Ultra Low Attachment flasks (Corning) to minimize adhesion to the plastic surface and facilitate the formation of EBs. Neuralization was induced by dual SMAD inhibition [496] using SB431542 (Sigma Aldrich) and LDN193189 (Stemgent). This was supplied for six days before addition of RA (Sigma Aldrich) to direct neural progenitors towards a spinal cord identity. Purmorphamine (Stemgent) was added to ventralize spinal cord progenitors [4, 248]. Maturation and survival were promoted with the addition of neurotrophic factors; BDNF, CNTF, GDNF, and IGF1. EBs were dissociated after 31 days of differentiation and seeded on polyornithine- (Sigma Aldrich) and laminin- (Sigma Aldrich) coated culture vessels for 10-12 days for further maturation [4] before analysis.

2D differentiation (Papers II-III)
2D differentiation was performed on adherent iPSCs in 6-well tissue culture vessels (9.6 cm^2). Cells were neuralized by dual SMAD inhibition using SB431542 (Sigma Aldrich) and LDN193189 (Stemgent) and SHH agonist (Sigma Aldrich) was used to induce ventralization and MN patterning [248, 496]. DAPT (Selleck Chemicals), a γ-secretase and Notch inhibitor, was added to promote neurogenesis as well as the FGF signalling inhibitor SU5402 (Sigma Aldrich), to further increase the yield of neurons [491].

IPSC-derived astrocytes
Patient-derived astrocyte lines were derived from 3D-differentiated MNCs. MNCs were passaged in DMEM supplemented with FBS, B-27 Supplement minus antioxidants, L-glutamine, NEAA and heparin [514] on polyornithine- (Sigma Aldrich) and laminin- (Sigma Aldrich) coated culture vessels to select for proliferating astrocytes.

IPSC-derived sensory neuron cultures
IPSCs were seeded at 0.4-0.5 $x10^5$ cells per cm^2 on Matrigel-coated plates in DEF-CS culture medium and differentiation was initiated at 60-80% confluence. Dual SMAD inhibition was performed using SB431542 (Sigma Aldrich) and LDN193189 (Stemgent). Following neuralization, cells were cultured in Knock Out-DMEM supplemented with L-glutamine, NEAA (Millipore), 2-mercaptoethanol (Sigma Aldrich) and Penicillin-Streptomycin, which was gradually was exchanged to 100% (v/v) N2-media (DMEM/F12 with glucose (Sigma Aldrich), sodium bicarbonate, putrescine (Sigma Aldrich), sodium selenite (Sigma Aldrich), progesterone (Sigma Aldrich), apo-transferrin (Sigma Aldrich), insulin (Sigma Aldrich), transferrin (Sigma Aldrich) and Penicillin-Streptomycin every second day (via 25 %, 50 % and 75 % (v/v), respectively). From day 2-12, media was supplemented with dual SMAD inhibitors SB431542 (Sigma Aldrich) and LDN193198 (Stemgent) together with CHIR99021 (Tocris), DAPT (Selleck Chemicals) and SU5402 (Sigma Aldrich). Differentiated cells were harvested using StemPro Accutase Cell Dissociation Reagent and seeded at a density of

50,000 cells/cm^2 on Matrigel-coated culture vessels in N2-media supplemented with NGF, BDNF, GDNF and ascorbic acid. Cells were harvested after 21 days of maturation.

Cell treatments
Fibroblasts were seeded in 60 mm cell culture vessels at a density of 0.8x10^4 cells per cm^2 and cultured for 24 h before treated with small molecules, or cultured under different oxygen tensions for defined periods of time following complete media change. MNCs were routinely seeded at a density of 0.5 x10^5 cells per cm^2 and matured for 10-12 days before treatment. MNCs were treated with Bortezomib (Millennium Pharmaceuticals) for 8 h and culture in low oxygen was done for 24 h.

Chemical treatments (Papers I-II and IV)
The small molecules used to treat cells included Bortezomib (Millennium Pharmaceuticals) to inhibit the proteasome, 3-methyladenine (3-MA, Sigma-Aldrich) to inhibit of autophagy, tunicamycin (Sigma Aldrich) as an inducer of ER-stress and rotenone (Sigma-Aldrich) to inhibit cellular respiration by blocking electron transport at mitochondrial Complex 1.

Low oxygen tension (Paper III)
Both fibroblasts and MNCs were exposed to different O_2 tensions at 37°C. For each experiment, control samples were maintained under standard tissue culture conditions (19% O_2, 5% CO_2, 76% N_2) whereas the test samples were transferred to a humidified incubator that was gassed with O_2 tensions ranging from 1-10% (1-10% O_2, 5% CO_2, 94-85% N_2). All cells were treated for 24 h at the indicated O_2 tension.

Sample fractionation
Cultures were washed in pre-warmed phosphate-buffered saline (PBS) containing iodoacetamide (IAM, Sigma Aldrich), which alkylates reduced cysteine residues, to prevent the formation of artificial disulphide bonds involving C57-C146 in misfolded SOD1 [203]. Cells were harvested using trypsin-EDTA, pelleted and snap-frozen on dry-ice and stored at -80°C until further analysis. At the time of analysis, cells were thawed at 25°C, put on ice and resuspended in ice-cold lysis buffer containing PBS with Complete EDTA-free Protease Inhibitor Cocktail (Roche), IAM and polyethylene glycol nonyl phenyl ether (Nonidet P-40, Roche) before sonication using a Sonifier Cell Disrupter (Branson). Cell lysates were centrifuged at 20,000 xg for 30 min. at 4°C. The supernatant, containing soluble SOD1, was analysed by misELISA and western blot. Pellets were processed further for detergent insoluble SOD1 aggregate analysis. To isolate detergent-resistant aggregates, pellets were washed and centrifuged twice more in the same lysis buffer before resuspension in sample buffer for analysis by western blotting. IAM was included throughout the protocol when samples were used for misELISA but omitted in samples used for western blotting to avoid possible effects on antibody binding due to alkylation of cysteine residues.

Quantification of SOD1 by ELISA
Soluble fractions of cell lysates were used to determine the amounts of soluble misfolded SOD1, as well as total SOD1, using two different sandwich ELISAs [202, 515]. ELISA assays were performed in 96-well Multisorb plates (Nunc) using three replicates samples; each analysed in duplicates wells.

Misfolded SOD1 ELISA (Papers I-IV)
A primary rabbit antibody raised against SOD1 peptide sequence 24-39 (Agrisera) [280] was used to capture misfolded SOD1. The antibody binds specifically to misfolded SOD1 but not to natively folded or murine protein [90, 409]. A goat anti-human antibody raised against denatured SOD1 was used as a secondary detection antibody [515]. The amount of misfolded SOD1 present in each sample was calibrated against a standard of the spinal cord from a *SOD1* transgenic mouse expressing human mutant G127X. The G127X truncated protein lacking C146 is unable to adapt a native fold and is thus completely unfolded. In the misfolded SOD1 ELISA, one unit of misfolded SOD1 was defined as the amount of misfolded protein present in 1 g wet weight of a terminal G127X mouse spinal cord [202]. Misfolded SOD1 values, expressed as μU/mg protein, were normalized to total cellular protein using the bicinchoninic acid assay (BCA) Protein Assay kit to account for differences in cell numbers between cultures.

Total SOD1 ELISA (Papers I-IV)
Total SOD1 was analysed by ELISA using a rabbit primary capture and a goat secondary detection antibody. Both were raised against native human SOD1. The values were normalized to a standard of human hemolysate (non-disease control) in which the SOD1 concentration had been determined by quantitative amino acid analysis [219]. Native SOD1 values, expressed as ng/mg protein, were normalized to total cellular protein using the BCA Protein Assay kit to account for differences in cell numbers between cultures. The native SOD1 ELISA may also detect some misfolded SOD1 species [515] and is thus referred to as a total SOD1 ELISA. The total SOD1 ELISA was used to quantify SOD1 expression in different lines and cell types. It was also used to normalize misfolded SOD1 to total SOD1, which indicates the stability of the mutant protein [197, 210].

Size exclusion chromatography
Size exclusion chromatography (SEC) was performed to study the composition of SOD1 in soluble cell extracts from G85S MNCs. Samples were applied to a Superdex 75 column (GE Healthcare) and eluted at 4°C in PBS containing IAM to avoid oxidation of disulphide-reduced SOD1 and collected in fractions for further analysis. The column was calibrated with standards including; blue dextran (2 kDa), thyroglobulin (669 kDa), ferritin (440 kDa), aldolase (158 kDa), conalbumin (75 kDa), BSA (69 kDa), ovalbumin (44 kDa), hSOD1 (32 kDa), and ribonuclease A (13.7 kDa). Misfolded SOD1 was analysed by misELISA. Total SOD1 (relative band intensity) was analysed by western blotting. The apparent molecular weight of the fractions representing each peak of misfolded or native SOD1 was determined in relation to the standards.

CytoTox-Glo Cytotoxicity Assay
The relative number of dead cells in a culture was analysed using the CytoTox-Glo Cytotoxicity Assay (Promega) in 96-well plates. This was used to quantify the number of live and dead cells following exposure to low O_2 tensions, or bortezomib treatment (Millennium Pharmaceuticals). The proportions of dead cells were determined by measuring a protease activity as an indicator of compromised cell membranes. Following protease release and cleavage of the AAF-aminoluciferin (AAF-Glo) substrate, which cannot enter living cells, aminoluciferin is released as a substrate, which is consumed by luciferase and produces a luminescent signal. This can be detected by a luminometer (Synergy 2 multi-mode microplate reader, Biotek). Once the signal from dead cells initially present in the culture has been measured, a detergent is added to lyse all cells and a second reading results in a measure of the total cell population. Thus, the relative proportion of dead cells following cell treatment can be quantified.

Proteasome analysis
The 20S core particle holds the constitutively expressed subunits β1 (caspase-like protease), β2 (trypsin-like protease) and β5 (chymotrypsin-like protease) sites, which are responsible for substrate cleavage. The activity of each subunit was determined by measuring cleavage of Z-nLPnLD-aminoluciferin for caspase-like activity, Z-LRR-aminoluciferin for trypsin-like activity and Suc-LLVY-aminoluciferin for chymotrypsin-like activity using Cell-Based Proteasome Glo assay (Promega). Following cleavage of each substrate, a luminescent signal was detected as described for the CytoTox-Glo Cytotoxicity Assay. The luminescent signal is proportional to the activity of each proteasome subunit in the sample.

***In vitro* translation and proteasome degradation (Paper II)**
In vitro translated proteins were used to investigate the degradation of SOD1 using purified proteasomes. SOD1 and ubiquitin-tagged GFP were translated using PureExpress protein synthesis kit (New England Biolabs). Human wt SOD1 was translated from a plasmid DNA template (pET-3a-wtSOD1; gift of Jens Danielsson, Stockholm University). The ubiquitin-GFP fusion protein template was generated by PCR from Ub-G76V-GFP [516]. Protein synthesis was conducted at 37°C and integrity of the product was established by western blotting. SOD1 and ubiquitin protein products were digested with purified proteasomes; 26S, 20S and i20S (all from Boston Biochem) in the absence, or presence, of MG132 (Sigma-Aldrich) to inhibit the proteasome. Reactions included DL-Dithiothreitol (DTT; Sigma-Aldrich) to prevent disulphide bond formation. Reactions were stopped at set time points by addition of SDS sample buffer and boiling for 5 min. Samples were run on 18% (w/v) Criterion TGX Precast gels (Bio-Rad Laboratories). SOD1 was quantified by western blotting using the SOD1 24-39 antibody (see Primary antibodies in Table 3) and band intensities were quantified using ImageLab software (Bio-Rad Laboratories).

Proteasome activity in cell extracts (Paper II)
Cells in culture media were trypsinized using trypsin/EDTA, pelleted at 1000 xg and washed in PBS before cells were lysed in buffer containing HEPES (pH 7.5), glycerol, Protease Inhibitor Cocktail (Roche), ATP and $MgCl_2$ and sonicated using a Sonifier Cell Disrupter (Branson). The lysate was centrifuged at 20,000 xg at 4°C, and the supernatants were snap-frozen before being stored at -80°C. Proteasome complexes were resolved in freshly-thawed lysates by native polyacrylamide gel electrophoresis (PAGE) in 3-8% (w/v) Criterion XT Tris-Acetate Precast gels (Bio-Rad Laboratories). Gels were incubated in a buffer with fluorogenic substrate Suc-LLVY-AMC (Boston Biochem) to measure the chymotrypsin-like activity in the resolved proteasome complexes. Gels were imaged under trans-UV illumination using a Chemidoc MP system and quantified using ImageLab software (Bio-Rad Laboratories).

Proteasome activity in cells (Paper II)
To visualize active proteasomes and their localization, live cells were labeled using Me4BodipyFL-Ahx3Leu3VS (Boston Biochem) before fixation and immunocytochemistry.

Immunocapture of misfolded SOD1
Misfolded SOD1 was immunocaptured using the rabbit anti-human SOD1 antibody raised against SOD1 sequence 24-39 coupled to Dynabeads M-270 Epoxy with the Dynabeads Antibody Coupling Kit. The beads were isolated magnetically, washed with the supplied buffers to remove unbound antibody and equilibrated with PBS containing Complete EDTA-free Protease Inhibitor Cocktail (Roche), IAM and Nonidet P-40 (Roche). Antibody-coated beads were incubated with cell extracts (20,000 xg fraction). The beads were washed extensively with PBS Complete EDTA-free protease inhibitor cocktail, IAM and Nonidet P-40 and bound proteins were eluted by boiling in SDS sample buffer containing IAM. Samples were analysed by non-reducing PAGE and western blotting.

Immunocytochemistry
Cells were cultured on nitric acid washed coverslips and fixed with formaldehyde (Sigma-Aldrich) for 10 min. at room temperature before immunostaining. Cells were permeabilized and blocked using Triton X-100 (Sigma-Aldrich) and FBS in PBS before incubation with primary antibody at 4°C overnight. Secondary antibody (Alexa Fluor conjugated) incubation was done for 1 h at room temperature and nuclei were counterstained with 4',6-diamidino-2-phenylindole (DAPI, Sigma-Aldrich) in PBS. Coverslips were mounted in Fluorescence Mounting Medium (Dako) on glass slides before images were obtained using confocal microscopy (Nikon A1) and pictures processed using Fiji image analysis software [517]. A list of antibodies used is summarized in Table 3.

Western Blotting
Western blotting was performed according to standard procedures using AnyKD or 18% Criterion TGX precast gels and Trans-Blot Turbo Midi

Nitrocellulose membranes (Bio-Rad Laboratories). Protein concentrations were determined using the BCA method (Pierce BCA Protein Assay Kit). The amount of disulphide-reduced and -oxidized SOD1 was determined using non-reduced gels by omitting 2-mercaptoethanol and adding IAM to the sample buffer [202, 203, 518].

Primary antibodies, raised in rabbit against human SOD1 peptide sequences (24-39, 57-72 or 144-153) [280], were used for detection of soluble misfolded SOD1 and detergent insoluble aggregates (see section 'Sample Fractionation' for extract preparation). Total SOD1 concentration in the extracts was determined using a known human SOD1 standard [219]. Primary incubation was done at 4°C overnight followed by secondary horseradish peroxidase (HRP)-conjugated polyclonal anti-rabbit IgG (Dako) for 1 h at room temperature with several washing steps in between. The signal was detected using ECL Chemiluminescent Detection Reagent (GE Healthcare) and measured with a ChemiDoc imaging system (Bio-Rad Laboratories). Quantification was performed using ImageLab software (BioRad Laboratories) and the amount of misfolded SOD1 was determined by comparison to a SOD1 standard normalized to anti-β-actin as a loading control.

Statistical analysis

Statistical analysis was performed using GraphPad Prism version 6.0h for Mac OS X (GraphPad Software). Data include a minimum of 3 technical replicates in each experiment performed on a minimum of 3 independent sets, referred to as n = 3 unless stated. Multiple groups were compared using one-way analysis of variance (ANOVA) with Tukey's post hoc test for multiple comparisons. Unpaired two-tailed Student's t-test was used to determine significance between two groups. F-test was used to test for variance between treated an untreated group followed by Welch's test for unequal variance and unpaired t-test for equal variance. A significance level of 0.05 was used for all analysis and results are presented as +/- SD.

Table 3 Primary antibodies used for immunocytochemistry and western blotting

Antibody	Source	Conentration
Immunocytochemistry		
GFAP	DAKO, clone 6F2	1:1000
Hoxb4	DSHB, I12	1:20
HuNu	Chemicon, clone 235-1, MAB 1281	1:100
ISLET1/2	DSHB, 39.4D5	1:50
LCN2	Sigma Aldrich, HPA002695	1:50
MAP2	Millipore, MAB3418A5	1:500
MAPT	Sigma Aldrich, T9450	1:2000
Peripherin	Millipore, ab1530	1:100
S100B	Sigma Aldrich, HPA015768	1:200

SMI31	Covance, SMI-31R	1:1000
SMI32	Covance, SMI-32R	1:1000
TUBB3	Covance, PRB-435P	1:7500
Vimentin	Progene, gp53	1:1000
Western blotting		
β-actin	Millipore, MAB1501R	1:200 000
CCS 252-270	Agrisera	0.9 µg/ml
GAPDH (14C10)	Cell signalling, #2118	1:1000
Glutaredoxin	R&D Systems, AF3399	1:2000
Grp78	Novous Biologicals, NB100-91794	1:5000
HIF-1α	BD Biosciences, 610958	1:500
LC3B	Sigma Aldrich, L7543	1:1000
SOD1 24-39	Agrisera	2.3 µg/ml
SOD1 57-72	Agrisera	1.6 µg/ml
SOD1 144-153	Agrisera	5.2 µg/ml
Ubiquitin	Cell Signalling, #3933	1:1000

Results

Paper I
Effects of Cellular Pathway Disturbances on Misfolded Superoxide Dismutase-1 in Fibroblasts Derived from ALS Patients

Mutations in the *SOD1* gene are associated with a toxic gain of function phenotypes in ALS. Several cellular pathways are disrupted in ALS, including protein degradation by the UPS [289, 317] and autophagy [334, 338, 519] but also induction of ER-stress [351, 352, 355] and mitochondrial dysfunction [383, 384, 520]. The toxic phenotypes are related to misfolded mutant SOD1 and proteotoxicity in FALS, but the pathogenesis of the disease is not understood. Moreover, it is not clear which of these phenotypes are primarily caused by misfolded SOD1 and which are secondary effects of proteotoxic stress, which in turn could promote SOD1 misfolding. Studies regarding mutant SOD1 toxicity have mainly been performed in transgenic models overexpressing human mutant SOD1. High levels of mutant protein expression influences the disease phenotype [217, 521] and induces abnormal protein interactions [387], which could lead to an incomplete understanding of ALS pathogenesis.

The aim of this study was to determine the possible relationship between disturbances in cellular pathways that are involved in ALS and misfolded SOD1. To analyze the misfolded protein at a physiological level of *SOD1* expression, we utilized a set of fibroblast lines from FALS patients (carrying *SOD1* and *C9ORF72* mutations) and non-disease controls. Cells were subjected to pharmacological treatments to disrupt cellular pathways involved in protein homeostasis and energy production. The levels of soluble misfolded, as well as native/total, SOD1 were quantified in cell extracts via a misfolded SOD1 specific (misELISA), or a total SOD1 ELISA, respectively. Detergent-insoluble (aggregated) SOD1 was analysed by western blotting.

Levels of SOD1 protein analysed by western blotting varied between patient-derived lines (Paper I, Figure 1A-B). Lines carrying mutant proteins including D90A, G93A and N86S expressed similar amount of protein to wt SOD1 in controls. However, in A4V, H46R, E78_R79insSI and L117V lines, levels were slightly reduced. In contrast, only the wt SOD1 protein (expressed from the wt allele) was detected in the truncated SOD1 mutants D125Tfs*24 and G127X by western blotting, since they are unstable and rapidly degraded.

Misfolded SOD1 can be degraded by the UPS [289, 317, 522-524]. To investigate SOD1 degradation by the proteasome, we used the proteasome inhibitor bortezomib (5 ng/ml for 24 h [525]). Increased levels of soluble misfolded SOD1 were found in all SOD1 lines, non-*SOD1* FALS and non-disease control lines after this treatment (Paper I, Figure 2A-B). Levels of total SOD1 also increased in the majority of lines (Paper I, Figure 2C) but were not the cause of the elevation of misfolded SOD1 as an increase was also seen following normalization to total SOD1 levels (Paper I, Figure 2B). Hence, both mutant and wt misfolded SOD1 are degraded by the

proteasome. Increased levels of soluble misfolded SOD1 are not due to enhanced SOD1 expression.

Detergent insoluble SOD1 is degraded by autophagy [334, 337, 519]. The role of autophagy in the degradation of soluble misfolded SOD1 was investigated by utilizing 3-MA (10 mM for 24 h [526]) resulting in a moderate inhibition of autophagosome formation (Paper I, S1 Figure C). Under these conditions, soluble misfolded SOD1 did not increase significantly. On the contrary, levels were decreased to varying extents in all *SOD1* FALS lines tested, whereas misfolded SOD1 in non-disease controls and *C9orf72* cells remained unaffected or slightly increased (Paper I, Figure 2D-E). 3-MA is not a specific inhibitor of autophagy [331] and it is possible that either use of other inhibitors, such as chloroquine or Bafilomycin A1, which inhibits autolysosome formations, or prolonged treatment, would have affected the clearance of misfolded SOD1.

Misfolded SOD1 induces ER-stress [352, 353, 355, 357], a response that is initially protective through the activation of the UPR [343, 345, 346, 527]. To investigate the effect of ER-stress on SOD1 misfolding we treated cells with tunicamycin, which is commonly used to induce ER-stress [528]. Tunicamycin is an antibiotic that inhibits N-linked glycosylation and leads to UPR due to an accumulation of improperly folded glycoproteins in the ER [529]. Strong induction of ER-stress was observed following tunicamycin treatment (0.5 µg/ml, 24 h), as measured by the induction of the ER-chaperone GRP78 (Paper I, S1 Figure C). However, no clear changes of soluble misfolded SOD1 levels were detected (Paper I, Figure 3A-B). These results suggest that induction of ER-stress does not increase misfolded SOD1 species fibroblasts. However, it cannot be ruled out that in other cell types such as MNs, chronic ER-stress may lead to an increase in misfolded SOD1 levels.

Misfolded SOD1 also causes early alterations in morphology and transportation of mitochondria [357, 381, 530, 531]. The effect of inhibiting mitochondrial ATP production on levels of soluble misfolded SOD1 was investigated by using rotenone, an inhibitor of the mitochondrial respiratory chain complex I ([532]; 24 h, 5 mM). As seen with 3-MA treatment, soluble misfolded SOD1 levels decreased in all *SOD1* FALS lines tested, whereas in non-disease controls and *C9ORF72* lines, the levels remained largely unchanged (Paper I, Figure 3D-E). Hence, disruption of mitochondrial function does not result in increased levels of misfolded SOD1.

Soluble misfolded SOD1 monomers are the template for SOD1 aggregation [199, 200, 213] Hence, a lack of response in soluble misfolded SOD1 levels could indicate that misfolded monomers are recruited to form insoluble aggregates [338]. Therefore, we also quantified the amount of detergent insoluble SOD1 following the various pharmacological interventions (Paper I, Figure 4 and Table 1). Proteasome inhibition led to an increase in detergent insoluble SOD1 aggregates in *SOD1* FALS lines carrying A4V, H46R, G93A, G127X and D125Tfs*24 mutations. Levels of aggregation in other FALS lines, as well as in controls, were below the detection limit of the assay, even following bortezomib treatment (Paper I, Figure 4 and Table 1). The truncation mutants D125Tfs*24 and G127X were the only ones with distinct aggregation in the absence of pharmacological intervention and the same lines also had the most significant accumulation of aggregated SOD1

after proteasome inhibition. Hence, the aggregation propensity of SOD1 differs between mutations.

In summary, patient-derived fibroblasts offer a useful model with which to study misfolded SOD1 in relation to known cellular disturbances in ALS. Using this model we were able to recapitulate an increase in both soluble and aggregated misfolded protein, which is a characteristic phenotype of *SOD1* FALS *in vivo*. Soluble misfolded SOD1 was evident in *SOD1* FALS, as well as non-disease control and non-*SOD1* FALS lines containing wt SOD1. However, proteasome inhibition was the only intervention tested that led to a significant increase in the levels of soluble misfolded and aggregated SOD1. Interestingly, proteasome activity is altered in *SOD1* FALS models at symptomatic stages of disease [315-317, 524] and in SALS patients [319]. Protein homeostasis is important for cellular health, particularly in postmitotic MNs [533] and has been suggested to decline with age [320, 534]. Our results suggest that an age-related decline in proteasome activity could be associated with accumulation of misfolded SOD1, and contribute to mid-life onset of ALS.

Paper II
Enhanced protein misfolding in patient-derived models of amyotrophic lateral sclerosis.

Aggregates of misfolded SOD1 are typically present in both FALS and SALS MNs, as well as in astrocytes [83, 90, 280, 281]. However, it is not known why misfolding and aggregation of the ubiquitously expressed SOD1 protein elicits the selective degeneration of MNs. We have previously established a model in which misfolded SOD was analysed under a physiological level of SOD1 expression in patient-derived fibroblast [212]. To investigate misfolded SOD1 in cells more relevant to ALS, we used patient-derived fibroblast that were reprogrammed to iPSCs and differentiated them to MN cultures [4, 488, 489]. In this model system, we investigated whether misfolded SOD1 is specifically enhanced in patient-derived MNs and astrocytes, which could help to explain their specific vulnerability in ALS.

We utilized a set of cell lines from FALS patients (*SOD1* and non-*SOD1*), a SALS patient and non-disease controls as well as human *SOD1* expressing mESC-derived MNC lines (Paper II, Supplemental Table 1). Using the same misELISA as in Paper I, we first compared levels of misfolded SOD1 between patient-derived fibroblasts, iPSCs and iPSC-derived MNCs (Paper II, Figure 1A, S1 and Supplemental Table 2) from two non-disease control lines. Levels of misfolded SOD1 were elevated in MNCs compared to non-neuronal cells in both lines (Paper II, Figure 1B). Hence, increased misfolding of wt SOD1 is present in MNCs, even in the absence of a *SOD1* mutation.

We continued to analyse misfolded SOD1 in ALS patient-derived MNCs (Paper II, Figure 2A and S1). Non-*SOD1* FALS (with mutations in *FUS, TARDBP* and *ANG*), as well as SALS MNCs, had similar levels of misfolded wt SOD1 to MNCs from non-disease controls (Paper II, Figure 2B). However, *SOD1* FALS lines with L144F and G85S mutations had significantly enhanced levels of misfolded SOD1. Compared to control

MNCs, misfolded SOD1 was elevated 2-fold in L144F MNCs and 80-fold in G85S (Paper II, Figure 2B).

We further compared patient-derived MNCs with MNCs differentiated from mESCs overexpressing human wt or G93A mutant *SOD1* (Paper II, Figure 2A and S2A). Despite a 6-fold higher expression of wt SOD1, the levels of misfolded SOD1 were comparable between non-disease patient lines and the wt mouse MNCs (Paper II, Figure 2B and S2B). The level of SOD1 overexpression was not as high in the G93A mouse MNC compared to *SOD1* FALS MNCs (3-fold, Paper II, Figure S2B). However, the amount of misfolded protein in the murine cells was elevated 230-fold (Paper II, Figure 2B). Hence, although the amounts of misfolded SOD1 in patient-derived MNCs vary between patient lines, levels are significantly enhanced over non-disease controls and considerably lower than the amounts in the G93A mouse model.

To test if the increase in misfolded SOD1 was specific to MNCs, we compared them with differentiated sensory neuron cultures (SNCs), since sensory neurons are not a primary target of ALS (Paper II, Figure 2C). We detected significantly elevated levels of misfolded protein in SOD1 A4V MNCs compared to SNCs (Paper II, Figure 2D). Hence, SOD1 misfolding is enhanced in MNCs. We cannot conclude whether SOD1 is less stable in MNCs or if it is less efficiently degraded. Nevertheless, we show inherently elevated SOD1 misfolding in ALS-susceptible MNCs compared to other neuronal and non-neuronal cell types.

Increased SOD1 misfolding could result from unknown genetic factors in the MNCs. To determine if elevated misfolded SOD1 levels are dependent on a *SOD1* mutation we utilized iPSCs carrying a *SOD1* A4V mutation and its isogenic control where the mutation has been corrected to wt [357, 376]. Total SOD1 ELISA showed decreased SOD1 expression in the A4V mutant MNCs compared to the isogenic line with wt *SOD1* (Paper II, Figure S2D). This is likely to reflect the reduced stability of mutant SOD1 in the *SOD1* A4V lines. Yet, the level of misfolded SOD1 was increased in *SOD1* A4V line (Paper II, Figure 2D).

The *SOD1* A4V and isogenic control iPSCs were also differentiated to SNCs (Paper II, Figure 2C). Interestingly, as seen in MNCs, A4V SNCs also had reduced SOD1 expression (Paper II, Figure S2D) as well as enhanced levels of misfolded protein compared to the isogenic line (Paper II, Figure 2D). Therefore, SOD1 misfolding is increased in MNCs in the presence of a SOD1 mutation.

Degeneration of motor neurons is a hallmark of ALS pathology [7, 13, 101]. MN toxicity is both cell-autonomous [419] and non-cell autonomous involving astrocytes [268, 271, 424-426, 445, 535]. However, the relative levels of misfolded SOD1 in astrocytes and MNs are not known. The cultures of patient-derived MNC contain both MNs and proliferating astrocytes (Paper II, Supplemental Table 2). By subculturing MNCs in serum-containing media, we generated pure iPSC-derived astrocyte cultures (iPSC-Astros) (Paper II, Figure 3A). Using the iPSC-Astros and the misELISA assay, we could investigate the levels of misfolded SOD1 in astrocytes.

Total SOD1 levels in G85S iPSC-Astros (Paper II, Figure 3A panel a-d) were comparable to those of MNCs (Paper II, Figure S3A). However,

misfolded SOD1 was significantly increased in G85S iPSC-Astros compared to MNCs (Paper II, Figure 3B). Elevated misfolded SOD1 was also present in A4V iPSC-Astros compared to MNCs (Paper II, Figure 3C). Thus, increased misfolded SOD1 is not only a feature of MNs but also present in iPSC-Astros. In contrast to A4V iPSC-Astros, G85S astrocytes were small and contained very little cytoplasm with disorganized filaments (Paper II, Figure 3A and S3C). High levels of misfolded SOD1 in such G85S iPSC-Astros could be responsible for the increased levels of misfolded SOD1 in G85S MNCs (Paper II, Figure 2B). We addressed this question by seeding MNCs on a confluent layer of mouse primary astrocytes (Paper II, Figure 3A, panel i-k). These MNC cultures contained 82% neurons of which half were MNs (Paper II, Supplemental Table 2). In these co-cultures, misfolded SOD1 in G85S MNCs was decreased to levels similar to those of A4V MNCs (Paper II, Figure 3B-C). Hence, the highly proliferative iPSC-Astros were mainly accountable for the very high levels of misfolded SOD1 in G85S MNCs. However, our results could not determine if the high levels of misfolded SOD1 were responsible for the altered phenotype of G85S astrocytes.

SOD1 aggregates are a hallmark of *SOD1* FALS [536, 537] and are also found in non-*SOD1* FALS patients [90, 280, 281]. Soluble misfolded SOD1 in *SOD1*-FALS transgenic mouse models lack the stabilizing C57-C146 intrasubunit disulphide bond [202, 203], which is important for protein stability [175, 176]. Disulphide-reduced SOD1 species are the substrate for aggregation [199, 200, 213], which implicate them in the propagation of disease. However, the form of soluble misfolded SOD1 in patient-derived cells in not known. To address this question, we characterized soluble misfolded SOD1 in patient-derived G85S MNCs by size exclusion chromatography [202] and immunocapture. Size exclusion chromatography was used to fractionate extracts of G85S MNCs in which misfolded SOD1 was analysed by misELISA and total SOD1 by western blotting (Paper II, Figure 4A). Similar to *SOD1* FALS mouse models [202], the majority of misfolded SOD1 in patient-derived MNCs was found to be highly disordered monomers. To investigate the disulphide status of the monomers, we immunocaptured misfolded SOD1 using the same antibody as in the misELISA assay. By using non-reducing native PAGE and western blotting, the majority of SOD1 in A4V MNCs and iPSC-Astros was identified as oxidized with intact disulphide bond. However, following immunocapture, all of the misfolded SOD1 monomers were disulphide-reduced. The amounts also increased with proteasome inhibition using bortezomib (Paper II, Figure 4B). Hence, soluble misfolded SOD1 in patient-derived MNCs and astrocytes exists as disulphide-reduced and disordered monomers.

As previously stated, disulphide-reduced and misfolded SOD1 species are the substrate for aggregation *in vivo*. However, the relationship between soluble and aggregated SOD1 in patient-derived MNCs in not known. We investigated this by analysing soluble and aggregated misfolded SOD1 in MNCs from G85S and non-disease control line as well as in MNCs from A4V and its isogenic control line. We treated the MNCs with bortezomib to enhance levels of misfolded SOD1 and analysed soluble levels by misELISA and insoluble aggregates using western blotting. Proteasome inhibition increased levels of soluble misfolded SOD1 in MNCs. The increase ranged

from 1.2-fold in non-disease controls to 1.8-fold in G85S MNCs. (Paper II, Figure 4C). However, aggregation only increased significantly in A4V MNCs (Paper II, Figure 4D). Thus, levels of soluble and aggregated misfolded SOD1 do not necessarily correlate and differ between G85S and A4V mutations.

Soluble misfolded monomers become depleted as aggregation progresses *in vivo* [338]. This could possibly explain the different levels of soluble and aggregated misfolded SOD1 found in A4V and G85S lines. However, the events leading to the initiation of aggregation are unknown. Misfolded proteins are generally degraded by the UPS [291, 312] and proteasome degradation can either be ubiquitin (Ub)-dependent (26S), or Ub-independent (20S) [286, 300, 301]. In the immunocapture analysis, we did not identify any SOD1 species with a higher molecular weight that would suggest that SOD1 was ubiquitinated (Paper II, 4B). Hence, the apparent lack of ubiquitination suggests that misfolded SOD1 is degraded by the 20S proteasome.

To investigate whether misfolded SOD1 is degraded through a ubiquitin-independent mechanism, we generated unfolded SOD1 by *in vitro* translation. The efficiency of degradation by purified 26S, 20S or i20S proteasomes over a 4 h time course was quantified by western blotting using an antibody recognizing misfolded SOD1. We first confirmed that the 26S proteasome degraded an ubiquitin-GFP fusion protein [516] more efficiently than the 20S proteasome (Paper II, Figure S4A). When analysing SOD1, no signification degradation was detected by the 26S proteasome (Paper II Figure 5A). However, SOD1 was degraded efficiently by 2 h by the 20S proteasome (Paper II, Figure 5B). We also tested the i20S proteasome, which is upregulated in early stages of disease in ALS mouse models [317, 523]. The i20S proteasome degraded SOD1 but much less efficient compared to the 20S proteasome (Paper II, Figure 5C). Hence, we can conclude that misfolded SOD1 is a substrate for degradation by the ubiquitin-independent 20S proteasome.

The difference in misfolded SOD1 levels that we identified between cell types (Paper II, Figure 1B, 2D and 3B-C) and mutations (Paper II, Figure 2B, 2D and 3B-C) could stem from dissimilarities of 26S and 20S proteasomes activities. We investigated this by analyzing the activities of 26S and 20S proteasome in MNCs, iPSC-Astros and SNCs using the A4V and isogenic control lines. Cell extracts were separated by native PAGE and activities measured by hydrolysis of fluorogenic substrate suc-LLVY-AMC. The relative activities of 26S and 20S were similar across cell types for both A4V and isogenic controls (Paper II, Figure 5D-F and S4B). Furthermore, we did not identify any differences in the ratio of 26/20S between A4V and isogenic controls in any of the cell types (Paper II, Figure S4C). Hence, no differences in proteasome activity could be detected in the patient-derived cultures. However, when labeling MNCs with a proteasome activity probe, we did discover a difference in proteasome distribution between MNs and astrocytes. Proteasomes were located in the nucleus in both cell types (Paper II, Figure S4D). However, in contrast to astrocytes, MNs also had active proteasomes distributed throughout the cytoplasm. The difference in proteasome distribution in MNCs was present in both A4V and isogenic control lines (Paper II, Figure S4D). Hence, we did detect a difference in

localization of proteasomes in the patient-derived MNC and astrocytes, but the increased levels of misfolded SOD1 do not seem to be due to a dysfunctional proteasome system.

In summary, we have shown that misfolded SOD1 is elevated in patient-derived MNC and astrocyte cultures, which could explain their vulnerability and involvement in ALS. Misfolded SOD1 in patient-derived cells exists as the same disulphide-reduced monomeric form as in murine overexpressing models and is a substrate for degradation by the 20S proteasome. These findings show that iPSC-derived models can serve as a foundation from which to understand the mechanisms that lead to SOD1 misfolding and pathological alterations in ALS.

Paper III
Low oxygen tension induces misfolding and aggregation of superoxide dismutase 1 in ALS patient-derived motor neurons.

Holo-SOD1 is an extremely stable protein [538]. An important determinant of its stability is the intrasubunit disulphide bond [175, 176]. The status of the disulphide bond is regulated through oxidation of C57 and C146 in SOD1 [175, 176], which can be CCS-independent or CCS and O_2-dependent [185, 193, 539, 540]. However, to achieve full SOD1 maturation and activation, both CCS and O_2 are required [175, 191]. Disulphide-reduction on the other hand is performed by glutaredoxin and GSH [540].

GSH is the main cellular redox buffer and scavenger of ROS [155]. The ratio of GSH/GSSG in the ER ranges between 3:1 to 1:1 [541] creating an oxidizing environment that facilitates the formation of disulphide bonds within newly synthesized proteins. The cytosol typically has a GSH/GSSG ratio of 30/1 or 100/1 and is highly reducing [155] and thus not favourable for maintaining oxidized disulphide bonds. Since SOD1 is mainly located in the reducing cytoplasm of cells, the disulphide bond is a potential Achilles heel for the stability of the protein [204]. However, formation of the disulphide bond in SOD1 is not associated with the GSH/GSSG ratio, but dependent on oxidation by O_2 catalyzed by CCS [175, 185, 191, 542]. Hence, O_2 availability could be a determinant of SOD1 stability.

Soluble misfolded SOD1 exists as disulphide-reduced monomers in mouse models expressing human mutant and wt *SOD1* [202, 203]. Reduced SOD1 monomers are substrates for aggregation [199, 200, 213] and a major component of aggregates *in vivo* [201, 543]. We have further demonstrated enhanced levels of misfolded, disulphide-reduced monomers in patient-derived MNCs (Paper II). However, whether decreased O_2 tensions affect SOD1 *in vitro* has not been tested. To investigate factors impacting on SOD1 misfolding in patient-derived cells, we analysed the role of O_2 tensions and redox status of the disulphide bond on the stability of SOD1.

Cell cultures are typically maintained under 19% O_2 tension *in vitro*. However, the levels in the CNS range between 0.2-5% making standard cultures hyperoxic rather than normoxic [544, 545]. We characterized levels of misfolded and aggregated SOD1 in patient-derived fibroblasts and MNCs cultured under O_2 tensions ranging from 19% (standard conditions) down to 1%, which we have referred to as low oxygen tension, or hypoxia. Misfolded

SOD1 was characterized in *SOD1* FALS, non-*SOD1* FALS and non-disease control lines by misELISA, immunocapture and western blotting.

We have established that patient-derived fibroblasts are a useful model with which to study misfolded SOD1 (Paper I). Therefore, exposure to low O_2 tensions (1-5% for 24 h) was first investigated in fibroblast lines. Culture under 1% O_2 induced the strongest hypoxic response as measured by induction of hypoxia inducible factor 1 alpha subunit (HIF1A) expression in non-disease control lines with wt *SOD1* as well as *SOD1* A4V, G93A and G127X fibroblast lines (Paper III; Figure 1A-B). Hence, 1% O_2 tension was used to examine the effect of hypoxia on SOD1 misfolding by misELISA. Enhanced levels of misfolded SOD1 cultured at 1% O_2 tension was evident in a range of full-length *SOD1* mutant fibroblast lines as well as in non-*SOD1* FALS and control lines with wt *SOD1* (Paper III, Figure 1C and S1). The truncated G127X and D125Tfs*24 lines, which lack C146 and cannot form the disulphide bond, did not exhibit increased misfolded SOD1 when cultured under low O_2. Hence, enhanced SOD1 misfolding in patient-derived fibroblasts in response to hypoxic conditions is dependent on the presence of the C57-C146 disulphide bond. A dose-dependent increase of soluble misfolded SOD1 was seen in the E78_79insSI and N86S fibroblasts but not in the truncated G127X mutation line (Paper III, Figure S2A). The response in the E78_79insSI and N86S fibroblasts also increased with time when comparing 1 h-4 h-8 h and 24 h exposures (Paper III, Figure S2B). Hence, the enhanced levels of misfolded SOD1 in response to low O_2 were both dose- and time-dependent in fibroblasts.

We have previously established that misfolded SOD1 is enhanced in patient-derived MNCs (Paper II). To test if reduced O_2 tension affected misfolded SOD1 in MNCs, we exposed cultures to low O_2 (19% vs 2% for 24 h) and analysed misfolded SOD1 by misELISA (Paper III, Figure S4 and S5). Culture under low O_2 tension (1% for 24 h) resulted in axonal fragmentation detected by immunocytochemical staining using antibodies against TUBB3, MAP2 and SMI32. This was rarely observed under 2% for 24 h (Paper III, Figure S5). Moreover, these conditions did not affect the viability of MNCs as measured by quantification of an assay for plasma membrane integrity or ATP levels (Paper III, Figure S6A-B). Hence, the investigated O_2 tensions were not cytotoxic. MNCs cultured under hypoxic conditions demonstrated more pronounced misfolding of SOD1 compared to the corresponding fibroblasts (Paper III, Figure 3 and S7A). The effect was largest in full-length mutant SOD1 lines but also evident in the control lines expressing wt *SOD1*. In contrast to fibroblasts, MNCs lines lacking the C57-C146 disulphide bond (G127X and D125Tsf*24) also demonstrate enhanced misfolding (Paper III, Figure 3). We hypothesize that this is a result of increased wt SOD1 misfolding, which is more prominent in MNCs compared to fibroblasts. Similar to fibroblasts, we also identified a dose-response to O_2 in MNCs (Paper III, Figure 4).

Proteasome inhibition led to elevated levels of misfolded soluble and aggregated SOD1 in patient-derived fibroblasts (Paper I) and MNCs (Paper II). Enhanced levels of misfolded SOD1 could result from compromized proteasome activity in cells cultured under hypoxic conditions. When analysing the chymotrypsin-like activity of the proteasome in *SOD1* FALS

lines cultured under low O_2 tension (19% vs 2% for 24 h), no consistant changes were detected (Paper III, Figure S7B). Hence, increased levels of misfolded protein were not a result of compromised proteasome activity.

To determine the disulphide status of SOD1 in response to low O_2 tension (2% for 24 h), we analysed MNCs extracts by non-reducing PAGE and western blotting, also following immunocapture. Disulphide-reduced SOD1 can be distinguished from oxidized SOD1 by its' migration pattern since oxidized SOD1 migrates faster in non-denaturing PAGE than reduced SOD1 (Paper III, Figure 5A). We detected an increased proportion of disulphide-reduced SOD1 following culture under 2% O_2 tension in all *SOD1* FALS MNC lines, as well as in non-disease control lines with wt *SOD1* (Paper III, Figure 5B). This was further supported by immunocapture where an antibody to misfolded SOD1 (same as the one used in the misELISA) only captured disulphide-reduced SOD1 (Paper III, Figure 6). Hence, exposure to low O_2 tension increase the levels of reduced misfolded SOD1 species in MNCs *in vitro*.

Disulphide-reduced and misfolded SOD1 lead to aggregation *in vitro* [199, 200, 213] and *in vivo* [201, 543]. To determine the effect of O_2 tension on aggregate formation in our cell model, we cultured MNCs under low O_2 tension (2% for 24 h) and quantified detergent-insoluble aggregates by western blotting. No significant increase in aggregation was seen in the H46R MNCs. However, increased aggregation was evident in E78_79insSI, N86S, G93A and A4V *SOD1* FALS MNCs (Paper III, Figure 7). Hence, reduction of disulphide bond in response to low O_2 tension was associated with increased aggregation in patient-derived cells.

The status of the disulphide bond is regulated by CCS and glutaredoxin [540 175, 176]. We did not detect and differences in their levels in response to low O_2 (Paper III, Figure 8). Hence, altered levels of CCS or glutaredoxin were not the cause of SOD1 dilsulphide-reduction.

As a main mediator of cellular redox balance, together with SOD1, GSH is a scavenger of ROS, and its ratio to GSSG can be used as a marker of oxidative stress. Therefore, the ratio of GSH/GSSG is expected to increase in cells cultures under low O_2 tension due to the decreased production of ROS and thus reduced demand of GSH. We determined the effect of low O_2 tension (1% or 2% for 24 h in fibroblast and MNCs, respectively) on the levels of GSH and GSSH in the cultures. GSH was significantly elevated in MNC compared to fibroblasts (Paper III; Figure 9A) and GSSG levels were extremely low in fibroblasts (Paper III; Figure 9B). This resulted in a very high ratio of GSH/GSSG in fibroblast compared to MNCs (Paper III, Figure 9C). However, we did not detect any clear changes in response to low O_2.

In conclusion, we demonstrate that enhanced reduction of the C57-C146 bond, misfolding and aggregation of SOD1 is dependent on the O_2 tension in patient-derived cells *in vitro*. Disulphide-reduction and SOD1 misfolding promote nucleation and growth of SOD1 aggregates. Hence, areas with sustained low oxygen perfusion could serve as a potential initiation site of ALS *in vivo*.

Paper IV
A Novel mutation D96Mfs*8 in *SOD1* identified in a Swedish ALS patient results in a truncated and heavily aggregation-prone protein

SOD1 aggregates are implicated in the pathology of ALS and are a key feature of both FALS and SALS [83, 280-282]. Truncation mutations lacking C146 are unable to fold natively making the proteins highly unstable and demonstrate increased aggregation compared to full-length mutant SOD1 (Paper I and III). Mutations including G127X and D125Tfs*24 cause ALS with no clinical [211] or neuropathological [90] differences compared to missense mutations in *SOD1*. Moreover, no null mutation has been identified in ALS. Hence, *SOD1* ALS pathology is not dependent on the presence of full-length SOD1.

Nonsense-mediated mRNA decay protects against translation of mRNA with premature stop codons, expression of which could be toxic to cells [546]. G127X and D125Tfs*24 SOD1 are translated, but mutant proteins are efficiently degraded *in vitro* (Paper I) [212]. The shortest pathogenic *SOD1* mutation described so far is the V118X mutation, which is 121 residues long including four non-native amino acids and a stop codon [547]. We have previously determined increased levels of misfolded SOD1 in patient-derived fibroblasts (Paper I) [212] and MNCs, where soluble misfolded monomers are disulphide-reduced (Paper II). However, it is not known which part(s) of SOD1 peptide sequence are required for misfolded SOD1 pathogenicity. To further investigate this important question, we characterized a novel D96Mfs*8 *SOD1* mutation in patient-derived cells *in vitro*.

The D96Mfs*8 mutation has a heterozygous deletion of a G-nucleotide in codon 96 in the *SOD1* sequence. The deletion induces a frameshift and a neopeptide of seven non-native amino acids followed by a stop codon. The stop codon causes an early truncation where part of the C-terminal sequence is absent, including C146, which is important for stabilization of the intrasubunit disulphide bond (Paper IV, Figure 1). To our knowledge, this is the shortest SOD1 peptide described. The mutation was identified in an individual diagnosed with ALS at 57 years of age after an asymmetrical onset of paresis and muscle wasting, initially in the left leg. Disease progression was slow, and 48 months after onset, the patient continues to use an electrical wheel chair for transportation and shows no signs of sensory or cognitive impairment. When investigating the family history, the patient's father was identified as mutation carrier, whom despite advanced age shows no signs of neurological disease (Paper IV, Figure 1).

The truncated D96Mfs*8 protein contains a seven amino acid long, positively charged, C-terminal neo-peptide (Paper IV, Figure 1). To investigate whether the D96Mfs*8 mutant protein led to increased levels of misfolded SOD1, we analysed fibroblasts derived from both the ALS patient and the unaffected mutation carrier. Soluble misfolded SOD1 was analysed by misELISA. We compared misfolded SOD1 in the novel D96Mfs*8 mutation with the common and frequently studied A4V and G93A mutations, as well as the G127X truncation mutation and wt SOD1 in a non-disease control. D96Mfs*8 protein expression was reduced compared to wt

SOD1 in the non-disease control fibroblasts but similar to other *SOD1* FALS mutations (Paper IV, Figure S1A). Enhanced levels of soluble misfolded SOD1 was identified in the D96Mfs*8 patient line as well as in the non-affected mutation carrier by misELISA (Paper IV, Figure 2A). The amount of misfolded SOD1 was in the same range as those in A4V, G93A and G127X mutations.

We have previously shown that proteasome inhibition leads to enhanced levels of soluble misfolded SOD1 in patient-derived fibroblasts (Paper I) [212] and MNCs (Paper II). Significantly elevated levels of soluble misfolded SOD1 was also evident in in the D96Mfs*8 lines following proteasome inhibition (Paper IV, Figure S1B). However, there was no apparent difference in amounts of soluble misfolded protein in fibroblasts between the D96Mfs*8 patient line and the unaffected carrier (Paper IV, Figure 2A and S2B).

The net charge of SOD1 is important for its propensity to aggregate [548]. SOD1 has a net negative and repulsive charge that counteracts aggregation to maintain the protein in solution [195]. The neo-peptide sequence in the D96Mfs*8 modified the protein's charge and makes it more positive (Paper IV, Figure 1). Moreover, aggregation is favored by the presence of reduced, misfolded SOD1 monomers [199, 200, 213]. However, truncated proteins are highly unstable and quickly degraded *in vitro* [212] and whether the structural changes in D96Mfs*8 affect aggregation of misfolded SOD1, is not known.

We used western blotting to analyze insoluble SOD1 aggregates in the same patient-derived fibroblast extracts as previously used to determine soluble misfolded SOD1 by ELISA. Proteasome inhibition using bortezomib (5 ng/ml, 24 h) was included to enhance levels of misfolded SOD1. The D96Mfs*8 truncated SOD1 protein, estimated to a molecular weight of about 10 kDa, was not detected in the soluble fraction by western blotting (Paper IV, Figure 2B) indicating that soluble misfolded SOD1 is quickly degraded by the proteasome. However, aggregates of insoluble D96Mfs*8 truncated protein were present in the pellet fraction following proteasome inhibition (Paper IV, Figure 2B). Hence, D96Mfs*8 SOD1 aggregates readily and can be detected in patient-derived fibroblasts.

D96Mfs*8 was also characterized in patient-derived MNCs (Paper IV, Figure S1C). Levels of soluble misfolded SOD1 was enhanced in both D96Mfs*8 patient and mutation carrier MNCs compared to wt *SOD1* in non-disease control MNCs analysed by misELISA (Paper IV, Figure 2C). Interestingly, in contrast to fibroblasts, soluble misfolded SOD1 was increased in the patient line compared to the non-affected mutation carrier (Paper IV, Figure 2C). Hence, soluble misfolded SOD1 is increased in D96Mfs*8 MNCs and further elevated in the ALS-patient line.

We also tested inhibition of the proteasome with bortezomib (5 ng/ml, 8 h) to increase levels of misfolded SOD1 in MNCs (Paper IV, Figure S2D). Interestingly, we detected a difference in the levels of soluble misfolded D96Mfs*8 SOD1 following proteasome inhibition between the MNCs and fibroblasts using the misELISA assay. To our surprise, the absolute levels of misfolded SOD1 in D96Mfs*8 lines was enhanced about 14-fold in fibroblasts following proteasome inhibition, compared to a 3-fold elevation in MNCs. Soluble misfolded SOD1 has been shown to decrease as

aggregation initiates in G127X transgenic mice [338]. Furthermore, we have demonstrated that the relative levels of soluble misfolded and aggregated SOD1 are different in patient-derived *SOD1* G85S and A4V MNCs (Paper II), which could underlie the differences in soluble levels of misfolded SOD1 in the D96Mfs*8 fibroblasts and MNCs lines.

To test whether we could detect any additional differences between the patient- and mutation carrier-derived MNCs, and also potential differences in aggregation compared to fibroblasts, we analysed soluble and aggregated misfolded SOD1 in MNCs by western blotting. As in fibroblasts (Paper I), soluble misfolded protein was quickly degraded and not detectable by western blotting (Paper IV, Figure 2D). However, in contrast to fibroblasts, aggregates of truncated D96Mfs*8 SOD1 in the detergent insoluble fraction were detected without proteasome inhibition (Paper IV, Figure 2D). Use of proteasome inhibition increased aggregation in both the D96Mfs*8 patient line but also the in non-affected mutation carrier. However, aggregation was more prominent in ALS patient-derived MNCs compared to the mutation carrier cells (Paper IV, Figure 2D). Hence, the *SOD1* mutant D96Mfs*8 protein is highly aggregation prone, especially in ALS-patient-derived MNCs, which could explain the moderate levels of misfolded soluble SOD1 present in D96Mfs*8 MNCs.

In conclusion, we demonstrate a novel D96Mfs*8 *SOD1* mutation, the protein resulting from this mutation is very unstable in patient-derived cells and is efficiently degraded by the proteasome. The mutant protein is extremely prone to aggregation in MNCs, highlighting the importance of a functional degradation system. Although we cannot conclude whether D96Mfs*8 is pathogenic or not, our observations suggest that heterozygosity for this novel mutations could be associated with reduced penetrance

Discussion

It is difficult to Early stages of ALS in patients, as with other neurodegenerative proteinopathies, such as AD and PD. This partly because the disease initiation occurs long before symptom onset. Moreover, the cells in the brain and spinal cord that are primarily affected are inaccessible. Patient studies are typically performed *post mortem* after significant degeneration and loss of the affected cells. Early stages of disease have commonly been investigated in transgenic models overexpressing human mutant proteins. However, most cases of neurodegenerative diseases are sporadic, without a known genetic cause, and cannot be studied in overexpression models. Patient-derived models enable the investigation of mechanisms of disease pathogenesis in both familial and sporadic patients, under physiologically-relevant levels of disease associated gene expression.

Fibroblasts are not a primary target of ALS but provide a useful model to study SOD1 misfolding since they express physiological levels of mutant, as well as of wt SOD1, with a patient-specific, human genetic background. Patient-derived fibroblasts have also been used to investigate pathological changes associated with PD [549, 550], AD [551] as well as ALS [552]. Fibroblasts are relatively accessible through skin biopsies and can be expanded in culture at a relatively low cost, which is useful since analyzing misfolded SOD1 by ELISA requires large amounts of material. With the identification of increased levels of soluble and aggregated SOD1 in *SOD1* FALS lines, albeit aggregated SOD1 species at low levels, we have found that important aspects of SOD1-mediated FALS pathogenesis are recapitulated in fibroblasts. However, since fibroblasts are proliferative cells, the fact that they are actively dividing could affect the handling of misfolded SOD1 compared to non-dividing or 'aged' neurons. A further advantage of fibroblasts is that they are suitable cells for reprogramming to iPSCs.

IPSCs retain the genetic background of their 'parental' fibroblasts and can be differentiated to different cell types, including MNs [454]. Several reprogramming methods have been developed using different somatic cell types as a source of cells, factors and/or delivery methods [455, 457, 460, 462, 553, 554]. Methods vary greatly in efficacy, duration and technical difficulties. Reprogramming using mRNA requires daily, time sensitive transfections, and is both more technically challenging and expensive, e.g. compared to episomal plasmid-based methods. We have utilized iPSCs reprogrammed by lentiviral transduction, mRNA transfection as well as episomal plasmid transfection. The choice of reprogramming method, as well as the culture system utilized to maintain undifferentiated iPSCs, could have an effect on the downstream differentiation efficiency. However, following analysis of cells reprogrammed with different methods, we found that increase in SOD1 misfolding was consistent in *SOD1* mutant lines and not associated with iPSC reprogramming method.

A variety of MN differentiation protocols for human iPSCs have been published and used to model ALS *in vitro* [4, 244, 488, 490-492, 498] and the yield of mature MNs is likey to be of importance when studying the pathogenesis of ALS. Apart from the use of different media formulations to maintain iPSCs

as pluripotent cells, as well as small molecules used to induce differentiation, protocols vary in the form of culture (adherent cells or EBs in suspension), period of differentiation and duration of neuronal maturation, as reviewed by Sances and colleagues [497]. Such variances are likely to affect both the efficiency of differentiation as well as the maturation of differentiated cell types. Conflicting reports of pathogenic phenotypes demonstrated in patient-derived MNs, e.g. whether FALS-derived MNs are hyper- or hypoexcitable [376, 555], could be related to variations in differentiation and maturation before analyses. We found similar levels of misfolded SOD1 in MNCs and cultures with pure astrocytes. Hence, misfolded SOD1 is enhanced in both cell types, and the yield of MNs in the differentiation was not critical for analysing levels of misfolded SOD1. The protocols we used to differentiate MNCs generate electrically active neurons 10 days after EB dissociation [4]. Other protocols require longer differentiation [498] or maturation time [492] to produce neurons with induced or spontaneous action potentials. We have shown that is it possible to analyse factors affecting SOD1 misfolding in early MNs, which is an advantage with this model system.

Different human iPSCs, as well as ESCs, are variable in their 'willingness' to convert to the neural lineage [556]. For the different lines that we have studied, cell populations were not quantified immediately after differentiation. Instead, MNCs were matured for 10 days after dissociation of differentiated cultures. At this stage, we observed varying percentages of neurons, MNs and astrocytes amongst different patient lines. This was partly a result of differences in the proliferation of a subset of cells in the cultures, as shown for a population of aberrant astrocytes in the *SOD1* G85S line (Paper II).

To investigate the role of *SOD1* FALS mutations, comparisons between patient lines and non-disease controls should be, as far as possible, performed between cultures with similar proportions of cell types. However, comparing patient-lines with perfectly matched controls is difficult, especially since differentiation efficacy may vary even between different iPSC clones from the same line [556]. Cells derived from a patients siblings, or spouse, are often used as controls to minimize differences in genetic backgrounds and help control for differences in environmental factors, respectively. However, the ideal controls are likely to be the patient's own cells. Using iPSCs, it is possible to genetically modify cells and establish an isogenic line where the mutation has been corrected. These cells have an identical genetic and epigenetic background but lack the disease causing mutation. Our results show that the differentiation efficacy is very similar between *SOD1* mutant and isogenic control lines. Hence, isogenic lines are a suitable control to study the effect of a mutant SOD1 protein. Genetic modification of iPSCs also permits insertion of mutations into wt cells, making it possible to study the effect of different *SOD1* mutations, or a combination of mutations in more than one gene, in the same genetic background. Together these techniques will be valuable for further studies of the role of misfolded SOD1 on ALS pathogenesis.

Differentiation protocols have been established to produce several ALS-relevant cells types apart from MNs, e.g. astrocytes [514], oligodendrocytes [557], microglia [558] and muscle cells [559]. The role of isolated cell types in ALS has

typically been investigated using transgenic mouse models or patient-derived cells at end stage of disease [411]. In iPSC models, comparison of isolated cell types, and co-cultures of different human and/or murine cell types can be utilized to investigate the non-cell autonomous contribution of mutant *SOD1* to early disease stages without protein overexpression.

We have characterized soluble and aggregated misfolded SOD1 in patient-derived cultures with a mixture of MNs and astrocytes and identified increased levels of misfolded SOD1 without any significant alteration in total SOD1 expression. This has not been reported previously in such a wide range of patient lines. Enhanced soluble and aggregated TARDBP has been reported in iPSC-derived MNs [508]. However, this was found to be coincident with an increase in total TARBDP protein levels in mutant cells compared to controls. By comparing misfolded SOD1 in patient-derived fibroblasts, iPSC-derived MNCs, astrocytes and SNCs, we were able to determine that SOD1 misfolding is enhanced in MNCs and astrocytes. Thus, to our knowledge, our results provide the first demonstration of increased misfolding of a ubiquitous disease-associated protein in a patient-derived model without a simultaneous increase in protein expression.

The fact that the MNCs we have used contain a mixture of MNs and astrocytes is likely to be beneficial for the survival of MNs. Although the models we have utilized did not contain other cell types that are involved in ALS including oligodendrocytes [436, 438] or microglia [422, 423, 434], our MNC model should better reflects the situation *in vivo* compared to a culture of highly purified MNs grown in isolation. However, the analysis of MNC extracts by the misELISA does not allow us to determine the level of SOD1 in defined cell types. FACS is typically used to obtain purified populations of MNs [247, 357, 376, 507]. We could not purify MNs in sufficient numbers to measure misfolded SOD1 by ELISA without incurring additional misfolding during the process. To circumvent this issue, we subcultured MNCs to establish pure astrocyte cultures and also seeded MNCs on a confluent layer of wt mouse primary astrocytes to retard the proliferation of human astrocytes. This enabled us to enrich the cultures in MNs. We could then rely upon the specificity of antibodies for misfolded human SOD1 to quantify misfolding in human astrocytes and MN-enriched populations. Using this approach enabled us to identify not only increased misfolded SOD1 in neurons but also in astrocytes. Culture of mutant MNs on wt non-neuronal cells is known to delay onset in *SOD1* G37R mice [428]. It is possible that co-culture of patient-derived MNs on mouse wt astrocytes suppress the level of misfolded SOD1 in the MNs. Our finding that astrocytes contain similar or higher levels of misfolded SOD1 compared to MNCs also raises the possibility of bidirectional signalling between MNs and astrocytes and that this may dampen misfolding of SOD1 in astrocytes non-cell autonomously. Further elucidation of this could provide important information on novel mechanisms of MN to astrocyte crosstalk.

By comparing MNCs with non-neuronal cells and SNCs, which are not a primary target in ALS, we have demonstrated that misfolded SOD1 is enhanced in ALS-associated MNCs, even in the absence of a *SOD1* mutation. Hence, our results suggest that vulnerability of MNCs could stem from

inherently high levels of misfolded SOD1 in MNs and motor area cells. MNCs depend on an efficient degradation of aberrant proteins to avoid accumulation of misfolded proteins that could trigger ALS. We have determined that soluble misfolded SOD1 is degraded by the proteasome in both fibroblasts and MNCs. By further characterization of SOD1 degradation, we identified misfolded SOD1 as a substrate for ubiquitin-independent 20S proteasome degradation. However, we did not detect any differences in the levels of proteasome activity, either between *SOD1* A4V and isogenic control lines, or between MNCs, SNCs and astrocytes, which could explain the differences in soluble misfolded SOD1 levels.

Studies in the G93A mouse model have demonstrated early alterations in proteasome composition with a reduction in the constitutive proteasome, accompanied by induction of the i20S proteasome [315, 317]. Hence, even though we did not detect an overall change in proteasome activity, misfolded SOD1 could lead to subtle alterations in proteasome composition. ALS is similar to other neurodegenerative diseases regarding accumulation of misfolded proteins and degeneration of selective neuronal subtypes. Holo-SOD1 is a very stable and ordered protein, especially in comparison with the inherently disordered proteins associated with other neurodegenerative diseases, including Tau in AD [560], and alpha synuclein in PD [561]. By identifying that misfolded SOD1 is a specific substrate for the 20s proteasome, in addition to Tau [303, 304] and alpha synuclein {Tofaris, 2001 #2272, we have helped shed light on the 20S proteasome as possible common pathway for the degradation of disease-associated misfolded proteins. Hence, the 20S proteasome seems to play an important role in the degradation of prion-competent substrates in several neurodegenerative diseases.

We found that misfolded SOD1 in patient-derived MNCs mainly exists as disulphide-reduced monomers, which corresponds to the form of misfolded SOD1 previously determined in *SOD1* transgenic mouse models [202]. SOD1 is primarily a cytoplasmic protein, but its' stability is dependent on the C57-C146 disulphide bond. However, the environment in the cytoplasm is highly reducing and is thus not favourable for maintaining C57-C146 in an oxidized state. Since the formation of the disulpfide bond is determined by O_2 and CCS [175, 191] we hypothesized that low O_2 tension could decrease the stability of SOD1. We established that low O_2 tension increased disulphide-reduction, misfolding and aggregation in mutant *SOD1*-expressing MNC as well as wt *SOD1*-expressing control MNCs. Reduced vascular perfusion could be common denominator of risk factors associated with ALS, including ageing [31], smoking [40] and stroke [30]. The amount of misfolded SOD1 is linked to disease onset [222, 230] and we show that in the event of prolonged hypoxia, the risk of SOD1 misfolding could increase significantly. Therefore, areas of localized hypoxia could serve as initiation sites of ALS.

Soluble misfolded and disulphide-reduced SOD1 are substrates for aggregation [199]. When analyzing both soluble and aggregated SOD1 by misELISA and western blotting, we found that the levels do not necessarily correlate between patient lines or cell types. *SOD1* A4V MNCs contained lower levels of soluble misfolded SOD1, but displayed a higher level of aggregated SOD1 protein, in comparison to G85S MNCs. This suggests that

misfolded SOD1 in A4V MNCs is more prone to aggregate. The A4V MNCs we have analysed have been shown to exhibit disease-associated phenotypes including mitochondrial dysfunction, hyperexcitability, ER-stress and UPR, which were found to be associated with MN degeneration after 30 days of culture [357, 376]. We did not analyse MN survival in relation to SOD1 misfolding, but in the same lines, our results indicate that a 2-fold increase in soluble and/or aggregated misfolded SOD1 at Day 10 precedes the subsequent degeneration of MNs degeneration by Day 30. Hence, a minor increase of misfolded SOD1 have the potential to trigger disease-associated pathways in *SOD1* mutant cells [357, 376].

We have established that soluble misfolded SOD1 is degraded by the proteasome *in vitro*. In the truncation mutant lines; *G127X, D125Tfs*24* and *D96Mfs*8*, we identified several fold increased levels of soluble misfolded SOD1 by misELISA after proteasome inhibition in fibroblasts. Surprisingly, in the *D96Mfs*8* lines, the increase was significantly higher in fibroblasts compared to MNCs. Further analysis of MNCs showed enhanced aggregation in MNCs, which was undetectable in fibroblasts. The *D96Mfs*8* mutation leads to a premature stop codon but also introduces seven non-native amino acids forming a C-terminal neo-peptide. The neo-peptide alters the predicted charge and hydrophobicity of the mutant protein, which is likely to increase its' aggregation propensity. The same aggregation prone protein is expressed in both fibroblasts and MNCs, present in minute amounts in its soluble form, still the D96Mfs*8 aggregate, but accumulation is enhanced in MNCs. The observed difference could be related to different aggregation propensities of mutant SOD1 in the cell types, or to the differences in the number of proliferative versus post-mitotic cells in each culture. Moreover, increased levels of soluble misfolded protein do not necessarily correlate with high levels of aggregated SOD1 as seen in *SOD1* A4V and G85S lines (Paper II). Hence, our findings show that it is important to quantify both soluble and aggregated forms of SOD1.

When comparing patient-derived D96Mfs*8 MNCs with those from a non-affected mutation carrier MNCs, aggregation was found to be more prominent in ALS-patient line. Although the patient-derived line had slightly increased levels of soluble misfolded SOD1, this implies that handling of misfolded SOD1 and/or the propensity for aggregation may different between individuals carrying the same *SOD1* mutations. It is unknown how the aggregates that we have quantified over 10 days of culture relate to those that develop over months in mice or decades in patients. Moreover, it is unclear at what threshold misfolded/aggregated SOD1 starts to aggregate, or at what stage this trigger a pathogenic response. However, iPSC-based models could be used to investigate this further, following careful quantification of misfolded SOD1 species. This would enable the role of misfolded and aggregated SOD1 in MN degeneration to be better defined.

We have determined that increased SOD1 misfolding and aggregation is associated with the presence of *SOD1* mutations in patient-derived cells *in vitro*. However, soluble misfolded SOD1 is enhanced in MNCs even in the absence of a *SOD1* mutation. This suggests that wt *SOD1* could be involved in pathogenesis in non-*SOD1* ALS. The accumulation of misfolded wt and

mutant SOD1 species in MNCs could presumably result from an increased rate of misfolding or reduced rate of degradation.

Onset of ALS is dependent on the dosage of misfolded SOD in both transgenic mouse models [217, 521] and in patients where homozygous carriers of *SOD1* mutations have earlier onset and more rapid progression compared to heterozygous carriers [562-564]. However, ALS is associated with reduced penetrance, and not all mutation carriers develop disease. This is exemplified by the *D96Mfs*8* mutation. We identified the mutation in a patient diagnosed with ALS, but also in the patient's father, who has lived with the mutation for over eight decades without any signs of neurodegenerative disease. Still, MNCs derived from both individuals displayed increased levels of soluble misfolded SOD1. Hence, the development of ALS is likely to be multifactorial [565]. Incomplete penetrance of *SOD1* ALS could be explained by an undefined compensatory mechanism that can handle enhanced levels of misfolded protein in some individuals, but not others. Alternatively, prion-like propagation of protein misfolding has been suggested to transmit AD and PD [566] and also ALS [407, 408]. If prion-conversion is a rare event in ALS but required for initiation of disease, this could also help explain the incomplete penetrance.

In conclusion, the methods we have established can be used to quantify and characterize misfolded and aggregated SOD1, not just in cells derived from patients carrying *SOD1* mutations, but also in other FALS and SALS patients that express only wt *SOD1*. These methods could be applied to discover protective or antagonistic factors, for example in unaffected mutation carriers, which would help to understand reduced penetrance in ALS. Analysis of soluble and aggregated misfolded SOD1 *in vitro* is a valuable tool to study early stages of disease in patient-derived cells. Our approach could also be used to better understand the pathogenic mechanisms of SOD1-mediated ALS, as well as a tool to screen for or validate, therapeutic drugs.

Conclusions

1. Mitochondrial dysfunction, decline in autophagy and induction of ER-stress are all associated with normal ageing as well as ALS. However, their induction- or dysfunction, did not affect levels of soluble or aggregated misfolded SOD1 in patient-derived fibroblasts.
2. The proteasome is the main degradation pathway for misfolded SOD1 in fibroblasts and MNCs.
3. An age-related decline in proteasome activity could lead to an accumulation of soluble and aggregated misfolded SOD1 and might be a key factor behind late-onset ALS.
4. Patient-derived fibroblasts expressing physiological levels of SOD1 are a useful model in which to study disease pathways related to misfolded SOD1 and ALS.
5. In iPSC-derived mixed motor neuron/astrocyte cultures (MNCs) from *SOD1* FALS patients, misfolded SOD1 exists in the same, disulphide-reduced form as in *SOD1* transgenic models.
6. Misfolded SOD1 is more abundant in MNCs and astrocytes and further elevated by *SOD1* mutations.
7. Misfolded SOD1 is degraded by the ubiquitin-independent 20S proteasome.
8. O_2 tension is a main determinant of SOD1 misfolding and aggregation in patient-derived cells.
9. Low O_2 tension resulted in increased SOD1 disulphide-reduction, misfolding and aggregation of SOD1 in cells carrying *SOD1* mutations and also only containing wt SOD1.
10. The response was time- and O_2 concentration-dependent and the effects were much greater in MNCs compared to fibroblasts, and enhanced by *SOD1* mutations.
11. Areas of the brain with low O_2 tension could be susceptible to increased misfolding and aggregation of SOD1. These could act as foci for the initiation of ALS.
12. The *SOD1* D96Mfs*8 mutation is to the shortest SOD1 peptide sequence yet described.
13. The D96Mfs *8 protein is unable to adopt a native fold and is efficiently degraded by the proteasome but is also prone to aggregation.
14. Heterozygosity of *D96Mfs*8* mutation could be associated with reduced penetrance of ALS.

Acknowledgements

I have been lucky enough to work with many great colleagues that have supported me and helped make these years memorable, and for that I am very grateful!

Jonathan Gilthorpe, you probably didn't expect me to stick around this long when you first agreed to let me work in your lab over the summer, but I've truly enjoyed working in your lab so thanks a lot for having me! I have never met anyone so enthusiastic and full of new ideas! Thank you for believing in me and always pushing me to become better, I have learned a lot from you!

I have also been fortunate enough to have several co-supervisors that have been closely involved in my projects. **Stefan Marklund,** you always have time to discuss results and plan new experiments, and no one knows SOD better than you! Special thanks to **Peter Andersen** for sharing your clinical knowledge with me and for inviting me to meet with patients, it gave me another perspective on the daily work. Thanks to **Thomas Brännström** for all education on neuropathology, especially during autopsies, I learn a lot from those opportunities. **Ulrika Nordström,** I'm so glad you joined the lab and I wish I was half as good as you when it comes to discussions! Thank you for all your help and questions!

Agneta Öberg and **Eva Jonsson**, I honestly could not have done this without you and all of your help! You are amazing, and without you there would be no thesis. Together with **Ann-Charloth Nilsson**, **Eva Bern, Helena Alstermark** and **Anna Birve** you have been great company in the lab and you've all always helped me out and supported me whenever I needed. Thank you!

Manuela and **Işil**, I'm so lucky that I got to share my time as a PhD student with you! Thanks for all the fun times we've had in- and outside the lab and at conferences! I'll never forget the sweaty cellar and shoe-smelling party in Leuven or getting lost twice (!) with Işil in Milan. And Manuela, thanks for knowing what I'm trying to say even when I'm too confused to form my thoughts into words! You are both great friends and have always been there for me and for that I'm always grateful! You have also, in your own way, taught me how to be a little less Swedish when necessary ;) Thanks also to all present and past members of the ALS group in Umeå who have all contributed to this thesis and made work, and social events, with the group fun: **Anna W, Anton, Ann-Christin, Anna-Karin R, Elaheh, Erica, Frida, Johan, Karin F, Karin H, Matthew, Mariusz, Monica, Per, Ulla-Stina, Angelica, Chizuru, Eiichi, Reza and Åsa.**

The Gilthorpe lab members over the years **Uma, Bala, Ann, Ash, Harsha, Anna-Karin J, Anna-Lena** and all project students, thanks for all your help and encouragement, not to mention the great company in the lab, at BBQs by the lake and during fika in our corner! Thanks also to **Denise** and **Lelle**, I've really enjoyed sharing the very 'politically correct' office with you ;)

Special thanks also to **Iwan Jones**, you taught me how to work in the lab from day one and have never stopped helping me out. Thanks for all your tips when I killed cells rather than culture them, for all jokes and great company!

Thanks also to **Agneta Valleskog, Birgitta Nordin, Clara Olsson, Clas Wikström, Lina Sollén, Sara Widmark** and **Terry Persson** for all the administrative help over the years. Thanks also to **Monica H** and all helpful people at **UCMM** and **Medical Biosciences/Pathology,** especially **Per-Arne Lundström** for keeping track and fixing my orders when I screw up!

Lunch and social (beer) corner people! Meeting up with you guys and talk about all the crazy things we always end up discussing has always made me laugh! Thank you **Andreas, Bethie, Björn, Erik D, Fredrick, Greg, Helena, Hélène, Kerstin, Lee-Ann, Linda, Mahmood, Maria, Mariam, Mattias, Mona, Oleg, Oskari, Sihan, Simona, Stefan, Valeria, Xingru and Zahra** for all the good times we've shared around those crowded tables ☺ **Richard**, you and your astrocytes have come to my rescue more times than I can count, thank you for saving my experiments! Thanks also to **Ida, Andreas and Anders,** without you, I would never have made it through the Biomedicine program to start with, and I would never have made such great friends!

Jag vill också passa på att tacka familj och vänner utanför jobbet.

Alla mina fantastiska vänner, tack för alla skidresor till Björkliden/Riksgränsen, Kittelfjäll och Hemavan, för alla Springsteenkonserter, bröllop, födelsedagsfester, hockeymatcher, kräftskivor och allmänt häng i alltifrån Köpenhamn, Stockholm, Göteborg, Umeå, Boden, Ekorrträsk, Rogsta och Rågoliden. Allt blir roligt när man är med er med och jag längtar alltid till nästa gång vi träffas!

Till världens bästa **mamma och pappa**! Tack för att ni stöttar mig och tycker att det jag gör är bra, även om det inte alltid är sant ;) Att komma hemma är bland det bästa som finns och det är tack vare er! Tack också till **Niklas, Maria** och mina favoriter **Tilde, Nelly och Armida**, ser fram emot att hänga mycket mer med er framöver! **Frida** 'my best friend *and* my sister' och **Nils**, tack för allt häng under åren i Umeå, ska bli kul att kolla in mitt nya rum i Skellefteå ;) Jag älskar er allihopa!

Jag har också turen att kunna komma 'hem' även till Boden och Henriksfjäll, tack **Mats, Doris och Margit**, nu finns det förhoppningsvis mer tid till både loppisar, bastubygge och fiske!

Sist men inte minst **Erik**. Du är så mycket som jag inte är och tur är väl det ☺ Tack för att du alltid finns där och lyssnar, även de gångerna när ja vet att du inte hör ett ord av vad ja säger ;) Utan dig hade jag aldrig klarat av det här! Jag älskar dig!

I would also like to express my gratitude to all of the patients and their families for their contribution to this work and to the funding organization that has supported this research including the Bertil Hållsten Foundation, Kempe Foundations, Knut and Alice Wallenberg Foundation, the StartNeuro Initiative, Swedish Brain Fund, the Swedish Research Council, Torsten and Ragnar Söderberg Foundation, Ulla-Carin Lindquist Foundation, the Umeå University Research Foundation and Västerbotten County Council.

References

1. Charcot, J.M., and Joffroy, A. (1869). Deux cas d'atrophie musculaire progressive : avec l sions de la substance grise et des faisceaux ant rolat raux de la moelle pini re. Arch Physiol Neurol Path 2, 744-760.
2. Charcot, J.M. (1873). Lecons sur les maladies du système nervaux. 2nd series, collected by Bourneville. Charcot, J.M. (1881) Lectures on the diseases of the nervous system, Vol 2, series 2, Sigersen G (trans and ed). London: New Sydenham Society, 163-20
3. Strange, R.W. et al. The structure of holo and metal-deficient wild-type human Cu, Zn superoxide dismutase and its relevance to familial amyotrophic lateral sclerosis. *J Mol Biol* **328**, 877-91 (2003).
4. Amoroso, M.W. et al. Accelerated high-yield generation of limb-innervating motor neurons from human stem cells. *J Neurosci* **33**, 574-86 (2013).
5. Ravits, J., Laurie, P., Fan, Y. & Moore, D.H. Implications of ALS focality: rostral-caudal distribution of lower motor neuron loss postmortem. *Neurology* **68**, 1576-82 (2007).
6. Ravits, J., Paul, P. & Jorg, C. Focality of upper and lower motor neuron degeneration at the clinical onset of ALS. *Neurology* **68**, 1571-5 (2007).
7. Cleveland, D.W. & Rothstein, J.D. From Charcot to Lou Gehrig: deciphering selective motor neuron death in ALS. *Nat Rev Neurosci* **2**, 806-19 (2001).
8. Lyall, R.A., Donaldson, N., Polkey, M.I., Leigh, P.N. & Moxham, J. Respiratory muscle strength and ventilatory failure in amyotrophic lateral sclerosis. *Brain* **124**, 2000-13 (2001).
9. Goetz, C.G. Amyotrophic lateral sclerosis: early contributions of Jean-Martin Charcot. *Muscle Nerve* **23**, 336-43 (2000).
10. Rowland, L.P. & Shneider, N.A. Amyotrophic lateral sclerosis. *N Engl J Med* **344**, 1688-700 (2001).
11. Ravits, J.M. & La Spada, A.R. ALS motor phenotype heterogeneity, focality, and spread: deconstructing motor neuron degeneration. *Neurology* **73**, 805-11 (2009).
12. Swinnen, B. & Robberecht, W. The phenotypic variability of amyotrophic lateral sclerosis. *Nat Rev Neurol* **10**, 661-70 (2014).
13. Wijesekera, L.C. & Leigh, P.N. Amyotrophic lateral sclerosis. *Orphanet J Rare Dis* **4**, 3 (2009).
14. Turner, M.R. et al. The diagnostic pathway and prognosis in bulbar-onset amyotrophic lateral sclerosis. *J Neurol Sci* **294**, 81-5 (2010).
15. Chio, A. et al. Phenotypic heterogeneity of amyotrophic lateral sclerosis: a population based study. *J Neurol Neurosurg Psychiatry* **82**, 740-6 (2011).
16. Chio, A. et al. Prognostic factors in ALS: A critical review. *Amyotroph Lateral Scler* **10**, 310-23 (2009).
17. Talbot, K. Motor neurone disease. *Postgrad Med J* **78**, 513-9 (2002).
18. Talbot, K. Motor neuron disease: the bare essentials. *Pract Neurol* **9**, 303-9 (2009).
19. Alonso, A., Logroscino, G., Jick, S.S. & Hernan, M.A. Incidence and lifetime risk of motor neuron disease in the United Kingdom: a population-based study. *Eur J Neurol* **16**, 745-51 (2009).
20. Al-Chalabi, A., van den Berg, L.H. & Veldink, J. Gene discovery in amyotrophic lateral sclerosis: implications for clinical management. *Nat Rev Neurol* **13**, 96-104 (2017).
21. Marin, B. et al. Variation in worldwide incidence of amyotrophic lateral sclerosis: a meta-analysis. *Int J Epidemiol* (2016).

22. Bettini, M., Vicens, J., Giunta, D.H., Rugiero, M. & Cristiano, E. Incidence and prevalence of amyotrophic lateral sclerosis in an HMO of Buenos Aires, Argentina. *Amyotroph Lateral Scler Frontotemporal Degener* **14**, 598-603 (2013).

23. Logroscino, G. et al. Incidence of amyotrophic lateral sclerosis in southern Italy: a population based study. *J Neurol Neurosurg Psychiatry* **76**, 1094-8 (2005).

24. Logroscino, G. et al. Incidence of amyotrophic lateral sclerosis in Europe. *J Neurol Neurosurg Psychiatry* **81**, 385-90 (2010).

25. Piemonte & Valle d'Aosta Register for Amyotrophic Lateral, S. Incidence of ALS in Italy: evidence for a uniform frequency in Western countries. *Neurology* **56**, 239-44 (2001).

26. Traynor, B.J. et al. Incidence and prevalence of ALS in Ireland, 1995-1997: a population-based study. *Neurology* **52**, 504-9 (1999).

27. Arthur, K.C. et al. Projected increase in amyotrophic lateral sclerosis from 2015 to 2040. *Nat Commun* **7**, 12408 (2016).

28. Chancellor, A.M., Slattery, J.M., Fraser, H. & Warlow, C.P. Risk factors for motor neuron disease: a case-control study based on patients from the Scottish Motor Neuron Disease Register. *J Neurol Neurosurg Psychiatry* **56**, 1200-6 (1993).

29. Sutedja, N.A. et al. What we truly know about occupation as a risk factor for ALS: a critical and systematic review. *Amyotroph Lateral Scler* **10**, 295-301 (2009).

30. Turner, M.R., Goldacre, R., Talbot, K. & Goldacre, M.J. Cerebrovascular injury as a risk factor for amyotrophic lateral sclerosis. *J Neurol Neurosurg Psychiatry* **87**, 244-6 (2016).

31. Ingre, C., Roos, P.M., Piehl, F., Kamel, F. & Fang, F. Risk factors for amyotrophic lateral sclerosis. *Clin Epidemiol* **7**, 181-93 (2015).

32. Armon, C. An Evidence-Based Medicine Approach to the Evaluation of the Role of Exogenous Risk Factors in Sporadic Amyotrophic Lateral Sclerosis. *Neuroepidemiology* **22**, 217-228 (2003).

33. Chio, A., Benzi, G., Dossena, M., Mutani, R. & Mora, G. Severely increased risk of amyotrophic lateral sclerosis among Italian professional football players. *Brain* **128**, 472-6 (2005).

34. Chio, A. et al. ALS in Italian professional soccer players: the risk is still present and could be soccer-specific. *Amyotroph Lateral Scler* **10**, 205-9 (2009).

35. Abel, E.L. Football increases the risk for Lou Gehrig's disease, amyotrophic lateral sclerosis. *Percept Mot Skills* **104**, 1251-4 (2007).

36. Huisman, M.H. et al. Lifetime physical activity and the risk of amyotrophic lateral sclerosis. *J Neurol Neurosurg Psychiatry* **84**, 976-81 (2013).

37. Veldink, J.H. et al. Physical activity and the association with sporadic ALS. *Neurology* **64**, 241-5 (2005).

38. Gallo, V. et al. Physical activity and risk of Amyotrophic Lateral Sclerosis in a prospective cohort study. *Eur J Epidemiol* **31**, 255-66 (2016).

39. Armon, C. Smoking may be considered an established risk factor for sporadic ALS. *Neurology* **73**, 1693-8 (2009).

40. Gallo, V. et al. Smoking and risk for amyotrophic lateral sclerosis: analysis of the EPIC cohort. *Ann Neurol* **65**, 378-85 (2009).

41. Weisskopf, M.G. et al. Prospective study of cigarette smoking and amyotrophic lateral sclerosis. *Am J Epidemiol* **160**, 26-33 (2004).

42. Brooks, B.R., Miller, R.G., Swash, M., Munsat, T.L. & World Federation of Neurology Research Group on Motor Neuron, D. El Escorial revisited: revised criteria for the diagnosis of amyotrophic lateral sclerosis. *Amyotroph Lateral Scler Other Motor Neuron Disord* **1**, 293-9 (2000).

43. Ludolph, A. et al. A revision of the El Escorial criteria - 2015. *Amyotroph Lateral Scler Frontotemporal Degener* **16**, 291-2 (2015).

44. Leigh, P.N. et al. The management of motor neurone disease. *J Neurol Neurosurg Psychiatry* **74 Suppl 4**, iv32-iv47 (2003).

45. Chio, A. et al. Global epidemiology of amyotrophic lateral sclerosis: a systematic review of the published literature. *Neuroepidemiology* **41**, 118-30 (2013).

46. Brooks, B.R. El Escorial World Federation of Neurology criteria for the diagnosis of amyotrophic lateral sclerosis. Subcommittee on Motor Neuron Diseases/Amyotrophic Lateral Sclerosis of the World Federation of Neurology Research Group on Neuromuscular Diseases and the El Escorial "Clinical limits of amyotrophic lateral sclerosis" workshop contributors. *J Neurol Sci* **124** Suppl, 96-107 (1994).

47. Bensimon, G. et al. A study of riluzole in the treatment of advanced stage or elderly patients with amyotrophic lateral sclerosis. *J Neurol* **249**, 609-15 (2002).

48. Miller, R.G., Mitchell, J.D., Lyon, M. & Moore, D.H. Riluzole for amyotrophic lateral sclerosis (ALS)/motor neuron disease (MND). *Cochrane Database Syst Rev*, Cd001447 (2007).

49. Lacomblez, L. et al. Long-term safety of riluzole in amyotrophic lateral sclerosis. *Amyotroph Lateral Scler Other Motor Neuron Disord* **3**, 23-9 (2002).

50. Bellingham, M.C. A review of the neural mechanisms of action and clinical efficiency of riluzole in treating amyotrophic lateral sclerosis: what have we learned in the last decade? *CNS Neurosci Ther* **17**, 4-31 (2011).

51. Bensimon, G., Lacomblez, L. & Meininger, V. A controlled trial of riluzole in amyotrophic lateral sclerosis. ALS/Riluzole Study Group. *N Engl J Med* **330**, 585-91 (1994).

52. Lacomblez, L., Bensimon, G., Leigh, P.N., Guillet, P. & Meininger, V. Dose-ranging study of riluzole in amyotrophic lateral sclerosis. Amyotrophic Lateral Sclerosis/Riluzole Study Group II. *Lancet* **347**, 1425-31 (1996).

53. Sojka, P., Andersen, P.M. & Forsgren, L. Effects of riluzole on symptom progression in amyotrophic lateral sclerosis. *Lancet* **349**, 176-7 (1997).

54. Miller, R.G., Mitchell, J.D. & Moore, D.H. Riluzole for amyotrophic lateral sclerosis (ALS)/motor neuron disease (MND). *Cochrane Database Syst Rev*, CD001447 (2012).

55. Lamanauskas, N. & Nistri, A. Riluzole blocks persistent Na+ and Ca2+ currents and modulates release of glutamate via presynaptic NMDA receptors on neonatal rat hypoglossal motoneurons in vitro. *Eur J Neurosci* **27**, 2501-14 (2008).

56. Mohammadi, B., Krampfl, K., Moschref, H., Dengler, R. & Bufler, J. Interaction of the neuroprotective drug riluzole with GABA(A) and glycine receptor channels. *Eur J Pharmacol* **415**, 135-40 (2001).

57. Cheah, B.C., Vucic, S., Krishnan, A.V. & Kiernan, M.C. Riluzole, neuroprotection and amyotrophic lateral sclerosis. *Curr Med Chem* **17**, 1942-199 (2010).

58. Bryson, H.M., Fulton, B. & Benfield, P. Riluzole. A review of its pharmacodynamic and pharmacokinetic properties and therapeutic potential in amyotrophic lateral sclerosis. *Drugs* **52**, 549-63 (1996).

59. Vucic, S. et al. Riluzole exerts central and peripheral modulating effects in amyotrophic lateral sclerosis. *Brain* **136**, 1361-70 (2013).

60. Andersen, P.M. et al. Good practice in the management of amyotrophic lateral sclerosis: clinical guidelines. An evidence-based review with good practice points. EALSC Working Group. *Amyotroph Lateral Scler* **8**, 195-213 (2007).

61. Abe, K., Yuki, S. & Kogure, K. Strong attenuation of ischemic and postischemic brain edema in rats by a novel free radical scavenger. *Stroke* **19**, 480-5 (1988).

62. Abe, K. et al. Confirmatory double-blind, parallel-group, placebo-controlled study of efficacy and safety of edaravone (MCI-186) in amyotrophic lateral sclerosis patients. *Amyotroph Lateral Scler Frontotemporal Degener* **15**, 610-7 (2014).

63. Writing, G. & Edaravone, A.L.S.S.G. Safety and efficacy of edaravone in well defined patients with amyotrophic lateral sclerosis: a randomised, double-blind, placebo-controlled trial. *Lancet Neurol* **16**, 505-512 (2017).

64. Millecamps, S. & Julien, J.P. Axonal transport deficits and neurodegenerative diseases. *Nat Rev Neurosci* **14**, 161-76 (2013).

65. Kiernan, M.C. et al. Amyotrophic lateral sclerosis. *The Lancet* **377**, 942-955 (2011).

66. Barbeito, L.H. et al. A role for astrocytes in motor neuron loss in amyotrophic lateral sclerosis. *Brain Res Brain Res Rev* **47**, 263-74 (2004).

67. O'Reilly, S.A. et al. Motor neuron-astrocyte interactions and levels of Cu,Zn superoxide dismutase in sporadic amyotrophic lateral sclerosis. *Exp Neurol* **131**, 203-10 (1995).

68. Schiffer, D., Cordera, S., Cavalla, P. & Migheli, A. Reactive astrogliosis of the spinal cord in amyotrophic lateral sclerosis. *J Neurol Sci* **139 Suppl**, 27-33 (1996).

69. Schiffer, D. & Fiano, V. Astrogliosis in ALS: possible interpretations according to pathogenetic hypotheses. *Amyotroph Lateral Scler Other Motor Neuron Disord* **5**, 22-5 (2004).

70. Kawamata, T., Akiyama, H., Yamada, T. & McGeer, P.L. Immunologic reactions in amyotrophic lateral sclerosis brain and spinal cord tissue. *Am J Pathol* **140**, 691-707 (1992).

71. Engelhardt, J.I. & Appel, S.H. IgG reactivity in the spinal cord and motor cortex in amyotrophic lateral sclerosis. *Arch Neurol* **47**, 1210-6 (1990).

72. McGeer, P.L. & McGeer, E.G. Inflammatory processes in amyotrophic lateral sclerosis. *Muscle & Nerve* **26**, 459-470 (2002).

73. Lansbury, P.T. & Lashuel, H.A. A century-old debate on protein aggregation and neurodegeneration enters the clinic. *Nature* **443**, 774-9 (2006).

74. Blokhuis, A.M., Groen, E.J., Koppers, M., van den Berg, L.H. & Pasterkamp, R.J. Protein aggregation in amyotrophic lateral sclerosis. *Acta Neuropathol* **125**, 777-94 (2013).

75. Ross, C.A. & Poirier, M.A. Protein aggregation and neurodegenerative disease. *Nat Med* **10 Suppl**, S10-7 (2004).

76. Neumann, M. et al. Ubiquitinated TDP-43 in frontotemporal lobar degeneration and amyotrophic lateral sclerosis. *Science* **314**, 130-3 (2006).

77. Arai, T. et al. TDP-43 is a component of ubiquitin-positive tau-negative inclusions in frontotemporal lobar degeneration and amyotrophic lateral sclerosis. *Biochem Biophys Res Commun* **351**, 602-11 (2006).

78. Leigh, P.N. et al. New aspects of the pathology of neurodegenerative disorders as revealed by ubiquitin antibodies. *Acta Neuropathol* **79**, 61-72 (1989).

79. Ikemoto, A.H.I.A.A. Neuropathology of amyotrophic lateral sclerosis with extra-motor system degeneration: Characteristics and differences in the molecular pathology between ALS with dementia and Guamanian ALS. *Amyotrophic Lateral Sclerosis and Other Motor Neuron Disorders* **1**, 97-104 (2009).

80. Kawashima, T. et al. Skein-like inclusions in the neostriatum from a case of amyotrophic lateral sclerosis with dementia. *Acta Neuropathol* **96**, 541-5 (1998).

81. Hirano, A. Neuropathology of ALS: an overview. *Neurology* **47**, S63-6 (1996).

82. Arai, T. et al. Neuronal and glial inclusions in frontotemporal dementia with or without motor neuron disease are immunopositive for p62. *Neuroscience Letters* **342**, 41-44 (2003).

83. Kato, S. et al. New consensus research on neuropathological aspects of familial amyotrophic lateral sclerosis with superoxide dismutase 1 (SOD1) gene mutations: inclusions containing SOD1 in neurons and astrocytes. *Amyotroph Lateral Scler Other Motor Neuron Disord* **1**, 163-84 (2000).

84. Lin, W.L. & Dickson, D.W. Ultrastructural localization of TDP-43 in filamentous neuronal inclusions in various neurodegenerative diseases. *Acta Neuropathol* **116**, 205-13 (2008).

85. Shibata, N. et al. Intense superoxide dismutase-1 immunoreactivity in intracytoplasmic hyaline inclusions of familial amyotrophic lateral sclerosis with posterior column involvement. *J Neuropathol Exp Neurol* **55**, 481-90 (1996).

86. Shibata, N. et al. Cu/Zn superoxide dismutase-like immunoreactivity in Lewy body-like inclusions of sporadic amyotrophic lateral sclerosis. *Neurosci Lett* **179**, 149-52 (1994).

87. Okamoto, Y. et al. Colocalization of 14-3-3 proteins with SOD1 in Lewy body-like hyaline inclusions in familial amyotrophic lateral sclerosis cases and the animal model. *PLoS One* **6**, e20427 (2011).

88. He, C.Z. & Hays, A.P. Expression of peripherin in ubiquinated inclusions of amyotrophic lateral sclerosis. *Journal of the Neurological Sciences* **217**, 47-54 (2004).

89. Liu, Y., Brooks, B.R., Taniguchi, N. & Hartmann, H.A. CuZnSOD and MnSOD immunoreactivity in brain stem motor neurons from amyotrophic lateral sclerosis patients. *Acta Neuropathol* **95**, 63-70 (1998).

90. Forsberg, K., Andersen, P.M., Marklund, S.L. & Brannstrom, T. Glial nuclear aggregates of superoxide dismutase-1 are regularly present in patients with amyotrophic lateral sclerosis. *Acta Neuropathol* **121**, 623-34 (2011).

91. Wood, J.D., Beaujeux, T.P. & Shaw, P.J. Protein aggregation in motor neurone disorders. *Neuropathol Appl Neurobiol* **29**, 529-45 (2003).

92. Mizusawa, H. et al. Focal accumulation of phosphorylated neurofilaments within anterior horn cell in familial amyotrophic lateral sclerosis. *Acta Neuropathol* **79**, 37-43 (1989).

93. Sobue, G. et al. Phosphorylated high molecular weight neurofilament protein in lower motor neurons in amyotrophic lateral sclerosis and other neurodegenerative diseases involving ventral horn cells. *Acta Neuropathol* **79**, 402-8 (1990).

94. Okamoto, K., Hirai, S., Amari, M., Watanabe, M. & Sakurai, A. Bunina bodies in amyotrophic lateral sclerosis immunostained with rabbit anti-cystatin C serum. *Neurosci Lett* **162**, 125-8 (1993).

95. Mizuno, Y. et al. Transferrin localizes in Bunina bodies in amyotrophic lateral sclerosis. *Acta Neuropathol* **112**, 597-603 (2006).

96. Okamoto, K., Mizuno, Y. & Fujita, Y. Bunina bodies in amyotrophic lateral sclerosis. *Neuropathology* **28**, 109-15 (2008).

97. Mori, F., Kakita, A., Takahashi, H. & Wakabayashi, K. Co-localization of Bunina bodies and TDP-43 inclusions in lower motor neurons in amyotrophic lateral sclerosis. *Neuropathology* **34**, 71-6 (2014).

98. Tan, C.F. et al. TDP-43 immunoreactivity in neuronal inclusions in familial amyotrophic lateral sclerosis with or without SOD1 gene mutation. *Acta Neuropathol* **113**, 535-42 (2007).

99. Haverkamp, L.J., Appel, V. & Appel, S.H. Natural history of amyotrophic lateral sclerosis in a database population. Validation of a scoring system and a model for survival prediction. *Brain* **118 (Pt 3)**, 707-19 (1995).

100. Robberecht, W. & Philips, T. The changing scene of amyotrophic lateral sclerosis. *Nat Rev Neurosci* **14**, 248-64 (2013).

101. Andersen, P.M. & Al-Chalabi, A. Clinical genetics of amyotrophic lateral sclerosis: what do we really know? *Nat Rev Neurol* **7**, 603-15 (2011).

102. Gros-Louis, F., Gaspar, C. & Rouleau, G.A. Genetics of familial and sporadic amyotrophic lateral sclerosis. *Biochim Biophys Acta* **1762**, 956-72 (2006).

103. Schymick, J.C., Talbot, K. & Traynor, B.J. Genetics of sporadic amyotrophic lateral sclerosis. *Hum Mol Genet* **16 Spec No. 2**, R233-42 (2007).

104. Chen, S., Sayana, P., Zhang, X. & Le, W. Genetics of amyotrophic lateral sclerosis: an update. *Mol Neurodegener* **8**, 28 (2013).

105. Gitcho, M.A. et al. TDP-43 A315T mutation in familial motor neuron disease. *Ann Neurol* **63**, 535-8 (2008).

106. Kabashi, E. et al. TARDBP mutations in individuals with sporadic and familial amyotrophic lateral sclerosis. *Nat Genet* **40**, 572-4 (2008).

107. Mackenzie, I.R. et al. Pathological TDP-43 distinguishes sporadic amyotrophic lateral sclerosis from amyotrophic lateral sclerosis with SOD1 mutations. *Ann Neurol* **61**, 427-34 (2007).

108. Sreedharan, J. et al. TDP-43 mutations in familial and sporadic amyotrophic lateral sclerosis. *Science* **319**, 1668-72 (2008).

109. Kirby, J. et al. Broad clinical phenotypes associated with TAR-DNA binding protein (TARDBP) mutations in amyotrophic lateral sclerosis. *Neurogenetics* **11**, 217-25 (2010).

110. Daoud, H. et al. Contribution of TARDBP mutations to sporadic amyotrophic lateral sclerosis. *J Med Genet* **46**, 112-4 (2009).

111. Liu-Yesucevitz, L. et al. Tar DNA binding protein-43 (TDP-43) associates with stress granules: analysis of cultured cells and pathological brain tissue. *PLoS One* **5**, e13250 (2010).

112. Kedersha, N. & Anderson, P. Stress granules: sites of mRNA triage that regulate mRNA stability and translatability. *Biochem Soc Trans* **30**, 963-9 (2002).

113. Anderson, P. & Kedersha, N. Stress granules: the Tao of RNA triage. *Trends Biochem Sci* **33**, 141-50 (2008).

114. Lagier-Tourenne, C. & Cleveland, D.W. Rethinking ALS: the FUS about TDP-43. *Cell* **136**, 1001-4 (2009).

115. Vance, C. et al. Mutations in FUS, an RNA processing protein, cause familial amyotrophic lateral sclerosis type 6. *Science* **323**, 1208-11 (2009).

116. Kwiatkowski, T.J., Jr. et al. Mutations in the FUS/TLS gene on chromosome 16 cause familial amyotrophic lateral sclerosis. *Science* **323**, 1205-8 (2009).

117. Yan, J. et al. Frameshift and novel mutations in FUS in familial amyotrophic lateral sclerosis and ALS/dementia. *Neurology* **75**, 807-14 (2010).

118. Rademakers, R. et al. Fus gene mutations in familial and sporadic amyotrophic lateral sclerosis. *Muscle Nerve* **42**, 170-6 (2010).

119. Belzil, V.V. et al. Mutations in FUS cause FALS and SALS in French and French Canadian populations. *Neurology* **73**, 1176-9 (2009).

120. Bosco, D.A. et al. Mutant FUS proteins that cause amyotrophic lateral sclerosis incorporate into stress granules. *Hum Mol Genet* **19**, 4160-75 (2010).

121. Gal, J. et al. Nuclear localization sequence of FUS and induction of stress granules by ALS mutants. *Neurobiol Aging* **32**, 2323.e27-40 (2011).

122. Aulas, A. & Vande Velde, C. Alterations in stress granule dynamics driven by TDP-43 and FUS: a link to pathological inclusions in ALS? *Front Cell Neurosci* **9**, 423 (2015).

123. Neumann, M. et al. A new subtype of frontotemporal lobar degeneration with FUS pathology. *Brain* **132**, 2922-31 (2009).

124. Gao, X. & Xu, Z. Mechanisms of action of angiogenin. *Acta Biochim Biophys Sin (Shanghai)* **40**, 619-24 (2008).

125. Greenway, M.J. et al. ANG mutations segregate with familial and 'sporadic' amyotrophic lateral sclerosis. *Nat Genet* **38**, 411-3 (2006).

126. Gellera, C. et al. Identification of new ANG gene mutations in a large cohort of Italian patients with amyotrophic lateral sclerosis. *Neurogenetics* **9**, 33-40 (2008).

127. van Es, M.A. et al. A case of ALS-FTD in a large FALS pedigree with a K17I ANG mutation. *Neurology* **72**, 287-8 (2009).

128. Oosthuyse, B. et al. Deletion of the hypoxia-response element in the vascular endothelial growth factor promoter causes motor neuron degeneration. *Nat Genet* **28**, 131-8 (2001).

129. DeJesus-Hernandez, M. et al. Expanded GGGGCC hexanucleotide repeat in noncoding region of C9ORF72 causes chromosome 9p-linked FTD and ALS. *Neuron* **72**, 245-56 (2011).

130. Renton, A.E. et al. A hexanucleotide repeat expansion in C9ORF72 is the cause of chromosome 9p21-linked ALS-FTD. *Neuron* **72**, 257-68 (2011).

131. Nordin, A. et al. Extensive size variability of the GGGGCC expansion in C9orf72 in both neuronal and non-neuronal tissues in 18 patients with ALS or FTD. *Hum Mol Genet* **24**, 3133-42 (2015).

132. Majounie, E. et al. Frequency of the C9orf72 hexanucleotide repeat expansion in patients with amyotrophic lateral sclerosis and frontotemporal dementia: a cross-sectional study. *The Lancet Neurology* **11**, 323-330 (2012).

133. Aoki, Y. et al. C9orf72 and RAB7L1 regulate vesicle trafficking in amyotrophic lateral sclerosis and frontotemporal dementia. *Brain* **140**, 887-897 (2017).

134. Farg, M.A. et al. C9ORF72, implicated in amytrophic lateral sclerosis and frontotemporal dementia, regulates endosomal trafficking. *Hum Mol Genet* **23**, 3579-95 (2014).

135. Gitler, A.D. & Tsuiji, H. There has been an awakening: Emerging mechanisms of C9orf72 mutations in FTD/ALS. *Brain Res* **1647**, 19-29 (2016).

136. Gijselinck, I. et al. A C9orf72 promoter repeat expansion in a Flanders-Belgian cohort with disorders of the frontotemporal lobar degeneration-amyotrophic lateral sclerosis spectrum: a gene identification study. *The Lancet Neurology* **11**, 54-65 (2012).

137. Lagier-Tourenne, C. et al. Targeted degradation of sense and antisense C9orf72 RNA foci as therapy for ALS and frontotemporal degeneration. *Proc Natl Acad Sci U S A* **110**, E4530-9 (2013).

138. Dafinca, R. et al. C9orf72 Hexanucleotide Expansions Are Associated with Altered Endoplasmic Reticulum Calcium Homeostasis and Stress Granule Formation in Induced Pluripotent Stem Cell-Derived Neurons from Patients with Amyotrophic Lateral Sclerosis and Frontotemporal Dementia. *Stem Cells* **34**, 2063-78 (2016).

139. Mori, K. et al. Bidirectional transcripts of the expanded C9orf72 hexanucleotide repeat are translated into aggregating dipeptide repeat proteins. *Acta Neuropathol* **126**, 881-93 (2013).

140. Mori, K. et al. The C9orf72 GGGGCC repeat is translated into aggregating dipeptide-repeat proteins in FTLD/ALS. *Science* **339**, 1335-8 (2013).

141. Ash, P.E. et al. Unconventional translation of C9ORF72 GGGGCC expansion generates insoluble polypeptides specific to c9FTD/ALS. *Neuron* **77**, 639-46 (2013).

142. Freischmidt, A. et al. Haploinsufficiency of TBK1 causes familial ALS and fronto-temporal dementia. *Nat Neurosci* **18**, 631-6 (2015).

143. Cirulli, E.T. et al. Exome sequencing in amyotrophic lateral sclerosis identifies risk genes and pathways. *Science* **347**, 1436-41 (2015).

144. Le Ber, I. et al. TBK1 mutation frequencies in French frontotemporal dementia and amyotrophic lateral sclerosis cohorts. *Neurobiol Aging* **36**, 3116 e5-8 (2015).

145. Helgason, E., Phung, Q.T. & Dueber, E.C. Recent insights into the complexity of Tank-binding kinase 1 signaling networks: the emerging role of cellular localization in the activation and substrate specificity of TBK1. *FEBS Lett* **587**, 1230-7 (2013).

146. Sharma, S. et al. Triggering the interferon antiviral response through an IKK-related pathway. *Science* **300**, 1148-51 (2003).

147. Pilli, M. et al. TBK-1 promotes autophagy-mediated antimicrobial defense by controlling autophagosome maturation. *Immunity* **37**, 223-34 (2012).

148. Maruyama, H. et al. Mutations of optineurin in amyotrophic lateral sclerosis. *Nature* **465**, 223-6 (2010).

149. Fecto, F. et al. SQSTM1 mutations in familial and sporadic amyotrophic lateral sclerosis. *Arch Neurol* **68**, 1440-6 (2011).

150. Murphy, M.P. How mitochondria produce reactive oxygen species. *Biochem J* **417**, 1-13 (2009).

151. Guzik, T.J. & Harrison, D.G. Vascular NADPH oxidases as drug targets for novel antioxidant strategies. *Drug Discov Today* **11**, 524-33 (2006).

152. Fukai, T. & Ushio-Fukai, M. Superoxide dismutases: role in redox signaling, vascular function, and diseases. *Antioxid Redox Signal* **15**, 1583-606 (2011).

153. Raha, S. & Robinson, B.H. Mitochondria, oxygen free radicals, disease and ageing. *Trends Biochem Sci* **25**, 502-8 (2000).

154. Barber, S.C. & Shaw, P.J. Oxidative stress in ALS: key role in motor neuron injury and therapeutic target. *Free Radic Biol Med* **48**, 629-41 (2010).

155. Chakravarthi, S., Jessop, C.E. & Bulleid, N.J. The role of glutathione in disulphide bond formation and endoplasmic-reticulum-generated oxidative stress. *EMBO Rep* **7**, 271-5 (2006).

156. Zelko, I.N., Mariani, T.J. & Folz, R.J. Superoxide dismutase multigene family: a comparison of the CuZn-SOD (SOD1), Mn-SOD (SOD2), and EC-SOD (SOD3) gene structures, evolution, and expression. *Free Radic Biol Med* **33**, 337-49 (2002).

157. Mann, T. & Keilin, D. Haemocuprein and Hepatocuprein, Copper-Protein Compounds of Blood and Liver in Mammals. *Proceedings of the Royal Society of London. Series B, Biological Sciences* **126**, 303-315 (1938).

158. Markowitz, H., Cartwright, G.E. & Wintrobe, M.M. Studies on copper metabolism. XXVII. The isolation and properties of an erythrocyte cuproprotein (erythrocuprein). *J Biol Chem* **234**, 40-5 (1959).

159. Kimmel, J.R., Markowitz, H. & Brown, D.M. Some chemical and physical properties of erythrocuprein. *J Biol Chem* **234**, 46-50 (1959).

160. McCord, J.M. & Fridovich, I. Superoxide dismutase. An enzymic function for erythrocuprein (hemocuprein). *J Biol Chem* **244**, 6049-55 (1969).

161. Wispe, J.R. et al. Synthesis and processing of the precursor for human manganо-superoxide dismutase. *Biochim Biophys Acta* **994**, 30-6 (1989).

162. Weisiger, R.A. & Fridovich, I. Superoxide dismutase. Organelle specificity. *J Biol Chem* **248**, 3582-92 (1973).

163. Weisiger, R.A. & Fridovich, I. Mitochondrial superoxide simutase. Site of synthesis and intramitochondrial localization. *J Biol Chem* **248**, 4793-6 (1973).

164. Beck, Y. et al. Human Mn superoxide dismutase cDNA sequence. *Nucleic Acids Res* **15**, 9076 (1987).

165. Li, Y. et al. Dilated cardiomyopathy and neonatal lethality in mutant mice lacking manganese superoxide dismutase. *Nat Genet* **11**, 376-81 (1995).

166. Marklund, S.L. Human copper-containing superoxide dismutase of high molecular weight. *Proc Natl Acad Sci U S A* **79**, 7634-8 (1982).

167. Marklund, S.L. Properties of extracellular superoxide dismutase from human lung. *Biochem J* **220**, 269-72 (1984).

168. Hjalmarsson, K., Marklund, S.L., Engstrom, A. & Edlund, T. Isolation and sequence of complementary DNA encoding human extracellular superoxide dismutase. *Proc Natl Acad Sci U S A* **84**, 6340-4 (1987).

169. Qin, Z., Itoh, S., Jeney, V., Ushio-Fukai, M. & Fukai, T. Essential role for the Menkes ATPase in activation of extracellular superoxide dismutase: implication for vascular oxidative stress. *Faseb j* **20**, 334-6 (2006).

170. Jeney, V. et al. Role of antioxidant-1 in extracellular superoxide dismutase function and expression. *Circ Res* **96**, 723-9 (2005).

171. Barra, D. et al. The complete amino acid sequence of human Cu/Zn superoxide dismutase. *FEBS Lett* **120**, 53-6 (1980).

172. Parge, H.E., Hallewell, R.A. & Tainer, J.A. Atomic structures of wild-type and thermostable mutant recombinant human Cu,Zn superoxide dismutase. *Proc Natl Acad Sci U S A* **89**, 6109-13 (1992).

173. Jabusch, J.R., Farb, D.L., Kerschensteiner, D.A. & Deutsch, H.F. Some sulfhydryl properties and primary structure of human erythrocyte superoxide dismutase. *Biochemistry* **19**, 2310-6 (1980).

174. Forman, H.J. & Fridovich, I. On the stability of bovine superoxide dismutase. The effects of metals. *J Biol Chem* **248**, 2645-9 (1973).

175. Furukawa, Y., Torres, A.S. & O'Halloran, T.V. Oxygen-induced maturation of SOD1: a key role for disulfide formation by the copper chaperone CCS. *Embo j* **23**, 2872-81 (2004).

176. Arnesano, F. et al. The unusually stable quaternary structure of human Cu,Zn-superoxide dismutase 1 is controlled by both metal occupancy and disulfide status. *J Biol Chem* **279**, 47998-8003 (2004).

177. Cao, X. et al. Structures of the G85R Variant of SOD1 in Familial Amyotrophic Lateral Sclerosis. *Journal of Biological Chemistry* **283**, 16169-16177 (2008).

178. Getzoff, E.D. et al. Faster superoxide dismutase mutants designed by enhancing electrostatic guidance. *Nature* **358**, 347-51 (1992).

179. Stathopulos, P.B. et al. Calorimetric analysis of thermodynamic stability and aggregation for apo and holo amyotrophic lateral sclerosis-associated Gly-93 mutants of superoxide dismutase. *J Biol Chem* **281**, 6184-93 (2006).

180. Rakhit, R. & Chakrabartty, A. Structure, folding, and misfolding of Cu,Zn superoxide dismutase in amyotrophic lateral sclerosis. *Biochim Biophys Acta* **1762**, 1025-37 (2006).

181. Arnesano, F., Banci, L., Bertini, I. & Bonvin, A.M. A docking approach to the study of copper trafficking proteins; interaction between metallochaperones and soluble domains of copper ATPases. *Structure* **12**, 669-76 (2004).

182. Nordlund, A. & Oliveberg, M. SOD1-associated ALS: a promising system for elucidating the origin of protein-misfolding disease. *HFSP J* **2**, 354-64 (2008).

183. Leal, S.S., Cristovao, J.S., Biesemeier, A., Cardoso, I. & Gomes, C.M. Aberrant zinc binding to immature conformers of metal-free copper-zinc superoxide dismutase triggers amorphous aggregation. *Metallomics* **7**, 333-46 (2015).

184. Banci, L. et al. Human superoxide dismutase 1 (hSOD1) maturation through interaction with human copper chaperone for SOD1 (hCCS). *Proc Natl Acad Sci U S A* **109**, 13555-60 (2012).

185. Culotta, V.C. et al. The copper chaperone for superoxide dismutase. *J Biol Chem* **272**, 23469-72 (1997).

186. O'Halloran, T.V. & Culotta, V.C. Metallochaperones, an Intracellular Shuttle Service for Metal Ions. *Journal of Biological Chemistry* **275**, 25057-25060 (2000).

187. Rae, T.D., Torres, A.S., Pufahl, R.A. & O'Halloran, T.V. Mechanism of Cu,Zn-Superoxide Dismutase Activation by the Human Metallochaperone hCCS. *Journal of Biological Chemistry* **276**, 5166-5176 (2000).

188. Lamb, A.L., Torres, A.S., O'Halloran, T.V. & Rosenzweig, A.C. Heterodimer formation between superoxide dismutase and its copper chaperone. *Biochemistry* **39**, 14720-7 (2000).

189. Rothstein, J.D. et al. The copper chaperone CCS is abundant in neurons and astrocytes in human and rodent brain. *J Neurochem* **72**, 422-9 (1999).

190. Nordlund, A. et al. Functional features cause misfolding of the ALS-provoking enzyme SOD1. *Proc Natl Acad Sci U S A* **106**, 9667-72 (2009).

191. Brown, N.M., Torres, A.S., Doan, P.E. & O'Halloran, T.V. Oxygen and the copper chaperone CCS regulate posttranslational activation of Cu,Zn superoxide dismutase. *Proc Natl Acad Sci U S A* **101**, 5518-23 (2004).

192. Wong, P.C. et al. Copper chaperone for superoxide dismutase is essential to activate mammalian Cu/Zn superoxide dismutase. *Proc Natl Acad Sci U S A* **97**, 2886-91 (2000).

193. Leitch, J.M. et al. Activation of Cu,Zn-superoxide dismutase in the absence of oxygen and the copper chaperone CCS. *J Biol Chem* **284**, 21863-71 (2009).

194. Broom, H.R., Rumfeldt, J.A., Vassall, K.A. & Meiering, E.M. Destabilization of the dimer interface is a common consequence of diverse ALS-associated mutations in metal free SOD1. *Protein Sci* **24**, 2081-9 (2015).

195. Lindberg, M.J., Bystrom, R., Boknas, N., Andersen, P.M. & Oliveberg, M. Systematically perturbed folding patterns of amyotrophic lateral sclerosis (ALS)-associated SOD1 mutants. *Proc Natl Acad Sci U S A* **102**, 9754-9 (2005).

196. Tiwari, A. & Hayward, L.J. Familial amyotrophic lateral sclerosis mutants of copper/zinc superoxide dismutase are susceptible to disulfide reduction. *J Biol Chem* **278**, 5984-92 (2003).

197. Rodriguez, J.A. et al. Familial amyotrophic lateral sclerosis-associated mutations decrease the thermal stability of distinctly metallated species of human copper/zinc superoxide dismutase. *J Biol Chem* **277**, 15932-7 (2002).

198. Rodriguez, J.A. et al. Destabilization of apoprotein is insufficient to explain Cu,Zn-superoxide dismutase-linked ALS pathogenesis. *Proc Natl Acad Sci U S A* **102**, 10516-21 (2005).

199. Furukawa, Y., Kaneko, K., Yamanaka, K., O'Halloran, T.V. & Nukina, N. Complete loss of post-translational modifications triggers fibrillar aggregation of SOD1 in the familial form of amyotrophic lateral sclerosis. *J Biol Chem* **283**, 24167-76 (2008).

200. Chattopadhyay, M. et al. Initiation and elongation in fibrillation of ALS-linked superoxide dismutase. *Proc Natl Acad Sci U S A* **105**, 18663-8 (2008).

201. Bergemalm, D. et al. Superoxide dismutase-1 and other proteins in inclusions from transgenic amyotrophic lateral sclerosis model mice. *J Neurochem* **114**, 408-18 (2010).

202. Zetterstrom, P., Graffmo, K.S., Andersen, P.M., Brannstrom, T. & Marklund, S.L. Composition of soluble misfolded superoxide dismutase-1 in murine models of amyotrophic lateral sclerosis. *Neuromolecular Med* **15**, 147-58 (2013).

203. Zetterstrom, P. et al. Soluble misfolded subfractions of mutant superoxide dismutase-1s are enriched in spinal cords throughout life in murine ALS models. *Proc Natl Acad Sci U S A* **104**, 14157-62 (2007).

204. Lindberg, M.J., Normark, J., Holmgren, A. & Oliveberg, M. Folding of human superoxide dismutase: disulfide reduction prevents dimerization and produces marginally stable monomers. *Proc Natl Acad Sci U S A* **101**, 15893-8 (2004).

205. Rosen, D.R. et al. Mutations in Cu/Zn superoxide dismutase gene are associated with familial amyotrophic lateral sclerosis. *Nature* **362**, 59-62 (1993).

206. Shaw, C.E. et al. Mutations in all five exons of SOD-1 may cause ALS. *Ann Neurol* **43**, 390-4 (1998).

207. Felbecker, A. et al. Four familial ALS pedigrees discordant for two SOD1 mutations: are all SOD1 mutations pathogenic? *J Neurol Neurosurg Psychiatry* **81**, 572-7 (2010).

208. Pasinelli, P. & Brown, R.H. Molecular biology of amyotrophic lateral sclerosis: insights from genetics. *Nat Rev Neurosci* **7**, 710-23 (2006).

209. Andersen, P.M. et al. Sixteen novel mutations in the Cu/Zn superoxide dismutase gene in amyotrophic lateral sclerosis: a decade of discoveries, defects and disputes. *Amyotroph Lateral Scler Other Motor Neuron Disord* **4**, 62-73 (2003).

210. Lindberg, M.J., Tibell, L. & Oliveberg, M. Common denominator of Cu/Zn superoxide dismutase mutants associated with amyotrophic lateral sclerosis: decreased stability of the apo state. *Proc Natl Acad Sci U S A* **99**, 16607-12 (2002).

211. Andersen, P.M. et al. Phenotypic heterogeneity in motor neuron disease patients with CuZn-superoxide dismutase mutations in Scandinavia. *Brain* **120 (Pt 10)**, 1723-37 (1997).

212. Keskin, I. et al. Effects of Cellular Pathway Disturbances on Misfolded Superoxide Dismutase-1 in Fibroblasts Derived from ALS Patients. *PLoS One* **11**, e0150133 (2016).

213. Lang, L., Kurnik, M., Danielsson, J. & Oliveberg, M. Fibrillation precursor of superoxide dismutase 1 revealed by gradual tuning of the protein-folding equilibrium. *Proc Natl Acad Sci U S A* **109**, 17868-73 (2012).

214. Furukawa, Y. & O'Halloran, T.V. Amyotrophic lateral sclerosis mutations have the greatest destabilizing effect on the apo- and reduced form of SOD1, leading to unfolding and oxidative aggregation. *J Biol Chem* **280**, 17266-74 (2005).

215. Rakhit, R. et al. Monomeric Cu,Zn-superoxide dismutase is a common misfolding intermediate in the oxidation models of sporadic and familial amyotrophic lateral sclerosis. *J Biol Chem* **279**, 15499-504 (2004).

216. Wong, P.C. et al. An adverse property of a familial ALS-linked SOD1 mutation causes motor neuron disease characterized by vacuolar degeneration of mitochondria. *Neuron* **14**, 1105-16 (1995).

217. Gurney, M.E. et al. Motor neuron degeneration in mice that express a human Cu,Zn superoxide dismutase mutation. *Science* **264**, 1772-5 (1994).

218. Andersen, P.M. et al. Amyotrophic lateral sclerosis associated with homozygosity for an Asp90Ala mutation in CuZn-superoxide dismutase. *Nat Genet* **10**, 61-6 (1995).

219. Marklund, S.L. et al. Normal binding and reactivity of copper in mutant superoxide dismutase isolated from amyotrophic lateral sclerosis patients. *J Neurochem* **69**, 675-81 (1997).

220. Synofzik, M. et al. Mutant superoxide dismutase-1 indistinguishable from wild-type causes ALS. *Hum Mol Genet* **21**, 3568-74 (2012).

221. Jonsson, P.A., Graffmo, K.S., Andersen, P.M., Marklund, S.L. & Brannstrom, T. Superoxide dismutase in amyotrophic lateral sclerosis patients homozygous for the D90A mutation. *Neurobiol Dis* **36**, 421-4 (2009).

222. Jonsson, P.A. et al. Minute quantities of misfolded mutant superoxide dismutase-1 cause amyotrophic lateral sclerosis. *Brain* **127**, 73-88 (2004).

223. Kato, S. Amyotrophic lateral sclerosis models and human neuropathology: similarities and differences. *Acta Neuropathol* **115**, 97-114 (2008).

224. Bruijn, L.I. et al. ALS-linked SOD1 mutant G85R mediates damage to astrocytes and promotes rapidly progressive disease with SOD1-containing inclusions. *Neuron* **18**, 327-38 (1997).

225. Julien, J.P. & Kriz, J. Transgenic mouse models of amyotrophic lateral sclerosis. *Biochim Biophys Acta* **1762**, 1013-24 (2006).

226. Dal Canto, M.C. & Gurney, M.E. A low expressor line of transgenic mice carrying a mutant human Cu,Zn superoxide dismutase (SOD1) gene develops pathological changes that most closely resemble those in human amyotrophic lateral sclerosis. *Acta Neuropathol* **93**, 537-50 (1997).

227. Jonsson, P.A. et al. Motor neuron disease in mice expressing the wild type-like D90A mutant superoxide dismutase-1. *J Neuropathol Exp Neurol* **65**, 1126-36 (2006).

228. Epstein, C.J. et al. Transgenic mice with increased Cu/Zn-superoxide dismutase activity: animal model of dosage effects in Down syndrome. *Proc Natl Acad Sci U S A* **84**, 8044-8 (1987).

229. Andersen, P.M. et al. Autosomal recessive adult-onset amyotrophic lateral sclerosis associated with homozygosity for Asp90Ala CuZn-superoxide dismutase mutation. A clinical and genealogical study of 36 patients. *Brain* **119 (Pt 4)**, 1153-72 (1996).

230. Jaarsma, D. et al. Human Cu/Zn superoxide dismutase (SOD1) overexpression in mice causes mitochondrial vacuolization, axonal degeneration, and premature motoneuron death and accelerates motoneuron disease in mice expressing a familial amyotrophic lateral sclerosis mutant SOD1. *Neurobiol Dis* **7**, 623-43 (2000).

231. Graffmo, K.S. et al. Expression of wild-type human superoxide dismutase-1 in mice causes amyotrophic lateral sclerosis. *Hum Mol Genet* **22**, 51-60 (2013).

232. Petrov, D., Mansfield, C., Moussy, A. & Hermine, O. ALS Clinical Trials Review: 20 Years of Failure. Are We Any Closer to Registering a New Treatment? *Front Aging Neurosci* **9** (2017).

233. Berry, J.D. et al. Design and initial results of a multi-phase randomized trial of ceftriaxone in amyotrophic lateral sclerosis. *PLoS One* **8**, e61177 (2013).

234. Groeneveld, G.J. et al. A randomized sequential trial of creatine in amyotrophic lateral sclerosis. *Ann Neurol* **53**, 437-45 (2003).

235. Shefner, J.M. et al. A clinical trial of creatine in ALS. *Neurology* **63**, 1656-61 (2004).

236. Henriques, A., Pitzer, C. & Schneider, A. Neurotrophic growth factors for the treatment of amyotrophic lateral sclerosis: where do we stand? *Front Neurosci* **4**, 32 (2010).

237. Mitsumoto, H., Brooks, B.R. & Silani, V. Clinical trials in amyotrophic lateral sclerosis: why so many negative trials and how can trials be improved? *Lancet Neurol* **13**, 1127-38 (2014).

238. Schnaar, R.I. & Schaffner, A.E. Separation of cell types from embryonic chicken and rat spinal cord: characterization of motoneuron-enriched fractions. *J Neurosci* **1**, 204-17 (1981).

239. Kobayashi, M., Nakano, M., Atobe, Y., Kadota, T. & Funakoshi, K. Islet-1 expression in thoracic spinal motor neurons in prenatal mouse. *Int J Dev Neurosci* **29**, 749-56 (2011).

240. Beaudet, M.J. et al. High yield extraction of pure spinal motor neurons, astrocytes and microglia from single embryo and adult mouse spinal cord. *Sci Rep* **5**, 16763 (2015).

241. Gingras, M., Gagnon, V., Minotti, S., Durham, H.D. & Berthod, F. Optimized protocols for isolation of primary motor neurons, astrocytes and microglia from embryonic mouse spinal cord. *J Neurosci Methods* **163**, 111-8 (2007).

242. Tradewell, M.L. & Durham, H.D. Calpastatin reduces toxicity of SOD1G93A in a culture model of amyotrophic lateral sclerosis. *Neuroreport* **21**, 976-9 (2010).

243. Bar, P.R. Motor neuron disease in vitro: the use of cultured motor neurons to study amyotrophic lateral sclerosis. *Eur J Pharmacol* **405**, 285-95 (2000).

244. Hu, B.Y. & Zhang, S.C. Differentiation of spinal motor neurons from pluripotent human stem cells. *Nat Protoc* **4**, 1295-304 (2009).

245. Hester, M.E. et al. Rapid and efficient generation of functional motor neurons from human pluripotent stem cells using gene delivered transcription factor codes. *Mol Ther* **19**, 1905-12 (2011).

246. Allodi, I. & Hedlund, E. Directed midbrain and spinal cord neurogenesis from pluripotent stem cells to model development and disease in a dish. *Front Neurosci* **8**, 109 (2014).

247. Toli, D. et al. Modeling amyotrophic lateral sclerosis in pure human iPSc-derived motor neurons isolated by a novel FACS double selection technique. *Neurobiol Dis* **82**, 269-80 (2015).

248. Wichterle, H., Lieberam, I., Porter, J.A. & Jessell, T.M. Directed differentiation of embryonic stem cells into motor neurons. *Cell* **110**, 385-97 (2002).

249. Bryson, J.B. et al. Optical control of muscle function by transplantation of stem cell-derived motor neurons in mice. *Science* **344**, 94-7 (2014).

250. Taylor, A.R. et al. Astrocyte and muscle-derived secreted factors differentially regulate motoneuron survival. *J Neurosci* **27**, 634-44 (2007).

251. Schaller, S. et al. Novel combinatorial screening identifies neurotrophic factors for selective classes of motor neurons. *Proc Natl Acad Sci U S A* **114**, E2486-E2493 (2017).

252. Cashman, N.R. et al. Neuroblastoma x spinal cord (NSC) hybrid cell lines resemble developing motor neurons. *Dev Dyn* **194**, 209-21 (1992).

253. Johann, S., Dahm, M., Kipp, M., Zahn, U. & Beyer, C. Regulation of choline acetyltransferase expression by 17 beta-oestradiol in NSC-34 cells and in the spinal cord. *J Neuroendocrinol* **23**, 839-48 (2011).

254. Vijayalakshmi, K. et al. Cerebrospinal fluid from sporadic amyotrophic lateral sclerosis patients induces degeneration of a cultured motor neuron cell line. *Brain Res* **1263**, 122-33 (2009).

255. Vijayalakshmi, K. et al. Evidence of endoplasmic reticular stress in the spinal motor neurons exposed to CSF from sporadic amyotrophic lateral sclerosis patients. *Neurobiol Dis* **41**, 695-705 (2011).

256. Durham, H.D., Dahrouge, S. & Cashman, N.R. Evaluation of the spinal cord neuron X neuroblastoma hybrid cell line NSC-34 as a model for neurotoxicity testing. *Neurotoxicology* **14**, 387-95 (1993).

257. Madji Hounoum, B. et al. NSC-34 Motor Neuron-Like Cells Are Unsuitable as Experimental Model for Glutamate-Mediated Excitotoxicity. *Front Cell Neurosci* **10**, 118 (2016).

258. Abbondanzo, S.J., Gadi, I. & Stewart, C.L. Derivation of embryonic stem cell lines. *Methods Enzymol* **225**, 803-23 (1993).

259. Thomson, J.A. et al. Embryonic stem cell lines derived from human blastocysts. *Science* **282**, 1145-7 (1998).

260. Vazin, T. & Freed, W.J. Human embryonic stem cells: derivation, culture, and differentiation: a review. *Restor Neurol Neurosci* **28**, 589-603 (2010).

261. Bain, G., Kitchens, D., Yao, M., Huettner, J.E. & Gottlieb, D.I. Embryonic stem cells express neuronal properties in vitro. *Dev Biol* **168**, 342-57 (1995).

262. Itskovitz-Eldor, J. et al. Differentiation of human embryonic stem cells into embryoid bodies compromising the three embryonic germ layers. *Mol Med* **6**, 88-95 (2000).

263. Munoz-Sanjuan, I. & Brivanlou, A.H. Neural induction, the default model and embryonic stem cells. *Nat Rev Neurosci* **3**, 271-80 (2002).

264. Harland, R. Neural induction. *Curr Opin Genet Dev* **10**, 357-62 (2000).

265. Muhr, J., Graziano, E., Wilson, S., Jessell, T.M. & Edlund, T. Convergent inductive signals specify midbrain, hindbrain, and spinal cord identity in gastrula stage chick embryos. *Neuron* **23**, 689-702 (1999).

266. Briscoe, J., Pierani, A., Jessell, T.M. & Ericson, J. A homeodomain protein code specifies progenitor cell identity and neuronal fate in the ventral neural tube. *Cell* **101**, 435-45 (2000).

267. Ericson, J., Morton, S., Kawakami, A., Roelink, H. & Jessell, T.M. Two critical periods of Sonic Hedgehog signaling required for the specification of motor neuron identity. *Cell* **87**, 661-73 (1996).

268. Di Giorgio, F.P., Carrasco, M.A., Siao, M.C., Maniatis, T. & Eggan, K. Non-cell autonomous effect of glia on motor neurons in an embryonic stem cell-based ALS model. *Nat Neurosci* **10**, 608-14 (2007).

269. Di Giorgio, F.P., Boulting, G.L., Bobrowicz, S. & Eggan, K.C. Human embryonic stem cell-derived motor neurons are sensitive to the toxic effect of glial cells carrying an ALS-causing mutation. *Cell Stem Cell* **3**, 637-48 (2008).

270. Palmer, T.D. et al. Cell culture. Progenitor cells from human brain after death. *Nature* **411**, 42-3 (2001).

271. Haidet-Phillips, A.M. et al. Astrocytes from familial and sporadic ALS patients are toxic to motor neurons. *Nat Biotechnol* **29**, 824-8 (2011).

272. Saccon, R.A., Bunton-Stasyshyn, R.K., Fisher, E.M. & Fratta, P. Is SOD1 loss of function involved in amyotrophic lateral sclerosis? *Brain* **136**, 2342-58 (2013).

273. Deng, H.X. et al. Amyotrophic lateral sclerosis and structural defects in Cu,Zn superoxide dismutase. *Science* **261**, 1047-51 (1993).

274. Borchelt, D.R. et al. Superoxide dismutase 1 with mutations linked to familial amyotrophic lateral sclerosis possesses significant activity. *Proc Natl Acad Sci U S A* **91**, 8292-6 (1994).

275. Al-Chalabi, A. & Lewis, C.M. Modelling the effects of penetrance and family size on rates of sporadic and familial disease. *Hum Hered* **71**, 281-8 (2011).

276. Reaume, A.G. et al. Motor neurons in Cu/Zn superoxide dismutase-deficient mice develop normally but exhibit enhanced cell death after axonal injury. *Nat Genet* **13**, 43-7 (1996).

277. Andersen, P.M. Amyotrophic lateral sclerosis associated with mutations in the CuZn superoxide dismutase gene. *Curr Neurol Neurosci Rep* **6**, 37-46 (2006).

278. Taylor, J.P., Hardy, J. & Fischbeck, K.H. Toxic proteins in neurodegenerative disease. *Science* **296**, 1991-5 (2002).

279. Kabashi, E., Valdmanis, P.N., Dion, P. & Rouleau, G.A. Oxidized/misfolded superoxide dismutase-1: the cause of all amyotrophic lateral sclerosis? *Ann Neurol* **62**, 553-9 (2007).

280. Forsberg, K. et al. Novel antibodies reveal inclusions containing non-native SOD1 in sporadic ALS patients. *PLoS One* **5**, e11552 (2010).

281. Bosco, D.A. et al. Wild-type and mutant SOD1 share an aberrant conformation and a common pathogenic pathway in ALS. *Nat Neurosci* **13**, 1396-403 (2010).

282. Pokrishevsky, E. et al. Aberrant localization of FUS and TDP43 is associated with misfolding of SOD1 in amyotrophic lateral sclerosis. *PLoS One* **7**, e35050 (2012).

283. Bozaykut, P., Ozer, N.K. & Karademir, B. Regulation of protein turnover by heat shock proteins. *Free Radic Biol Med* **77**, 195-209 (2014).

284. Mogk, A., Kummer, E. & Bukau, B. Cooperation of Hsp70 and Hsp100 chaperone machines in protein disaggregation. *Front Mol Biosci* **2**, 22 (2015).

285. Liberek, K., Lewandowska, A. & Zietkiewicz, S. Chaperones in control of protein disaggregation. *Embo j* **27**, 328-35 (2008).

286. Ciechanover, A. & Kwon, Y.T. Degradation of misfolded proteins in neurodegenerative diseases: therapeutic targets and strategies. *Exp Mol Med* **47**, e147 (2015).

287. Lilienbaum, A. Relationship between the proteasomal system and autophagy. *Int J Biochem Mol Biol* **4**, 1-26 (2013).

288. Hjerpe, R. et al. UBQLN2 Mediates Autophagy-Independent Protein Aggregate Clearance by the Proteasome. *Cell* **166**, 935-49 (2016).

289. Kabashi, E. & Durham, H.D. Failure of protein quality control in amyotrophic lateral sclerosis. *Biochim Biophys Acta* **1762**, 1038-50 (2006).

290. Hollenbeck, P.J. Products of endocytosis and autophagy are retrieved from axons by regulated retrograde organelle transport. *J Cell Biol* **121**, 305-15 (1993).

291. Hoffman, E.K., Wilcox, H.M., Scott, R.W. & Siman, R. Proteasome inhibition enhances the stability of mouse Cu/Zn superoxide dismutase with mutations linked to familial amyotrophic lateral sclerosis. *J Neurol Sci* **139**, 15-20 (1996).

292. Hershko, A. & Ciechanover, A. The ubiquitin system. *Annu Rev Biochem* **67**, 425-79 (1998).

293. Ciechanover, A. Intracellular protein degradation: from a vague idea through the lysosome and the ubiquitin-proteasome system and onto human diseases and drug targeting. *Bioorg Med Chem* **21**, 3400-10 (2013).

294. Glickman, M.H. & Ciechanover, A. The ubiquitin-proteasome proteolytic pathway: destruction for the sake of construction. *Physiol Rev* **82**, 373-428 (2002).

295. Voges, D., Zwickl, P. & Baumeister, W. The 26S proteasome: a molecular machine designed for controlled proteolysis. *Annu Rev Biochem* **68**, 1015-68 (1999).

296. Kish-Trier, E. & Hill, C.P. Structural biology of the proteasome. *Annu Rev Biophys* **42**, 29-49 (2013).

297. Smith, D.M. et al. Docking of the proteasomal ATPases' carboxyl termini in the 20S proteasome's alpha ring opens the gate for substrate entry. *Mol Cell* **27**, 731-44 (2007).

298. Ben-Nissan, G. & Sharon, M. Regulating the 20S proteasome ubiquitin-independent degradation pathway. *Biomolecules* **4**, 862-84 (2014).

299. Asher, G., Reuven, N. & Shaul, Y. 20S proteasomes and protein degradation "by default". *Bioessays* **28**, 844-9 (2006).

300. Baugh, J.M., Viktorova, E.G. & Pilipenko, E.V. Proteasomes can degrade a significant proportion of cellular proteins independent of ubiquitination. *J Mol Biol* **386**, 814-27 (2009).

301. Tsvetkov, P. et al. Operational definition of intrinsically unstructured protein sequences based on susceptibility to the 20S proteasome. *Proteins* **70**, 1357-66 (2008).

302. Tofaris, G.K., Layfield, R. & Spillantini, M.G. alpha-synuclein metabolism and aggregation is linked to ubiquitin-independent degradation by the proteasome. *FEBS Lett* **509**, 22-6 (2001).

303. Cardozo, C. & Michaud, C. Proteasome-mediated degradation of tau proteins occurs independently of the chymotrypsin-like activity by a nonprocessive pathway. *Arch Biochem Biophys* **408**, 103-10 (2002).

304. David, D.C. et al. Proteasomal degradation of tau protein. *J Neurochem* **83**, 176-85 (2002).

305. Wang, X., Yen, J., Kaiser, P. & Huang, L. Regulation of the 26S proteasome complex during oxidative stress. *Sci Signal* **3**, ra88 (2010).

306. Grune, T. et al. HSP70 mediates dissociation and reassociation of the 26S proteasome during adaptation to oxidative stress. *Free Radic Biol Med* **51**, 1355-64 (2011).

307. Huang, Q., Wang, H., Perry, S.W. & Figueiredo-Pereira, M.E. Negative regulation of 26S proteasome stability via calpain-mediated cleavage of Rpn10 subunit upon mitochondrial dysfunction in neurons. *J Biol Chem* **288**, 12161-74 (2013).

308. Stadtmueller, B.M. & Hill, C.P. Proteasome activators. *Mol Cell* **41**, 8-19 (2011).

309. Seifert, U. et al. Immunoproteasomes preserve protein homeostasis upon interferon-induced oxidative stress. *Cell* **142**, 613-24 (2010).

310. Pickering, A.M. et al. The immunoproteasome, the 20S proteasome and the PA28alphabeta proteasome regulator are oxidative-stress-adaptive proteolytic complexes. *Biochem J* **432**, 585-94 (2010).

311. Ferrington, D.A. & Gregerson, D.S. Immunoproteasomes: structure, function, and antigen presentation. *Prog Mol Biol Transl Sci* **109**, 75-112 (2012).

312. Di Noto, L., Whitson, L.J., Cao, X., Hart, P.J. & Levine, R.L. Proteasomal degradation of mutant superoxide dismutases linked to amyotrophic lateral sclerosis. *J Biol Chem* **280**, 39907-13 (2005).

313. Johnston, J.A., Dalton, M.J., Gurney, M.E. & Kopito, R.R. Formation of high molecular weight complexes of mutant Cu, Zn-superoxide dismutase in a mouse model for familial amyotrophic lateral sclerosis. *Proc Natl Acad Sci U S A* **97**, 12571-6 (2000).

314. Urushitani, M., Kurisu, J., Tsukita, K. & Takahashi, R. Proteasomal inhibition by misfolded mutant superoxide dismutase 1 induces selective motor neuron death in familial amyotrophic lateral sclerosis. *J Neurochem* **83**, 1030-42 (2002).

315. Kabashi, E. et al. Proteasomes remain intact, but show early focal alteration in their composition in a mouse model of amyotrophic lateral sclerosis. *J Neurochem* **105**, 2353-66 (2008).

316. Kabashi, E., Agar, J.N., Taylor, D.M., Minotti, S. & Durham, H.D. Focal dysfunction of the proteasome: a pathogenic factor in a mouse model of amyotrophic lateral sclerosis. *J Neurochem* **89**, 1325-35 (2004).

317. Cheroni, C. et al. Functional alterations of the ubiquitin-proteasome system in motor neurons of a mouse model of familial amyotrophic lateral sclerosis. *Hum Mol Genet* **18**, 82-96 (2009).

318. Puttaparthi, K. & Elliott, J.L. Non-neuronal induction of immunoproteasome subunits in an ALS model: possible mediation by cytokines. *Exp Neurol* **196**, 441-51 (2005).

319. Kabashi, E., Agar, J.N., Strong, M.J. & Durham, H.D. Impaired proteasome function in sporadic amyotrophic lateral sclerosis. *Amyotroph Lateral Scler* **13**, 367-71 (2012).

320. Keller, J.N., Huang, F.F. & Markesbery, W.R. Decreased levels of proteasome activity and proteasome expression in aging spinal cord. *Neuroscience* **98**, 149-56 (2000).

321. Vilchez, D., Saez, I. & Dillin, A. The role of protein clearance mechanisms in organismal ageing and age-related diseases. *Nat Commun* **5**, 5659 (2014).

322. Saez, I. & Vilchez, D. The Mechanistic Links Between Proteasome Activity, Aging and Age-related Diseases. *Curr Genomics* **15**, 38-51 (2014).

323. Crippa, V. et al. The small heat shock protein B8 (HspB8) promotes autophagic removal of misfolded proteins involved in amyotrophic lateral sclerosis (ALS). *Hum Mol Genet* **19**, 3440-56 (2010).

324. Dantuma, N.P. & Bott, L.C. The ubiquitin-proteasome system in neurodegenerative diseases: precipitating factor, yet part of the solution. *Front Mol Neurosci* **7**, 70 (2014).

325. Ryter, S.W., Cloonan, S.M. & Choi, A.M. Autophagy: a critical regulator of cellular metabolism and homeostasis. *Mol Cells* **36**, 7-16 (2013).

326. Navone, F., Genevini, P. & Borgese, N. Autophagy and Neurodegeneration: Insights from a Cultured Cell Model of ALS. *Cells* **4**, 354-86 (2015).

327. Mizushima, N., Ohsumi, Y. & Yoshimori, T. Autophagosome formation in mammalian cells. *Cell Struct Funct* **27**, 421-9 (2002).

328. Lee, Y.K. & Lee, J.A. Role of the mammalian ATG8/LC3 family in autophagy: differential and compensatory roles in the spatiotemporal regulation of autophagy. *BMB Rep* **49**, 424-30 (2016).

329. Donaldson, K.M. et al. Ubiquitin-mediated sequestration of normal cellular proteins into polyglutamine aggregates. *Proc Natl Acad Sci U S A* **100**, 8892-7 (2003).

330. Wooten, M.W. et al. Signaling, polyubiquitination, trafficking, and inclusions: sequestosome 1/p62's role in neurodegenerative disease. *J Biomed Biotechnol* **2006**, 62079 (2006).

331. Mizushima, N., Yoshimori, T. & Levine, B. Methods in mammalian autophagy research. *Cell* **140**, 313-26 (2010).

332. Bjorkoy, G. et al. p62/SQSTM1 forms protein aggregates degraded by autophagy and has a protective effect on huntingtin-induced cell death. *J Cell Biol* **171**, 603-14 (2005).

333. Choi, A.M., Ryter, S.W. & Levine, B. Autophagy in human health and disease. *N Engl J Med* **368**, 1845-6 (2013).

334. Kabuta, T., Suzuki, Y. & Wada, K. Degradation of amyotrophic lateral sclerosis-linked mutant Cu,Zn-superoxide dismutase proteins by macroautophagy and the proteasome. *J Biol Chem* **281**, 30524-33 (2006).

335. Morimoto, N. et al. Increased autophagy in transgenic mice with a G93A mutant SOD1 gene. *Brain Res* **1167**, 112-7 (2007).

336. Zhang, X. et al. Rapamycin treatment augments motor neuron degeneration in SOD1(G93A) mouse model of amyotrophic lateral sclerosis. *Autophagy* **7**, 412-25 (2011).

337. Sasaki, S. Autophagy in spinal cord motor neurons in sporadic amyotrophic lateral sclerosis. *J Neuropathol Exp Neurol* **70**, 349-59 (2011).

338. Tokuda, E., Brannstrom, T., Andersen, P.M. & Marklund, S.L. Low autophagy capacity implicated in motor system vulnerability to mutant superoxide dismutase. *Acta Neuropathol Commun* **4**, 6 (2016).

339. Shibata, M. et al. Regulation of intracellular accumulation of mutant Huntingtin by Beclin 1. *J Biol Chem* **281**, 14474-85 (2006).

340. Braakman, I. & Hebert, D.N. Protein folding in the endoplasmic reticulum. *Cold Spring Harb Perspect Biol* **5**, a013201 (2013).

341. Matus, S., Valenzuela, V., Medinas, D.B. & Hetz, C. ER Dysfunction and Protein Folding Stress in ALS. *Int J Cell Biol* **2013**, 674751 (2013).

342. Walter, P. & Ron, D. The unfolded protein response: from stress pathway to homeostatic regulation. *Science* **334**, 1081-6 (2011).

343. Haze, K., Yoshida, H., Yanagi, H., Yura, T. & Mori, K. Mammalian transcription factor ATF6 is synthesized as a transmembrane protein and activated by proteolysis in response to endoplasmic reticulum stress. *Mol Biol Cell* **10**, 3787-99 (1999).

344. Cox, J.S., Shamu, C.E. & Walter, P. Transcriptional induction of genes encoding endoplasmic reticulum resident proteins requires a transmembrane protein kinase. *Cell* **73**, 1197-206 (1993).

345. Ron, D. & Walter, P. Signal integration in the endoplasmic reticulum unfolded protein response. *Nat Rev Mol Cell Biol* **8**, 519-29 (2007).

346. Harding, H.P., Zhang, Y. & Ron, D. Protein translation and folding are coupled by an endoplasmic-reticulum-resident kinase. *Nature* **397**, 271-4 (1999).

347. Schaheen, B., Dang, H. & Fares, H. Derlin-dependent accumulation of integral membrane proteins at cell surfaces. *J Cell Sci* **122**, 2228-39 (2009).

348. Olzmann, J.A., Kopito, R.R. & Christianson, J.C. The mammalian endoplasmic reticulum-associated degradation system. *Cold Spring Harb Perspect Biol* **5** (2013).

349. Lilley, B.N. & Ploegh, H.L. A membrane protein required for dislocation of misfolded proteins from the ER. *Nature* **429**, 834-40 (2004).

350. Tobisawa, S. et al. Mutant SOD1 linked to familial amyotrophic lateral sclerosis, but not wild-type SOD1, induces ER stress in COS7 cells and transgenic mice. *Biochemical and Biophysical Research Communications* **303**, 496-503 (2003).

351. Kikuchi, H. et al. Spinal cord endoplasmic reticulum stress associated with a microsomal accumulation of mutant superoxide dismutase-1 in an ALS model. *Proc Natl Acad Sci U S A* **103**, 6025-30 (2006).

352. Atkin, J.D. et al. Induction of the unfolded protein response in familial amyotrophic lateral sclerosis and association of protein-disulfide isomerase with superoxide dismutase 1. *J Biol Chem* **281**, 30152-65 (2006).

353. Atkin, J.D. et al. Endoplasmic reticulum stress and induction of the unfolded protein response in human sporadic amyotrophic lateral sclerosis. *Neurobiol Dis* **30**, 400-7 (2008).

354. Ito, Y. et al. Involvement of CHOP, an ER-stress apoptotic mediator, in both human sporadic ALS and ALS model mice. *Neurobiol Dis* **36**, 470-6 (2009).

355. Saxena, S., Cabuy, E. & Caroni, P. A role for motoneuron subtype-selective ER stress in disease manifestations of FALS mice. *Nat Neurosci* **12**, 627-36 (2009).

356. Nishitoh, H. et al. ALS-linked mutant SOD1 induces ER stress- and ASK1-dependent motor neuron death by targeting Derlin-1. *Genes Dev* **22**, 1451-64 (2008).

357. Kiskinis, E. et al. Pathways disrupted in human ALS motor neurons identified through genetic correction of mutant SOD1. *Cell Stem Cell* **14**, 781-95 (2014).

358. Meldrum, B.S. Glutamate as a neurotransmitter in the brain: review of physiology and pathology. *J Nutr* **130**, 1007s-15s (2000).

359. Van Den Bosch, L. & Robberecht, W. Different receptors mediate motor neuron death induced by short and long exposures to excitotoxicity. *Brain Res Bull* **53**, 383-8 (2000).

360. Van Den Bosch, L., Vandenberghe, W., Klaassen, H., Van Houtte, E. & Robberecht, W. Ca(2+)-permeable AMPA receptors and selective vulnerability of motor neurons. *J Neurol Sci* **180**, 29-34 (2000).

361. Stys, P.K. General mechanisms of axonal damage and its prevention. *J Neurol Sci* **233**, 3-13 (2005).

362. Carriedo, S.G., Yin, H.Z. & Weiss, J.H. Motor neurons are selectively vulnerable to AMPA/kainate receptor-mediated injury in vitro. *J Neurosci* **16**, 4069-79 (1996).

363. Damiano, M. et al. Neural mitochondrial Ca2+ capacity impairment precedes the onset of motor symptoms in G93A Cu/Zn-superoxide dismutase mutant mice. *J Neurochem* **96**, 1349-61 (2006).

364. Bonifacino, T. et al. In-vivo effects of knocking-down metabotropic glutamate receptor 5 in the SOD1G93A mouse model of amyotrophic lateral sclerosis. *Neuropharmacology* (2017).

365. Van Damme, P., Dewil, M., Robberecht, W. & Van Den Bosch, L. Excitotoxicity and amyotrophic lateral sclerosis. *Neurodegener Dis* **2**, 147-59 (2005).

366. Fray, A.E. et al. The expression of the glial glutamate transporter protein EAAT2 in motor neuron disease: an immunohistochemical study. *Eur J Neurosci* **10**, 2481-9 (1998).

367. Rothstein, J.D., Martin, L.J. & Kuncl, R.W. Decreased glutamate transport by the brain and spinal cord in amyotrophic lateral sclerosis. *N Engl J Med* **326**, 1464-8 (1992).

368. Spreux-Varoquaux, O. et al. Glutamate levels in cerebrospinal fluid in amyotrophic lateral sclerosis: a reappraisal using a new HPLC method with coulometric detection in a large cohort of patients. *J Neurol Sci* **193**, 73-8 (2002).

369. Wuolikainen, A., Moritz, T., Marklund, S.L., Antti, H. & Andersen, P.M. Disease-related changes in the cerebrospinal fluid metabolome in amyotrophic lateral sclerosis detected by GC/TOFMS. *PLoS One* **6**, e17947 (2011).

370. Doble, A. The role of excitotoxicity in neurodegenerative disease: implications for therapy. *Pharmacol Ther* **81**, 163-221 (1999).

371. Park, S.B., Kiernan, M.C. & Vucic, S. Axonal Excitability in Amyotrophic Lateral Sclerosis : Axonal Excitability in ALS. *Neurotherapeutics* **14**, 78-90 (2017).

372. Vucic, S. & Kiernan, M.C. Axonal excitability properties in amyotrophic lateral sclerosis. *Clin Neurophysiol* **117**, 1458-66 (2006).

373. Vucic, S., Nicholson, G.A. & Kiernan, M.C. Cortical hyperexcitability may precede the onset of familial amyotrophic lateral sclerosis. *Brain* **131**, 1540-50 (2008).

374. Leroy, F., Lamotte d'Incamps, B., Imhoff-Manuel, R.D. & Zytnicki, D. Early intrinsic hyperexcitability does not contribute to motoneuron degeneration in amyotrophic lateral sclerosis. *Elife* **3** (2014).

375. Saxena, S. et al. Neuroprotection through excitability and mTOR required in ALS motoneurons to delay disease and extend survival. *Neuron* **80**, 80-96 (2013).

376. Wainger, B.J. et al. Intrinsic membrane hyperexcitability of amyotrophic lateral sclerosis patient-derived motor neurons. *Cell Rep* **7**, 1-11 (2014).

377. Manfredi, G. & Xu, Z. Mitochondrial dysfunction and its role in motor neuron degeneration in ALS. *Mitochondrion* **5**, 77-87 (2005).

378. Beal, M.F. Mitochondrial dysfunction in neurodegenerative diseases. *Biochim Biophys Acta* **1366**, 211-23 (1998).

379. Liu, J. et al. Toxicity of familial ALS-linked SOD1 mutants from selective recruitment to spinal mitochondria. *Neuron* **43**, 5-17 (2004).

380. Vande Velde, C., Miller, T.M., Cashman, N.R. & Cleveland, D.W. Selective association of misfolded ALS-linked mutant SOD1 with the cytoplasmic face of mitochondria. *Proc Natl Acad Sci U S A* **105**, 4022-7 (2008).

381. Vande Velde, C. et al. Misfolded SOD1 associated with motor neuron mitochondria alters mitochondrial shape and distribution prior to clinical onset. *PLoS One* **6**, e22031 (2011).

382. Pasinelli, P. et al. Amyotrophic lateral sclerosis-associated SOD1 mutant proteins bind and aggregate with Bcl-2 in spinal cord mitochondria. *Neuron* **43**, 19-30 (2004).

383. Israelson, A. et al. Misfolded mutant SOD1 directly inhibits VDAC1 conductance in a mouse model of inherited ALS. *Neuron* **67**, 575-87 (2010).

384. Pedrini, S. et al. ALS-linked mutant SOD1 damages mitochondria by promoting conformational changes in Bcl-2. *Hum Mol Genet* **19**, 2974-86 (2010).

385. Shimizu, S., Narita, M. & Tsujimoto, Y. Bcl-2 family proteins regulate the release of apoptogenic cytochrome c by the mitochondrial channel VDAC. *Nature* **399**, 483-7 (1999).

386. Sturtz, L.A., Diekert, K., Jensen, L.T., Lill, R. & Culotta, V.C. A fraction of yeast Cu,Zn-superoxide dismutase and its metallochaperone, CCS, localize to the intermembrane space of mitochondria. A physiological role for SOD1 in guarding against mitochondrial oxidative damage. *J Biol Chem* **276**, 38084-9 (2001).

387. Bergemalm, D. et al. Overloading of stable and exclusion of unstable human superoxide dismutase-1 variants in mitochondria of murine amyotrophic lateral sclerosis models. *J Neurosci* **26**, 4147-54 (2006).

388. Zetterstrom, P., Graffmo, K.S., Andersen, P.M., Brannstrom, T. & Marklund, S.L. Proteins that bind to misfolded mutant superoxide dismutase-1 in spinal cords from transgenic amyotrophic lateral sclerosis (ALS) model mice. *J Biol Chem* **286**, 20130-6 (2011).

389. Chen, S. & Brown, I.R. Neuronal expression of constitutive heat shock proteins: implications for neurodegenerative diseases. *Cell Stress Chaperones* **12**, 51-8 (2007).

390. Wu, D.C., Re, D.B., Nagai, M., Ischiropoulos, H. & Przedborski, S. The inflammatory NADPH oxidase enzyme modulates motor neuron degeneration in amyotrophic lateral sclerosis mice. *Proc Natl Acad Sci U S A* **103**, 12132-7 (2006).

391. Marden, J.J. et al. Redox modifier genes in amyotrophic lateral sclerosis in mice. *J Clin Invest* **117**, 2913-9 (2007).

392. Wilkinson, B., Koenigsknecht-Talboo, J., Grommes, C., Lee, C.Y. & Landreth, G. Fibrillar beta-amyloid-stimulated intracellular signaling cascades require Vav for induction of respiratory burst and phagocytosis in monocytes and microglia. *J Biol Chem* **281**, 20842-50 (2006).

393. Harraz, M.M. et al. SOD1 mutations disrupt redox-sensitive Rac regulation of NADPH oxidase in a familial ALS model. *J Clin Invest* **118**, 659-70 (2008).

394. Polymenidou, M. et al. Misregulated RNA processing in amyotrophic lateral sclerosis. *Brain Res* **1462**, 3-15 (2012).

395. Lu, L. et al. Mutant Cu/Zn-superoxide dismutase associated with amyotrophic lateral sclerosis destabilizes vascular endothelial growth factor mRNA and downregulates its expression. *J Neurosci* **27**, 7929-38 (2007).

396. Donnelly, C.J. et al. RNA toxicity from the ALS/FTD C9ORF72 expansion is mitigated by antisense intervention. *Neuron* **80**, 415-28 (2013).

397. Polymenidou, M. & Cleveland, D.W. Prion-like spread of protein aggregates in neurodegeneration. *J Exp Med* **209**, 889-93 (2012).

398. Collins, S.R., Douglass, A., Vale, R.D. & Weissman, J.S. Mechanism of prion propagation: amyloid growth occurs by monomer addition. *PLoS Biol* **2**, e321 (2004).

399. Frost, B. & Diamond, M.I. Prion-like mechanisms in neurodegenerative diseases. *Nat Rev Neurosci* **11**, 155-9 (2010).

400. Walker, L.C. & Jucker, M. Neurodegenerative diseases: expanding the prion concept. *Annu Rev Neurosci* **38**, 87-103 (2015).

401. Chattopadhyay, M. & Valentine, J.S. Aggregation of copper-zinc superoxide dismutase in familial and sporadic ALS. *Antioxid Redox Signal* **11**, 1603-14 (2009).

402. Oztug Durer, Z.A. et al. Loss of metal ions, disulfide reduction and mutations related to familial ALS promote formation of amyloid-like aggregates from superoxide dismutase. *PLoS One* **4**, e5004 (2009).

403. Banci, L. et al. Metal-free superoxide dismutase forms soluble oligomers under physiological conditions: a possible general mechanism for familial ALS. *Proc Natl Acad Sci U S A* **104**, 11263-7 (2007).

404. Chia, R. et al. Superoxide dismutase 1 and tgSOD1 mouse spinal cord seed fibrils, suggesting a propagative cell death mechanism in amyotrophic lateral sclerosis. *PLoS One* **5**, e10627 (2010).

405. Grad, L.I. et al. Intercellular propagated misfolding of wild-type Cu/Zn superoxide dismutase occurs via exosome-dependent and -independent mechanisms. *Proc Natl Acad Sci U S A* **111**, 3620-5 (2014).

406. Munch, C., O'Brien, J. & Bertolotti, A. Prion-like propagation of mutant superoxide dismutase-1 misfolding in neuronal cells. *Proc Natl Acad Sci U S A* **108**, 3548-53 (2011).

407. Ayers, J.I. et al. Experimental transmissibility of mutant SOD1 motor neuron disease. *Acta Neuropathol* **128**, 791-803 (2014).

408. Ayers, J.I., Fromholt, S.E., O'Neal, V.M., Diamond, J.H. & Borchelt, D.R. Prion-like propagation of mutant SOD1 misfolding and motor neuron disease spread along neuroanatomical pathways. *Acta Neuropathol* **131**, 103-14 (2016).

409. Bergh, J. et al. Structural and kinetic analysis of protein-aggregate strains in vivo using binary epitope mapping. *Proc Natl Acad Sci U S A* **112**, 4489-94 (2015).

410. Bidhendi, E.E. et al. Two superoxide dismutase prion strains transmit amyotrophic lateral sclerosis-like disease. *J Clin Invest* **126**, 2249-53 (2016).

411. Ilieva, H., Polymenidou, M. & Cleveland, D.W. Non-cell autonomous toxicity in neurodegenerative disorders: ALS and beyond. *J Cell Biol* **187**, 761-72 (2009).

412. Lasiene, J. & Yamanaka, K. Glial Cells in Amyotrophic Lateral Sclerosis. *Neurology Research International* **2011**, 1-7 (2011).

413. Boillee, S., Vande Velde, C. & Cleveland, D.W. ALS: a disease of motor neurons and their nonneuronal neighbors. *Neuron* **52**, 39-59 (2006).

414. Ferraiuolo, L., Kirby, J., Grierson, A.J., Sendtner, M. & Shaw, P.J. Molecular pathways of motor neuron injury in amyotrophic lateral sclerosis. *Nat Rev Neurol* **7**, 616-30 (2011).

415. Henkel, J.S., Beers, D.R., Zhao, W. & Appel, S.H. Microglia in ALS: the good, the bad, and the resting. *J Neuroimmune Pharmacol* **4**, 389-98 (2009).

416. Taylor, J.P., Brown, R.H., Jr. & Cleveland, D.W. Decoding ALS: from genes to mechanism. *Nature* **539**, 197-206 (2016).

417. Lino, M.M., Schneider, C. & Caroni, P. Accumulation of SOD1 mutants in postnatal motoneurons does not cause motoneuron pathology or motoneuron disease. *J Neurosci* **22**, 4825-32 (2002).

418. Pramatarova, A., Laganiere, J., Roussel, J., Brisebois, K. & Rouleau, G.A. Neuron-specific expression of mutant superoxide dismutase 1 in transgenic mice does not lead to motor impairment. *J Neurosci* **21**, 3369-74 (2001).

419. Jaarsma, D., Teuling, E., Haasdijk, E.D., De Zeeuw, C.I. & Hoogenraad, C.C. Neuron-specific expression of mutant superoxide dismutase is sufficient to induce amyotrophic lateral sclerosis in transgenic mice. *J Neurosci* **28**, 2075-88 (2008).

420. Wang, L., Sharma, K., Grisotti, G. & Roos, R.P. The effect of mutant SOD1 dismutase activity on non-cell autonomous degeneration in familial amyotrophic lateral sclerosis. *Neurobiol Dis* **35**, 234-40 (2009).

421. Gong, Y.H., Parsadanian, A.S., Andreeva, A., Snider, W.D. & Elliott, J.L. Restricted expression of G86R Cu/Zn superoxide dismutase in astrocytes results in astrocytosis but does not cause motoneuron degeneration. *J Neurosci* **20**, 660-5 (2000).

422. Boillee, S. et al. Onset and progression in inherited ALS determined by motor neurons and microglia. *Science* **312**, 1389-92 (2006).

423. Beers, D.R. et al. Wild-type microglia extend survival in PU.1 knockout mice with familial amyotrophic lateral sclerosis. *Proc Natl Acad Sci U S A* **103**, 16021-6 (2006).

424. Yamanaka, K. et al. Astrocytes as determinants of disease progression in inherited amyotrophic lateral sclerosis. *Nat Neurosci* **11**, 251-3 (2008).

425. Nagai, M. et al. Astrocytes expressing ALS-linked mutated SOD1 release factors selectively toxic to motor neurons. *Nat Neurosci* **10**, 615-22 (2007).

426. Marchetto, M.C. et al. Non-cell-autonomous effect of human SOD1 G37R astrocytes on motor neurons derived from human embryonic stem cells. *Cell Stem Cell* **3**, 649-57 (2008).

427. Caroni, P. Overexpression of growth-associated proteins in the neurons of adult transgenic mice. *J Neurosci Methods* **71**, 3-9 (1997).

428. Yamanaka, K. et al. Mutant SOD1 in cell types other than motor neurons and oligodendrocytes accelerates onset of disease in ALS mice. *Proc Natl Acad Sci U S A* **105**, 7594-9 (2008).

429. Lobsiger, C.S. & Cleveland, D.W. Glial cells as intrinsic components of non-cell-autonomous neurodegenerative disease. *Nat Neurosci* **10**, 1355-60 (2007).

430. Sokolowski, J.D. & Mandell, J.W. Phagocytic clearance in neurodegeneration. *Am J Pathol* **178**, 1416-28 (2011).

431. Tang, Y. & Le, W. Differential Roles of M1 and M2 Microglia in Neurodegenerative Diseases. *Mol Neurobiol* **53**, 1181-94 (2016).

432. Hall, E.D., Oostveen, J.A. & Gurney, M.E. Relationship of microglial and astrocytic activation to disease onset and progression in a transgenic model of familial ALS. *Glia* **23**, 249-56 (1998).

433. Alexianu, M.E., Kozovska, M. & Appel, S.H. Immune reactivity in a mouse model of familial ALS correlates with disease progression. *Neurology* **57**, 1282-9 (2001).

434. Henkel, J.S. et al. Presence of dendritic cells, MCP-1, and activated microglia/macrophages in amyotrophic lateral sclerosis spinal cord tissue. *Ann Neurol* **55**, 221-35 (2004).

435. Lee, Y. et al. Oligodendroglia metabolically support axons and contribute to neurodegeneration. *Nature* **487**, 443-8 (2012).

436. Kang, S.H. et al. Degeneration and impaired regeneration of gray matter oligodendrocytes in amyotrophic lateral sclerosis. *Nat Neurosci* **16**, 571-9 (2013).

437. Kang, S.H., Fukaya, M., Yang, J.K., Rothstein, J.D. & Bergles, D.E. NG2+ CNS glial progenitors remain committed to the oligodendrocyte lineage in postnatal life and following neurodegeneration. *Neuron* **68**, 668-81 (2010).

438. Ferraiuolo, L. et al. Oligodendrocytes contribute to motor neuron death in ALS via SOD1-dependent mechanism. *Proc Natl Acad Sci U S A* **113**, E6496-E6505 (2016).

439. Ben Haim, L., Carrillo-de Sauvage, M.A., Ceyzeriat, K. & Escartin, C. Elusive roles for reactive astrocytes in neurodegenerative diseases. *Front Cell Neurosci* **9**, 278 (2015).

440. Sofroniew, M.V. & Vinters, H.V. Astrocytes: biology and pathology. *Acta Neuropathol* **119**, 7-35 (2010).

441. Kato, S. et al. Familial amyotrophic lateral sclerosis with a two base pair deletion in superoxide dismutase 1: gene multisystem degeneration with intracytoplasmic hyaline inclusions in astrocytes. *J Neuropathol Exp Neurol* **55**, 1089-101 (1996).

442. Kushner, P.D., Stephenson, D.T. & Wright, S. Reactive astrogliosis is widespread in the subcortical white matter of amyotrophic lateral sclerosis brain. *J Neuropathol Exp Neurol* **50**, 263-77 (1991).

443. Liddelow, S.A. et al. Neurotoxic reactive astrocytes are induced by activated microglia. *Nature* **541**, 481-487 (2017).

444. Clement, A.M. et al. Wild-type nonneuronal cells extend survival of SOD1 mutant motor neurons in ALS mice. *Science* **302**, 113-7 (2003).

445. Wang, L., Gutmann, D.H. & Roos, R.P. Astrocyte loss of mutant SOD1 delays ALS disease onset and progression in G85R transgenic mice. *Hum Mol Genet* **20**, 286-93 (2011).

446. Van Damme, P., Van Den Bosch, L., Van Houtte, E., Callewaert, G. & Robberecht, W. GluR2-dependent properties of AMPA receptors determine the selective vulnerability of motor neurons to excitotoxicity. *J Neurophysiol* **88**, 1279-87 (2002).

447. Van Damme, P., Braeken, D., Callewaert, G., Robberecht, W. & Van Den Bosch, L. GluR2 deficiency accelerates motor neuron degeneration in a mouse model of amyotrophic lateral sclerosis. *J Neuropathol Exp Neurol* **64**, 605-12 (2005).

448. Van Damme, P. et al. Astrocytes regulate GluR2 expression in motor neurons and their vulnerability to excitotoxicity. *Proc Natl Acad Sci U S A* **104**, 14825-30 (2007).

449. Howland, D.S. et al. Focal loss of the glutamate transporter EAAT2 in a transgenic rat model of SOD1 mutant-mediated amyotrophic lateral sclerosis (ALS). *Proc Natl Acad Sci U S A* **99**, 1604-9 (2002).

450. Rothstein, J.D., Van Kammen, M., Levey, A.I., Martin, L.J. & Kuncl, R.W. Selective loss of glial glutamate transporter GLT-1 in amyotrophic lateral sclerosis. *Ann Neurol* **38**, 73-84 (1995).

451. Gurdon, J.B. The developmental capacity of nuclei taken from intestinal epithelium cells of feeding tadpoles. *J Embryol Exp Morphol* **10**, 622-40 (1962).

452. Wilmut, I., Schnieke, A.E., McWhir, J., Kind, A.J. & Campbell, K.H. Viable offspring derived from fetal and adult mammalian cells. *Nature* **385**, 810-3 (1997).

453. Takahashi, K. & Yamanaka, S. Induction of pluripotent stem cells from mouse embryonic and adult fibroblast cultures by defined factors. *Cell* **126**, 663-76 (2006).

454. Takahashi, K., Okita, K., Nakagawa, M. & Yamanaka, S. Induction of pluripotent stem cells from fibroblast cultures. *Nat Protoc* **2**, 3081-9 (2007).

455. Yu, J. et al. Induced pluripotent stem cell lines derived from human somatic cells. *Science* **318**, 1917-20 (2007).

456. Nakagawa, M. et al. Generation of induced pluripotent stem cells without Myc from mouse and human fibroblasts. *Nat Biotechnol* **26**, 101-6 (2008).

457. Zhou, W. & Freed, C.R. Adenoviral gene delivery can reprogram human fibroblasts to induced pluripotent stem cells. *Stem Cells* **27**, 2667-74 (2009).

458. Malik, N. & Rao, M.S. A review of the methods for human iPSC derivation. *Methods Mol Biol* **997**, 23-33 (2013).

459. Yakubov, E., Rechavi, G., Rozenblatt, S. & Givol, D. Reprogramming of human fibroblasts to pluripotent stem cells using mRNA of four transcription factors. *Biochem Biophys Res Commun* **394**, 189-93 (2010).

460. Warren, L. et al. Highly efficient reprogramming to pluripotency and directed differentiation of human cells with synthetic modified mRNA. *Cell Stem Cell* **7**, 618-30 (2010).

461. Yu, J. et al. Human induced pluripotent stem cells free of vector and transgene sequences. *Science* **324**, 797-801 (2009).

462. Okita, K. et al. A more efficient method to generate integration-free human iPS cells. *Nat Methods* **8**, 409-12 (2011).

463. Schlaeger, T.M. et al. A comparison of non-integrating reprogramming methods. **33**, 58-63 (2015).

464. Stifani, N. Motor neurons and the generation of spinal motor neuron diversity. *Front Cell Neurosci* **8**, 293 (2014).

465. Jessell, T.M. Neuronal specification in the spinal cord: inductive signals and transcriptional codes. *Nat Rev Genet* **1**, 20-9 (2000).

466. Kanning, K.C., Kaplan, A. & Henderson, C.E. Motor neuron diversity in development and disease. *Annu Rev Neurosci* **33**, 409-40 (2010).

467. Lumsden, A. Neural development. A 'LIM code' for motor neurons? *Curr Biol* **5**, 491-5 (1995).

468. Liu, J.P., Laufer, E. & Jessell, T.M. Assigning the positional identity of spinal motor neurons: rostrocaudal patterning of Hox-c expression by FGFs, Gdf11, and retinoids. *Neuron* **32**, 997-1012 (2001).

469. Dasen, J.S., Liu, J.P. & Jessell, T.M. Motor neuron columnar fate imposed by sequential phases of Hox-c activity. *Nature* **425**, 926-33 (2003).

470. Dasen, J.S., Tice, B.C., Brenner-Morton, S. & Jessell, T.M. A Hox regulatory network establishes motor neuron pool identity and target-muscle connectivity. *Cell* **123**, 477-91 (2005).

471. Dasen, J.S., De Camilli, A., Wang, B., Tucker, P.W. & Jessell, T.M. Hox repertoires for motor neuron diversity and connectivity gated by a single accessory factor, FoxP1. *Cell* **134**, 304-16 (2008).

472. Rousso, D.L., Gaber, Z.B., Wellik, D., Morrisey, E.E. & Novitch, B.G. Coordinated actions of the forkhead protein Foxp1 and Hox proteins in the columnar organization of spinal motor neurons. *Neuron* **59**, 226-40 (2008).

473. Briscoe, J. & Ericson, J. Specification of neuronal fates in the ventral neural tube. *Curr Opin Neurobiol* **11**, 43-9 (2001).

474. Ericson, J. et al. Sonic hedgehog induces the differentiation of ventral forebrain neurons: a common signal for ventral patterning within the neural tube. *Cell* **81**, 747-56 (1995).

475. Kania, A. & Jessell, T.M. Topographic motor projections in the limb imposed by LIM homeodomain protein regulation of ephrin-A:EphA interactions. *Neuron* **38**, 581-96 (2003).

476. Pfaff, S.L., Mendelsohn, M., Stewart, C.L., Edlund, T. & Jessell, T.M. Requirement for LIM homeobox gene Isl1 in motor neuron generation reveals a motor neuron-dependent step in interneuron differentiation. *Cell* **84**, 309-20 (1996).

477. Ericson, J., Thor, S., Edlund, T., Jessell, T.M. & Yamada, T. Early stages of motor neuron differentiation revealed by expression of homeobox gene Islet-1. *Science* **256**, 1555-60 (1992).

478. Landmesser, L.T. The acquisition of motoneuron subtype identity and motor circuit formation. *Int J Dev Neurosci* **19**, 175-82 (2001).

479. Arber, S. et al. Requirement for the homeobox gene Hb9 in the consolidation of motor neuron identity. *Neuron* **23**, 659-74 (1999).

480. Westbury, D.R. A comparison of the structures of alpha and gamma-spinal motoneurones of the cat. *J Physiol* **325**, 79-91 (1982).

481. Henneman, E., Somjen, G. & Carpenter, D.O. FUNCTIONAL SIGNIFICANCE OF CELL SIZE IN SPINAL MOTONEURONS. *J Neurophysiol* **28**, 560-80 (1965).

482. Frey, D. et al. Early and selective loss of neuromuscular synapse subtypes with low sprouting competence in motoneuron diseases. *J Neurosci* **20**, 2534-42 (2000).

483. Theys, P.A., Peeters, E. & Robberecht, W. Evolution of motor and sensory deficits in amyotrophic lateral sclerosis estimated by neurophysiological techniques. *J Neurol* **246**, 438-42 (1999).

484. Hegedus, J., Putman, C.T., Tyreman, N. & Gordon, T. Preferential motor unit loss in the SOD1(G93A) transgenic mouse model of amyotrophic lateral sclerosis. *J Physiol* **586**, 3337-51 (2008).

485. Schaefer, A.M., Sanes, J.R. & Lichtman, J.W. A compensatory subpopulation of motor neurons in a mouse model of amyotrophic lateral sclerosis. *J Comp Neurol* **490**, 209-19 (2005).

486. Wada, T. et al. Highly efficient differentiation and enrichment of spinal motor neurons derived from human and monkey embryonic stem cells. *PLoS One* **4**, e6722 (2009).

487. Takazawa, T. et al. Maturation of spinal motor neurons derived from human embryonic stem cells. *PLoS One* **7**, e40154 (2012).

488. Boulting, G.L. et al. A functionally characterized test set of human induced pluripotent stem cells. *Nat Biotechnol* **29**, 279-86 (2011).

489. Dimos, J.T. et al. Induced pluripotent stem cells generated from patients with ALS can be differentiated into motor neurons. *Science* **321**, 1218-21 (2008).

490. Du, Z.W. et al. Generation and expansion of highly pure motor neuron progenitors from human pluripotent stem cells. *Nat Commun* **6**, 6626 (2015).

491. Maury, Y. et al. Combinatorial analysis of developmental cues efficiently converts human pluripotent stem cells into multiple neuronal subtypes. *Nat Biotechnol* **33**, 89-96 (2015).

492. Sareen, D. et al. Targeting RNA foci in iPSC-derived motor neurons from ALS patients with a C9ORF72 repeat expansion. *Sci Transl Med* **5**, 208ra149 (2013).

493. Gouti, M. et al. In vitro generation of neuromesodermal progenitors reveals distinct roles for wnt signalling in the specification of spinal cord and paraxial mesoderm identity. *PLoS Biol* **12**, e1001937 (2014).

494. Karumbayaram, S. et al. Directed differentiation of human-induced pluripotent stem cells generates active motor neurons. *Stem Cells* **27**, 806-11 (2009).

495. Dasen, J.S. & Jessell, T.M. Hox networks and the origins of motor neuron diversity. *Curr Top Dev Biol* **88**, 169-200 (2009).

496. Chambers, S.M. et al. Highly efficient neural conversion of human ES and iPS cells by dual inhibition of SMAD signaling. *Nat Biotechnol* **27**, 275-80 (2009).

497. Sances, S. et al. Modeling ALS with motor neurons derived from human induced pluripotent stem cells. *Nat Neurosci* **16**, 542-53 (2016).

498. Devlin, A.C. et al. Human iPSC-derived motoneurons harbouring TARDBP or C9ORF72 ALS mutations are dysfunctional despite maintaining viability. *Nat Commun* **6**, 5999 (2015).

499. Lee, H. et al. Directed differentiation and transplantation of human embryonic stem cell-derived motoneurons. *Stem Cells* **25**, 1931-9 (2007).

500. Qu, Q. et al. High-efficiency motor neuron differentiation from human pluripotent stem cells and the function of Islet-1. *Nat Commun* **5**, 3449 (2014).

501. Yin, Q.W., Johnson, J., Prevette, D. & Oppenheim, R.W. Cell death of spinal motoneurons in the chick embryo following deafferentation: rescue effects of tissue extracts, soluble proteins, and neurotrophic agents. *J Neurosci* **14**, 7629-40 (1994).

502. Myszczynska, M. & Ferraiuolo, L. New In Vitro Models to Study Amyotrophic Lateral Sclerosis. *Brain Pathol* **26**, 258-65 (2016).

503. de Boer, A.S. & Eggan, K. A perspective on stem cell modeling of amyotrophic lateral sclerosis. *Cell Cycle* **14**, 3679-88 (2015).

504. Chen, H. et al. Modeling ALS with iPSCs reveals that mutant SOD1 misregulates neurofilament balance in motor neurons. *Cell Stem Cell* **14**, 796-809 (2014).

505. Burkhardt, M.F. et al. A cellular model for sporadic ALS using patient-derived induced pluripotent stem cells. *Mol Cell Neurosci* **56**, 355-64 (2013).

506. Alves, C.J. et al. Gene expression profiling for human iPS-derived motor neurons from sporadic ALS patients reveals a strong association between mitochondrial functions and neurodegeneration. *Front Cell Neurosci* **9**, 289 (2015).

507. Egawa, N. et al. Drug screening for ALS using patient-specific induced pluripotent stem cells. *Sci Transl Med* **4**, 145ra104 (2012).

508. Bilican, B. et al. Mutant induced pluripotent stem cell lines recapitulate aspects of TDP-43 proteinopathies and reveal cell-specific vulnerability. *Proc Natl Acad Sci U S A* **109**, 5803-8 (2012).

509. Nishimura, A.L. et al. Allele-specific knockdown of ALS-associated mutant TDP-43 in neural stem cells derived from induced pluripotent stem cells. *PLoS One* **9**, e91269 (2014).

510. Ichiyanagi, N. et al. Establishment of In Vitro FUS-Associated Familial Amyotrophic Lateral Sclerosis Model Using Human Induced Pluripotent Stem Cells. *Stem Cell Reports* **6**, 496-510 (2016).

511. Liu, X. et al. The fused in sarcoma protein forms cytoplasmic aggregates in motor neurons derived from integration-free induced pluripotent stem cells generated from a patient with familial amyotrophic lateral sclerosis carrying the FUS-P525L mutation. *Neurogenetics* **16**, 223-31 (2015).

512. Akimoto, C. et al. A blinded international study on the reliability of genetic testing for GGGGCC-repeat expansions in C9orf72 reveals marked differences in results among 14 laboratories. *J Med Genet* **51**, 419-24 (2014).

513. Li, Y. et al. A comprehensive library of familial human amyotrophic lateral sclerosis induced pluripotent stem cells. *PLoS One* **10**, e0118266 (2015).

514. Roybon, L. et al. Human stem cell-derived spinal cord astrocytes with defined mature or reactive phenotypes. *Cell Rep* **4**, 1035-48 (2013).

515. Zetterstrom, P., Andersen, P.M., Brannstrom, T. & Marklund, S.L. Misfolded superoxide dismutase-1 in CSF from amyotrophic lateral sclerosis patients. *J Neurochem* **117**, 91-9 (2011).

516. Dantuma, N.P., Lindsten, K., Glas, R., Jellne, M. & Masucci, M.G. Short-lived green fluorescent proteins for quantifying ubiquitin/proteasome-dependent proteolysis in living cells. *Nat Biotechnol* **18**, 538-43 (2000).

517. Schindelin, J. et al. Fiji: an open-source platform for biological-image analysis. *Nat Methods* **9**, 676-82 (2012).

518. Jonsson, P.A. et al. Disulphide-reduced superoxide dismutase-1 in CNS of transgenic amyotrophic lateral sclerosis models. *Brain* **129**, 451-64 (2006).

519. Li, L., Zhang, X. & Le, W. Altered macroautophagy in the spinal cord of SOD1 mutant mice. *Autophagy* **4**, 290-3 (2008).

520. Li, Q. et al. ALS-linked mutant superoxide dismutase 1 (SOD1) alters mitochondrial protein composition and decreases protein import. *Proc Natl Acad Sci U S A* **107**, 21146-51 (2010).

521. Alexander, G.M. et al. Effect of transgene copy number on survival in the G93A SOD1 transgenic mouse model of ALS. *Brain Res Mol Brain Res* **130**, 7-15 (2004).

522. Kitamura, A. et al. Dysregulation of the proteasome increases the toxicity of ALS-linked mutant SOD1. *Genes Cells* **19**, 209-24 (2014).

523. Bendotti, C. et al. Dysfunction of constitutive and inducible ubiquitin-proteasome system in amyotrophic lateral sclerosis: implication for protein aggregation and immune response. *Prog Neurobiol* **97**, 101-26 (2012).

524. Cheroni, C. et al. Accumulation of human SOD1 and ubiquitinated deposits in the spinal cord of SOD1G93A mice during motor neuron disease progression correlates with a decrease of proteasome. *Neurobiol Dis* **18**, 509-22 (2005).

525. Paramore, A. & Frantz, S. Bortezomib. *Nat Rev Drug Discov* **2**, 611-2 (2003).

526. Seglen, P.O. & Gordon, P.B. 3-Methyladenine: specific inhibitor of autophagic/lysosomal protein degradation in isolated rat hepatocytes. *Proc Natl Acad Sci U S A* **79**, 1889-92 (1982).

527. Schroder, M. & Kaufman, R.J. ER stress and the unfolded protein response. *Mutat Res* **569**, 29-63 (2005).

528. Yan, W. et al. Control of PERK eIF2alpha kinase activity by the endoplasmic reticulum stress-induced molecular chaperone P58IPK. *Proc Natl Acad Sci U S A* **99**, 15920-5 (2002).

529. Nami, B., Donmez, H. & Kocak, N. Tunicamycin-induced endoplasmic reticulum stress reduces in vitro subpopulation and invasion of CD44+/CD24- phenotype breast cancer stem cells. *Exp Toxicol Pathol* **68**, 419-26 (2016).

530. De Vos, K.J. et al. Familial amyotrophic lateral sclerosis-linked SOD1 mutants perturb fast axonal transport to reduce axonal mitochondria content. *Hum Mol Genet* **16**, 2720-8 (2007).

531. Magrane, J., Cortez, C., Gan, W.B. & Manfredi, G. Abnormal mitochondrial transport and morphology are common pathological denominators in SOD1 and TDP43 ALS mouse models. *Hum Mol Genet* **23**, 1413-24 (2014).

532. Lindahl, P.E. & Oberg, K.E. The effect of rotenone on respiration and its point of attack. *Exp Cell Res* **23**, 228-37 (1961).

533. Dasuri, K. et al. Selective vulnerability of neurons to acute toxicity after proteasome inhibitor treatment: implications for oxidative stress and insolubility of newly synthesized proteins. *Free Radic Biol Med* **49**, 1290-7 (2010).

534. Koga, H., Kaushik, S. & Cuervo, A.M. Protein homeostasis and aging: The importance of exquisite quality control. *Ageing Res Rev* **10**, 205-15 (2011).

535. Re, D.B. et al. Necroptosis drives motor neuron death in models of both sporadic and familial ALS. *Neuron* **81**, 1001-8 (2014).

536. Durham, H.D., Roy, J., Dong, L. & Figlewicz, D.A. Aggregation of mutant Cu/Zn superoxide dismutase proteins in a culture model of ALS. *J Neuropathol Exp Neurol* **56**, 523-30 (1997).

537. Prudencio, M., Hart, P.J., Borchelt, D.R. & Andersen, P.M. Variation in aggregation propensities among ALS-associated variants of SOD1: correlation to human disease. *Hum Mol Genet* **18**, 3217-26 (2009).

538. Miller, A.F. Superoxide dismutases: ancient enzymes and new insights. *FEBS Lett* **586**, 585-95 (2012).

539. Leitch, J.M., Yick, P.J. & Culotta, V.C. The right to choose: multiple pathways for activating copper,zinc superoxide dismutase. *J Biol Chem* **284**, 24679-83 (2009).

540. Carroll, M.C. et al. The effects of glutaredoxin and copper activation pathways on the disulfide and stability of Cu,Zn superoxide dismutase. *J Biol Chem* **281**, 28648-56 (2006).

541. Go, Y.M. & Jones, D.P. Redox compartmentalization in eukaryotic cells. *Biochim Biophys Acta* **1780**, 1273-90 (2008).

542. Fetherolf, M.M. et al. Copper-zinc superoxide dismutase is activated through a sulfenic acid intermediate at a copper ion entry site. *J Biol Chem* **292**, 12025-12040 (2017).

543. Karch, C.M., Prudencio, M., Winkler, D.D., Hart, P.J. & Borchelt, D.R. Role of mutant SOD1 disulfide oxidation and aggregation in the pathogenesis of familial ALS. *Proc Natl Acad Sci U S A* **106**, 7774-9 (2009).

544. Erecinska, M. & Silver, I.A. Tissue oxygen tension and brain sensitivity to hypoxia. *Respir Physiol* **128**, 263-76 (2001).

545. Lyons, D.G., Parpaleix, A., Roche, M. & Charpak, S. Mapping oxygen concentration in the awake mouse brain. *Elife* **5** (2016).

546. Baker, K.E. & Parker, R. Nonsense-mediated mRNA decay: terminating erroneous gene expression. *Curr Opin Cell Biol* **16**, 293-9 (2004).

547. Jackson, M. et al. Copper/zinc superoxide dismutase 1 and sporadic amyotrophic lateral sclerosis: analysis of 155 cases and identification of a novel insertion mutation. *Ann Neurol* **42**, 803-7 (1997).

548. Nordlund, A. & Oliveberg, M. Folding of Cu/Zn superoxide dismutase suggests structural hotspots for gain of neurotoxic function in ALS: parallels to precursors in amyloid disease. *Proc Natl Acad Sci U S A* **103**, 10218-23 (2006).

549. Grunewald, A. et al. Mutant Parkin impairs mitochondrial function and morphology in human fibroblasts. *PLoS One* **5**, e12962 (2010).

550. Auburger, G. et al. Primary skin fibroblasts as a model of Parkinson's disease. *Mol Neurobiol* **46**, 20-7 (2012).

551. Johnston, J.A. et al. Increased beta-amyloid release and levels of amyloid precursor protein (APP) in fibroblast cell lines from family members with the Swedish Alzheimer's disease APP670/671 mutation. *FEBS Lett* **354**, 274-8 (1994).

552. Sabatelli, M. et al. Primary fibroblasts cultures reveal TDP-43 abnormalities in amyotrophic lateral sclerosis patients with and without SOD1 mutations. *Neurobiol Aging* **36**, 2005 e5-2005 e13 (2015).

553. Anokye-Danso, F. et al. Highly efficient miRNA-mediated reprogramming of mouse and human somatic cells to pluripotency. *Cell Stem Cell* **8**, 376-88 (2011).

554. Fusaki, N., Ban, H., Nishiyama, A., Saeki, K. & Hasegawa, M. Efficient induction of transgene-free human pluripotent stem cells using a vector based on Sendai virus, an RNA virus that does not integrate into the host genome. *Proc Jpn Acad Ser B Phys Biol Sci* **85**, 348-62 (2009).

555. Naujock, M. et al. 4-Aminopyridine Induced Activity Rescues Hypoexcitable Motor Neurons from Amyotrophic Lateral Sclerosis Patient-Derived Induced Pluripotent Stem Cells. *Stem Cells* **34**, 1563-75 (2016).

556. Bock, C. et al. Reference Maps of human ES and iPS cell variation enable high-throughput characterization of pluripotent cell lines. *Cell* **144**, 439-52 (2011).

557. Douvaras, P. et al. Efficient generation of myelinating oligodendrocytes from primary progressive multiple sclerosis patients by induced pluripotent stem cells. *Stem Cell Reports* **3**, 250-9 (2014).

558. Pandya, H. et al. Differentiation of human and murine induced pluripotent stem cells to microglia-like cells. *Nat Neurosci* **20**, 753-759 (2017).

559. Maffioletti, S.M. & Gerli, M.F. Efficient derivation and inducible differentiation of expandable skeletal myogenic cells from human ES and patient-specific iPS cells. **10**, 941-58 (2015).

560. Skrabana, R., Sevcik, J. & Novak, M. Intrinsically Disordered Proteins in the Neurodegenerative Processes: Formation of Tau Protein Paired Helical Filaments and Their Analysis. *Cellular and Molecular Neurobiology* **26**, 1083-1095 (2006).

561. van Rooijen, B.D., van Leijenhorst-Groener, K.A., Claessens, M.M. & Subramaniam, V. Tryptophan fluorescence reveals structural features of alpha-synuclein oligomers. *J Mol Biol* **394**, 826-33 (2009).

562. Alavi, A. et al. Genetic analysis and SOD1 mutation screening in Iranian amyotrophic lateral sclerosis patients. *Neurobiol Aging* **34**, 1516.e1-8 (2013).

563. Boukaftane, Y. et al. Identification of six novel SOD1 gene mutations in familial amyotrophic lateral sclerosis. *Can J Neurol Sci* **25**, 192-6 (1998).

564. Hayward, C., Brock, D.J., Minns, R.A. & Swingler, R.J. Homozygosity for Asn86Ser mutation in the CuZn-superoxide dismutase gene produces a severe clinical phenotype in a juvenile onset case of familial amyotrophic lateral sclerosis. *J Med Genet* **35**, 174 (1998).

565. Roche, J.C. et al. A proposed staging system for amyotrophic lateral sclerosis. *Brain* **135**, 847-52 (2012).

566. Brundin, P., Melki, R. & Kopito, R. Prion-like transmission of protein aggregates in neurodegenerative diseases. *Nat Rev Mol Cell Biol* **11**, 301-7 (2010).